Photoinduced and Microbial Degradation of Dissolved Organic Matter in Natural Waters

Khan M. G. Mostofa, Cong-qiang Liu, Daisuke Minakata, Fengchang Wu, Davide Vione, M. Abdul Mottaleb, Takahito Yoshioka and Hiroshi Sakugawa

1 Background

Solar radiation is a universal and regular phenomenon in biosphere that is vital for all life in the Earth's crust. It maintains all the physical, chemical, photoinduced and biological processes of organic matter and dissolved organic matter

---

K. M. G. Mostofa (✉) · C. Q. Liu
State Key Laboratory of Environmental Geochemistry, Institute of Geochemistry,
Chinese Academy of Sciences, Guiyang 550002, China
e-mail: mostofa@vip.gyig.ac.cn

D. Minakata
School of Civil and Environmental Engineering, Brook Byers Institute for Sustainable Systems,
Georgia Institute of Technology, 828 West Peachtree Street, Suite 320, Atlanta, GA 30332, USA

F. C. Wu
State Environmental Protection Key Laboratory of Lake Pollution Control,
Chinese Research Academy of Environmental Sciences, Chaoyang 100012, China

D. Vione
Dipartimento Chim Analit, University Turin, I-10125 Turin, Italy

Centro Interdipartimentale NatRisk, I-10095 Grugliasco, TO, Italy

M. A. Mottaleb
Department of Chemistry/Physics, Center for Innovation and Entrepreneurship (CIE),
Northwest Missouri State University, 800 University Drive, Maryville, MO 64468, USA

T. Yoshioka
Field Science Education and Research Center, Kyoto University, Kitashirakawa Oiwake-cho,
Sakyo-ku, Kyoto 606-8502, Japan

H. Sakugawa
Department of Environmental Dynamics and Management, Graduate School of Biosphere
Science, Hiroshima University, 1-7-1, Kagamiyama, Higashi-Hiroshima 739-8521, Japan

---

Note that 'Photoinduced and photolytically' has been used instead of "photochemical and photochemically" in this book.

K. M. G. Mostofa et al. (eds.), *Photobiogeochemistry of Organic Matter*,
Environmental Science and Engineering, DOI: 10.1007/978-3-642-32223-5_4,

(DOM) in natural waters. Photoinduced or photolytic processes can maintain the acidity-alkalinity, water transparency, thermal stratification, redox reactions, production of bioavailable carbon substrates to enhance biological productivity, nutrient concentrations, production of dissolved inorganic carbon (DIC), autochthonous production of DOM, photosynthesis, formation of surface chlorophyll *a* maxima (SCM) and so on (Harvey et al. 1995; Moran and Zepp 1997; Laurion et al. 2000; Kopacek et al. 2003; Barbiero and Tuchman 2004; Huisman et al. 2006; Mostofa et al. 2009a, b). Finally, solar radiation is a major source of energy that is of essential importance in natural water ecosystems. The Photoinduced degradation of DOM and its consequences on natural waters are significantly dependent on the spectral range of sunlight under consideration, namely the UV-A (315–400 nm), UV-B (280–315 nm) or visible light (400–700 nm). Depending on the wavelength, there are significant variations as far as sunlight penetration in the water column is concerned (Scully et al. 1996; Morris and Hargreaves 1997; Reche et al. 1999). DOM is typically able to absorb UV radiation in sea and lake water (Kirk 1994; Morris et al. 1995), thereby controlling the penetration of UV in the deep water layers. The penetration depths of UV radiation in natural waters are greatly varied, with typical penetration in clear ocean water of ~20 m for UV-B and ~50 m for UV-A radiation. In oligotrophic marine waters, penetration of UV-B radiation is 5–10 m and 0.5–3 m in freshwater (Kirk 1994; Smith and Baker 1981; Waiser and Robarts 2000). Therefore, any changes in the radiation wavelengths or an increase in global temperature can greatly impact on the various biogeochemical processes mentioned earlier. However, researchers do not pay much attention to photoinduced processes to assess the biogeochemical processes in natural waters.

The microbial process is a well-known observable fact that is typically responsible for the in situ generation of DOM, cycling of nutrients, occurrence of deep chlorophyll *a* maxima (DCM), photosynthesis, thermal energy and degradation of organic matter in soil or sediment porewaters, which are vital to water environments (Mostofa et al. 2009a, b; Conrad 1999; Guildford and Hecky 2000; Rochelle-Newall and Fisher 2002; Roberts et al. 2004; Lovley 2006; Yamashita and Tanoue 2008). Microbial process is generally controlled by bacterial cells and microorganisms, both autotrophs (plants, algae, bacteria) and heterotrophs (animals, fungi, bacteria) in the aquatic environments. Microbial activity is often taking place at the hypolimnion in natural waters as well as in sediment porewaters, and it is most significant in temperate, Arctic and Antarctic regions when the lake epilimnion is covered by ice. There is also no photoinduced degradation taking place at the epilimnion during the ice-covered period. The overall photoinduced and microbial changes in organic matter and DOM components in waters play a significant role in the global carbon cycle and in the biogeochemical processes in the aquatic environment.

This review will provide a common overview on biogeochemical functions of DOM for photoinduced and microbial processes, DOM degradation for a variety of waters, theoretical model and mechanisms for photoinduced and microbial degradation of organic matter and DOM components, reaction rate constants by functional group contribution method, kinetics of photoinduced degradation of DOM, and interactions between photoinduced and microbial degradation in waters. This study also discusses the key factors that may significantly affect the photoinduced and microbial activities in waters. Finally, this study summarizes the various photoproducts of DOM and depicts their importance on biogeochemical cycles in the aquatic environments.

1.1 Biogeochemical Functions of DOM for Photoinduced Processes in Natural Waters

Photoinduced reactions caused by solar radiation can produce various biogeochemical alterations of DOM that can be listed as follows (Mostofa et al. 2011):

(1) Photoinduced generation of free radicals, which are susceptible to induce photoinduced degradation of DOM in aqueous media. The free radicals sources include: (i) Photolysis of NO_2^- and NO_3^- ions inducing production of hydroxyl radical ($HO^\bullet$) in waters (Zafiriou and True 1979a, b; Takeda et al. 2004; Vione et al. 2006; Minero et al. 2007) (ii) Generation of free radical species such as superoxide ion ($O_2^{\bullet -}$), hydrogen peroxide (H_2O_2), organic peroxides (ROOH) and $HO^\bullet$ by photolysis of CDOM or FDOM in waters (Cooper et al. 1988; Moore et al. 1993; O'Sullivan et al. 2005; Mostofa and Sakugawa 2009); (iii) Photoinduced production of $HO^\bullet$ by the photo-Fenton (Zepp et al. 1992; White et al. 2003) as well as the photo-ferrioxalate/H_2O_2 reactions (Safarzadeh-Amiri et al. 1996, 1997; Southworth and Voelker 2003).

(2) Production of new organic substances by photorespiration or assimilation of particulate organic matter (POM: ca. algae or phytoplankton) and high molecular weight DOM. These processes have a deep impact on the carbon cycling and include: (i) Photo-respiration or assimilations of algae that can produce autochthonous fulvic acid and other organic substances as well as nutrients in the aquatic environments (Mostofa et al. 2009b; Thomas and Lara 1995; Fu et al. 2010). (ii) Photoinduced degradation of chlorophyll *a* with production of new organic substances; this process is typically occurring in the photic layer of natural lake and seawater (Rontani 2001; Cuny et al. 2002). (iii) Photoinduced assimilation or degradation of algal biomass in surface waters under natural sunlight, which may produce new DOM or FDOM species in the aquatic environments (Rochelle-Newall and Fisher 2002; Thomas and Lara 1995; Fu et al. 2010; Henrichs and Doyle 1986; Biddanda and Benner 1997; Carrillo et al. 2002; Mostofa KMG et al. unpublished). (iv) Microbial assimilation or degradation of algal biomass or phytoplankton; in vitro experiments have shown that under dark incubation these processes may produce new DOM or FDOM (Rochelle-Newall and Fisher 2002; Yamashita and Tanoue 2008; Fu et al. 2010; Biddanda and Benner 1997; Mostofa KMG et al. unpublished; Yamashita and Tanoue 2004; Stedmon and Markager 2005). (v) Photoinduced transformation of high-molecular weight DOM into low-molecular weight organic substances; in some cases the process can lead to complete mineralization (Moran and Zepp 1997; Dahlén et al. 1996; Ma and Green 2004; Vähätalo and Järvinen 2007; Vione et al. 2009).

(3) Photoinduced degradation can regulate water-quality parameters. In particular: (i) Photoinduced degradation changes the physical, chemical and optical properties of water (Kopacek et al. 2003; Vahatalo et al. 2000; Twardowski and Donaghay 2002; Mostofa et al. 2005; Mostofa et al. 2007a, b; Moran et al. 2000), the structure of DOM (Kramer et al. 1996; Kulovaara 1996; Bertilsson and Allard 1996) as well as its molecular weight (Twardowski and Donaghay 2002; Allard et al. 1994; Kaiser and Sulzberger 2004; Yoshioka et al. 2007); (ii) Photoinduced degradation processes can affect the acidity-alkalinity balance and the consumption of dissolved oxygen at the epilimnion level in both lacustrine and oceanic environments (Kopacek et al. 2003; Amon and Benner 1996; Gao and Zepp 1998); (iii) Photoinduced degradation decreases the absorbance of CDOM (and/or FDOM), which can result in water discoloration (Reche et al. 1999) and increases the water-column transparency. A notable consequence is the increased penetration of photosynthetically active radiation (PAR, 400–700 nm) but also of damaging UV radiation (280–400 nm) in the water column (Laurion et al. 2000). These effects have also an influence on the photoinduced degradation of deep-water DOM (Morris and Hargreaves 1997; Siegel and Michaels 1996); (iv) Photoinduced processes can induce the degradation of organic pollutants or contaminants. A wide variety of photogenerated transients is involved ($HO^{\bullet}$, $CO_3^{\bullet-}$, $^1O_2$, $^3CDOM^*$) (Maddigapu et al. 2011; Minella et al. 2011; Arsene C 2011), but the hydroxyl radical is the reactive species that is less likely to produce secondary toxic pollutants. Therefore, $HO^{\bullet}$-induced processes are most likely to achieve efficient decontamination. The photo-Fenton reaction or photo-ferrioxalate/H_2O_2 reactions are particularly effective to this purpose (Safarzadeh-Amiri et al. 1997; Southworth and Voelker 2003; Brezonik and Fulkerson-Brekken 1998); (v) Photoinduced degradation of DOM can interact with eutrophication by increasing the phosphate concentration upon decomposition of organic phosphorus present in DOM (Reche et al. 1999; Carpenter et al. 1998; Kim and Kim 2006; Li et al. 2008); (vi) Production of CO_2 as well as other dissolved inorganic carbon (DIC) species upon photoinduced degradation of DOM can potentially influence the carbon cycling, and may have an impact on climate change (Salonen and Vähätalo 1994; Graneli et al. 1996, 1998); (vii) The decomposition of DOM affects directly or indirectly the distribution of trace elements in natural waters (Kopacek et al. 2003; Kieber et al. 1989).

(4) Photoinduced degradation of DOM can be beneficial to the water ecosystem and provides energy for microbial loops. Its effects include: (i) Supply of nutrients, which are naturally important for plankton productivity in natural waters (Kim and Kim 2006; Kirchman et al. 1991; Salonen et al. 1992; Wetzel 1992); (ii) Increase in the pool of bioavailable carbon substrates, which are essential foods for microorganisms (Bertilsson and Allard 1996; Lindell et al. 1996; Wetzel et al. 1995; Benner and Biddanda 1998; Bertilsson and Tranvik 1998; Bertilsson et al. 1999); (iii) Photo-production of reactive species by CDOM or FDOM, such as hydrogen peroxide (H_2O_2), organic peroxides (ROOH) and $HO^{\bullet}$. These species can contribute damage to macromolecules such as DNA, proteins and lipids (O'Sullivan et al. 2005; Samuilov et al. 2001; Blokhina et al. 2003; Zhao et al. 2003). (iv) The simultaneous generation of H_2O_2, CO_2 and DIC from DOM

could favor the occurrence of photosynthesis in natural waters, where H_2O_2 instead of H_2O would be involved as reactant in photosynthesis ($xCO_2 + yH_2O_{2(H_2O)} + h\upsilon \rightarrow C_x(H_2O)_y + O_2$ + energy; and $2H_2O_2 + h\upsilon \rightarrow 2H_2O + O_2$) (Mostofa et al. 2009a; Komissarov 1994, 1995, 2003). (v) Production of CO_2 and DIC by photoinduced degradation of DOM and particulate organic matter (POM: ca. algae) can potentially influence carbon cycling and climate change (Ma and Green 2004; Salonen and Vähätalo 1994; Graneli et al. 1998; Clark et al. 2004; Xie et al. 2004; Borges et al. 2008; Kujawinski et al. 2009; Tranvik et al. 2009; Omar et al. 2010; Ballaré et al. 2011; Zepp et al. 2011).

1.2 Biogeochemical Functions of DOM for Microbial Processes in Natural Waters

The major changes in organic materials and DOM by microbial processes can be listed as follows:

(i) Microbial degradation of vascular plant material is the only anaerobic process that, according to physical (temperature, moisture), chemical (redox, nutrient availability) and microbial (microfloral successional patterns, availability of microorganisms) factors can diagenetically produce the humic substances (mostly fulvic and humic acids), proteins, carbohydrates, unidentified organic substances and nutrients in soil or sediment pore water environments (Mostofa et al. 2009a; Conrad 1999; Lovley 2006; Wetzel 1992; Malcolm 1985; Nakane et al. 1997; Uchida et al. 1998, 2000).

(ii) Microbial respiration or assimilation of POM (ca. algae or phytoplankton) can produce autochthonous fulvic acid-like substances (C- and M-like) (see the FDOM chapter for detailed description), various DOM components as well as nutrients at different rates in aquatic environments (Harvey et al. 1995; Mostofa et al. 2009b; Conrad 1999; Lovley 2006; Yamashita and Tanoue 2008; Fu et al. 2010; Weiss et al. 1991; Lehmann et al. 2002; Zhang et al. 2009). The microbial origin of these autochthonous organic substances and nutrients in association with photoinduced production are susceptible to control the organic carbon and nutrients dynamics in natural waters.

(iii) Microbial processes may generally affect the chemical composition of aliphatic carbon (e.g. carbohydrates) in macromolecules such as humic substances (fulvic and humic acids) of vascular plant origin, or autochthonous fulvic acids of algal or phytoplankton origin. Chemical alterations have been observed either experimentally under dark incubation or in sediment pore waters (Mostofa et al. 2007a, b, 2009b; Conrad 1999; Moran et al. 2000; Deshmukh et al. 2002; Li W et al., unpublished data). The changes in pore-water autochthonous fulvic acid of algal origin can be identified by the differences in excitation-emission matrix (EEM) spectra and by an increase with depth of fluorescence intensity in sediment pore waters. Studies observe that the relative increase in fluorescence intensity of peak C (relative to humic-like fluorophores) is 43 % in 20–40 cm and 88 % in 42–60 cm depth samples, compared to the average fluorescence intensity at 1–20 cm (Li W et al., unpublished data). Similarly, microbial processes can degrade the protein-like and tryptophan-like components, which are labile to microbial degradation. Microbial processing of these components can be monitored by a decrease in their fluorescence intensity, experimentally under dark incubation and in field observations in deeper layers of natural waters (Mostofa et al. 2005, 2010, 2011; Baker and Inverarity 2004).

(iv) Methanogenesis caused by microorganisms (methanogens and acetogens) is an important anaerobic process that can produce CH_4 and CO_2 by converting either acetate (and formate) or H_2/CO_2 in anaerobic environments (Conrad 1999; Zinder 1993; Lovley et al. 1996; Kotsyurbenko et al. 2001).

(v) Microbial changes either in organic substances (e.g. glucose) or in the functional groups of macromolecules such as fulvic and humic acids of vascular plant origin, as well as autochthonous fulvic acids of algal or phytoplankton origin, may occur with the release of a variety of byproducts such as CH_4, CO_2, DIC (sum of dissolved $CO_2 + H_2CO_3 + HCO_3^- + CO_3^{2-}$), PO_4^{3-}, NH_4^+, H_2O_2 and organic peroxides in waters (Conrad 1999; Mostofa and Sakugawa 2009; Fu et al. 2010; Ma and Green 2004; Li et al. 2008; Tranvik et al. 2009; Zhang et al. 2009; Li W et al., unpublished data; Lovley et al. 1996; Palenik and Morel 1988; Zhang et al. 2004; Kim et al. 2006).

(vi) The *Nitrospira* genus and *Nitrobacter* species are the key nitrite-oxidizing bacteria (NOB) in nitrifying waste water treatment plants, which are likely to depend mostly on nitrite concentration (Kim and Kim 2006). In addition, extracellular polymeric substances (EPSs), biologically produced by most bacteria, are composed of a mixture of polysaccharides, mucopolysacharides and proteins (Arundhati Pal 2008). EPSs produced by anaerobic sludge under sulfate-reducing conditions are capable of biosorption of heavy metals and can remove them from the waste water treatment plant (Chen et al. 1995; Zhang et al. 2010).

(vii) A new metabolic class of microorganisms demonstrates that a wide diversity of organic compounds can be effectively converted to electricity in self- sustaining microbial fuel cells with long-term stability (Lovley 2006; Chaudhuri and Lovley 2003; Logan and Regan 2006; Cheng and Logan 2007; Li and Fang 2007; Rozendal et al. 2007; Call and Logan 2008; Lee et al. 2008; Lee and Rittmann 2009, 2010; Premier et al. 2012). These organisms, known as electricigens, can completely oxidize organic compounds to carbon dioxide, with direct quantitative electron transfer to electrodes that serve as the sole electron acceptor (Lovley 2006).

2 Theoretical Model for DOM Degradation in Natural Waters

Solar radiation causes the sequential degradation of functional groups in DOM, which can be optically detected either as chromophoric dissolved organic matter (CDOM, Fig. 1a–c) or as fluorescent dissolved organic matter (FDOM, Fig. 1d–f).

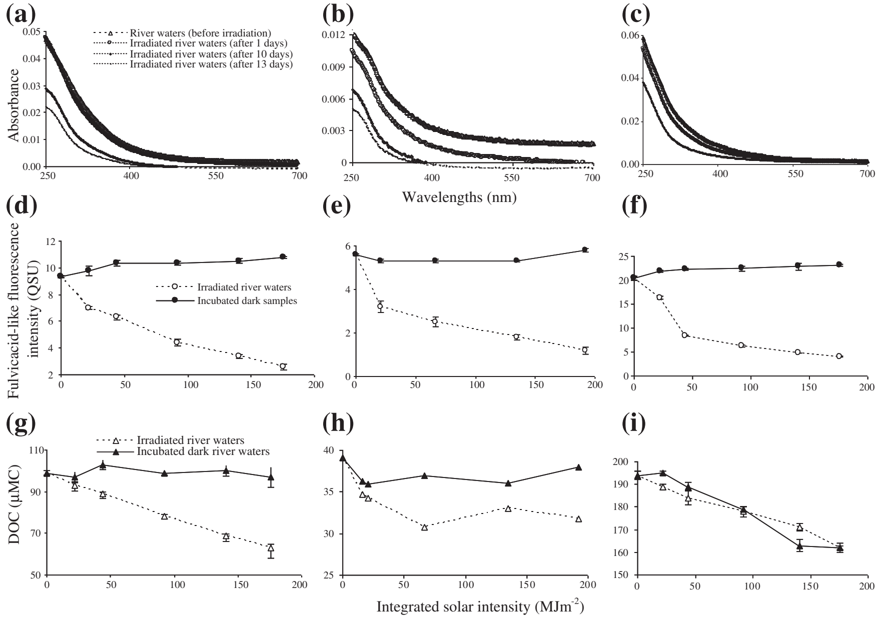

Fig. 1 Photoinduced and/or microbial mineralization of chromophoric dissolved organic matter (CDOM) (**a**, **b**, **c**), fulvic acid-like fluorescence intensity at peak C (**d**, **e**, **f**), and dissolved organic carbon (DOC) concentration (**g**, **h**, **i**) in the upstream waters of Kago and Nishi-Mataya as well as in the downstream waters of Yasu River, respectively. Photoexperiments are conducted under natural sunlight with integrated solar intensity (0, 22, 44, 92, 141, and 176 MJ m^{-2}) during the irradiation period (0, 1, 4, 7, 10, and 13 days, respectively) and microbial experiments are conducted on the filtered samples under dark condition. The quinine sulfate unit (QSU) is estimated using the fluorescence of standard quinine sulfate solution for 1 μg $L^{-1} = 1$ QSU. The error bar indicates the standard deviation between triplicate samples. *Data source* Mostofa et al. (2007); Mostofa KMG et al. (unpublished)

Degradation takes place with simultaneous mineralization of dissolved organic carbon (DOC) (Fig. 1g–i) in natural waters (Fig. 1) (Vione et al. 2009; Vahatalo et al. 2000; Mostofa et al. 2005; Mostofa et al. 2007; Moran et al. 2000; Bertilsson and Allard 1996; Allard et al. 1994; Mostofa et al. 2005; Amador et al. 1989; Vähätalo and Wetzel 2004; del Vecchio and Blough 2002). The functional groups in stream humic substances (fulvic and humic acids), with ^{14}C age = 0 (Malcolm 1990), are highly photosensitive/photoreactive, particularly in rivers (Mostofa et al. 2005, 2007; Wu et al. 2005). Photosensitivity sequentially decreases during water transportation from source (stream water) to rivers and then to lakes or coastal or marine waters on the basis of water residence time (Mostofa et al. 2005a, b, 2007; Malcolm 1990; Kieber et al. 1990; Mopper et al. 1991; Miller and Zepp 1995). The functional groups in DOM (either chromophores in CDOM or fluorophores in FDOM) can efficiently absorb solar radiation in natural waters (Mostofa and Sakugawa 2009; Wu et al. 2005; Zafiriou et al. 1984; Mopper and Zhou 1990;

Cooper et al. 1989; Senesi 1990). This can subsequently lead to the decomposition of those functional groups in DOM, thereby causing either losses of absorbance in the UV and visible wavelength regions(Fig. 1a–c) (Vahatalo et al. 2000; Vähätalo and Wetzel 2004; del Vecchio and Blough 2002; Blough and del Vecchio 2002) or losses in fluorescence intensity of FDOM in natural waters (Fig. 1d–f) (Mostofa et al. 2005a, b, 2007; Moran et al. 2000). It can be noted that photoinduced degradation is generally occurring in the mixing zone and decreases with an increase in water depth in natural waters (Vahatalo et al. 2000; Graneli et al. 1996; Mostofa et al. 2005; Bertilsson and Tranvik 2000). Photoinduced degradation can reduce the mean molecular size of the high molecular weight DOM (Moran and Zepp 1997; Yoshioka et al. 2007; Amador et al. 1989; Amon and Benner 1994), which subsequently produces low molecular weight (LMW) intermediate substances (Moran and Zepp 1997; Dahlén et al. 1996; Bertilsson and Tranvik 1998; Mopper et al. 1991). This process ultimately ends up in mineralization with formation of e.g. COS, CO, CO_2, DIC, ammonium, gaseous hydrocarbons and so on in natural waters (Moran and Zepp 1997; Ma and Green 2004; Gao and Zepp 1998; Graneli et al. 1996, 1998; Clark et al. 2004; Xie et al. 2004; Borges et al. 2008; Kujawinski et al. 2009; Tranvik et al. 2009; Omar et al. 2010; Ballaré et al. 2011; Zepp et al. 2011; Mopper et al. 1991; Miller and Zepp 1995; Bertilsson and Tranvik 2000; Chen et al. 1978; Fujiwara et al. 1995; Bushaw et al. 1996; Miller and Moran 1997; Stiller and Nissenbaum 1999; White et al. 2010; Cai 2011).

The rate of photoinduced mineralization of DOM at the depth z (pm_z, mol C m^{-3} d^{-1}), modified by Vähätalo et al. (2000) from Schwarzenbach 1993) and Miller (1998), can be expressed as follows:

$$pm_z = \int_{\lambda_{\min}}^{\lambda_{\max}} \varphi_\lambda Q_{s,z,\lambda} a_{CDOM,\lambda}\, d\lambda \tag{2.1}$$

where φ_λ is the spectrum of the apparent quantum yield for photoinduced mineralization (mol produced DIC/mol absorbed photons), $Q_{s,z,\lambda}$ is the scalar photon flux density spectrum at a depth z (also referred to as actinic flux, mol photons m^{-2} d^{-1}), and $a_{CDOM,\lambda}$ is the absorption spectrum of CDOM (m^{-1}). CDOM or FDOM is the part of DOM that can absorb solar radiation. The parameters λ_{max} and λ_{min} are the minimum and maximum wavelengths contributing to photoinduced mineralization.

In the whole water column the rate of photoinduced mineralization, modified by Vähätalo et al. (2000) from Miller (1998), can be expressed as follows:

$$pm = \int_{\lambda_{\min}}^{\lambda_{\max}} \varphi\lambda Q a_{,\lambda} (a_{CDOM,\lambda}/a_{tot,\lambda})\, d\lambda \tag{2.2}$$

where $Q_{a,\lambda}$ represents the photons absorbed by the water column (mol photons m^{-2} d^{-1}) and the $a_{CDOM,\lambda}/a_{tot,\lambda}$ ratio expresses how much CDOM contributes to the total absorption. In infinitely deep waters, $Q_{a,\lambda}$ roughly equals the downward vector photon flux density just below the surface $Q_{d,v,0-\lambda}$, (Sikorski and Zika 1993a, b).

The quantum yields related to DOM decrease exponentially with increasing wavelength (Moran and Zepp 1997; Vahatalo et al. 2000; Gao and Zepp 1998; Sikorski and Zika 1993; Ratte et al. 1998). A generalized equation to find an exponential relation between quantum yield and wavelength (Vahatalo et al. 2000) can be expressed below:

$$\varphi_{\lambda} = \mathrm{c} \times 10^{-\mathrm{d}\lambda} \tag{2.3}$$

where c (dimensionless) and d (nm^{-1}) are positive constants and λ is a wavelength (nm). Different combinations of c and d can cover a wide range of exponential relationships between quantum yield and wavelength.

2.1 Photoinduced Degradation of DOM in Natural Waters

Photoinduced degradation can decompose the DOM, estimated as dissolved organic carbon (DOC) concentration, in natural waters. This has been verified in photoexperiments conducted on waters by using direct natural sunlight or artificial UV radiation in laboratory. Photoirradiation of the samples can gradually decrease the DOC concentration as a function of integrated solar intensity ($\mathrm{MJ\ m}^{-2}$) during the irradiation period (Fig. 1g–i). The initial DOC concentration, the changes in DOC changes including relative percentages (%), as well as experimental conditions in photoinduced degradation experiments are summarized in Table 1 (Morris and Hargreaves 1997; Ma and Green 2004; Mostofa et al. 2007; Bertilsson and Allard 1996; Amon and Benner 1996; Mostofa et al. 2005; Vähätalo and Wetzel 2004; Miller and Moran 1997; Mostofa K et al., unpublished; Mostofa and Sakugawa unpublished data; Borisover et al. 2011; Pullin et al. 2004; Shiller et al. 2006; Brooks et al. 2007; Corin et al. 1996; Winter et al. 2007; Skoog et al. 1996). It is shown that DOC concentration photolytically decreases by approximately 21–36 % in stream waters during 12–13 days, 2–54 % in downstream river waters during hours to 10 days, 6–41 % in lake waters during hours to 70 days, 31–36 % in Estuarine waters during 71 days, 3–7 % in seawater during hours to 6 days of irradiation (Table 1). Photoirradiation can decompose 35 % of Nordic Reference humic acid (NoHA) and 24 % of Nordic Reference fulvic acid (NoFA) extracted from humus-rich pond water (Table 1).

It is shown that DOC concentration in rivers photolytically decreases a little, approximately 1–2 % in the surface layer (0 m), during 5.5–15.5 h of sunlight irradiation. The DOC losses decrease in deeper layers (<1 % at 6.5 and 24 m), as has been observed in an in situ photo experiment conducted on rivers submerging at different vertical depths (0, 6.5 and 24 m) in Lake Superior (Table 1) (Ma and Green 2004). In lake waters the DOC mineralization is 22–23 % at the surface layer (0 m), 23–24 % at 6.5 m and 4–9 % at 24 m depth, respectively, during the 5.5–15.5 h irradiation period. The results show that DOM mineralization gradually decreases from surface (0 m) to deeper layers because of declining solar radiation that penetrates into lake water.

Table 1 Photoinduced and microbial changes of dissolved organic carbon (DOC) concentration during photoirradiation experiments conducted on natural waters as reported elsewhere

Type of samples/Locations	Filtration size/type (μm)	Irradiation time (h, or, day)	Solar intensity (MJm^{-2})	DOC Before irradiation	Changes in DOC		Changes in DOC		References
					Photoirradiation	Microbial	Photoirradiation	Microbial	
				(μM C)	(μM C)		%		
Kago upstream (July 2000), Japan (35°N)	0.45	12 (irradiated)	192	119	−29	na	−24	na	Mostofa et al. (2005b)
Kago upstream (July 2000), Japan (35°N)	0.45	12 (dark)	192	119	na	1[a]	na	1[a]	Mostofa et al. (2005b)
Kago upstream (June 2001), Japan (35°N)	0.45	13 (irradiated)	176	99	−36	na	−36	na	Mostofa et al. (2007a)
Kago upstream (June 2001), Japan (35°N)	0.45	13 (dark)	176	99	na	−2	na	−2	Mostofa et al. (2007a)
Nishi-Mataya upstream, Japan (35°N)	0.45	13 (irradiated)	176	38	−12	na	−32	na	Mostofa et al. (2007a)
Nishi-Mataya upstream, Japan (35°N)	0.45	13 (dark)	176	38	na	−3	na	−8	Mostofa K et al. (2007a)
Nishi-Mataya upstream, Japan (35°N)	0.45	12 (irradiated)	192	39	−8	na	−21	na	Mostofa K et al. (unpublished data)
Nishi-Mataya upstream, Japan (35°N)	0.45	12 (dark)	192	39	na	−1	na	−3	Mostofa K et al. (unpublished data)
Yasu River, Japan (35°N)	0.45	13 (irradiated)	176	194	−32	na	−16	na	Mostofa et al. (2007a)
Yasu River, Japan (35°N)	0.45	13 (dark)	176	194	na	−32	na	−16	Mostofa et al. (2007a)
Kurose River (Izumi site), 34°N	0.20	6 (irradiated)	118.5	406	−220	na	−54	na	Mostofa K et al. (unpublished data)

(continued)

Table 1 (continued)

Type of samples/Locations	Filtration size/type (μm)	Irradiation time (h, or, day)	Solar intensity (MJm^{-2})	DOC Before irradiation	Changes in DOC		Changes in DOC		References
					Photoirradiation	Microbial	Photoirradiation	Microbial	
				(μM C)	(μM C)		%		
Kurose River (Izumi site), 34°N	0.45	6 (dark)	118.5	433	na	−235	na	−82	Mostofa K et al. (unpublished data)
Kurose River (Izumi site), 34°N	unfiltered[b]	6 (irradiated)	118.5	406	81[a]	na	20[a]	na	Mostofa K et al. (unpublished data)
Kurose River (Izumi site), 34°N	unfiltered[b]	6 (dark)	118.5	433	na	−367	na	−85	Mostofa K et al. (unpublished data)
Kurose River (Hinotsume site), 34°N	0.20	10 (irradiated)	152.5	412	−90	na	−22	na	Mostofa K et al. (unpublished data)
Kurose River (Hinotsume site), 34°N	0.45	10 (dark)	152.5	412	na	−132	na	−32	Mostofa K et al. (unpublished data)
Kurose River (Hinotsume site), 34°N	unfiltered[b]	10 (irradiated)	152.5	441	−7	na	−2	na	Mostofa K et al. (unpublished data)
Kurose River (Hinotsume site), 34°N	unfiltered[b]	10 (dark)	152.5	441	na	−161	na	−37	Mostofa K et al. (unpublished data)
Kishon River, Israel	filtered (0.20)	10 (dark)	na	792–1100	na	−(167–350)	na	−(22–34)	Borisover et al. (2011)
Parker River, near caostal (USA)		15	nd	703	−27	na	−3.8	na	Pullin et al. (2004)

(continued)

Table 1 (continued)

Type of samples/Locations	Filtration size/type (µm)	Irradiation time (h, or, day)	Solar intensity (MJm^{-2})	DOC Before irradiation	Changes in DOC		Changes in DOC		References
					Photoirradiation	Microbial	Photoirradiation	Microbial	
				(µM C)	(µM C)		%		
Parker River, near caostal (USA) + ·OH		15	nd	703	−29	na	−4	na	Pullin et al. (2004)
Rio Negro water, Amazon River, 3°S	0.20	3 (irradiated)	nd	~835	−98	na	−15	na	Amon and Benner (1996)
Rio Negro water, Amazon River, 3°S	0.20	3 (dark)	nd	nm	nm	nm	nm	1.2–2.7	Amon and Benner (1996)
Rio Negro water, Amazon River, 3°S	0.20	10 h (1 day)	nd	800	−41	na	−5	na	Amon and Benner (1996)
Rio Negro water, Amazon River, 3°S	0.20	4 h	nd	~785	−18	na	−2	na	Amon and Benner (1996)
Pearl River, Mississippi: 30°N	0.22	21 (irradiated)	nd	~565	−113	NMD	−20	NMD	Shiller et al. (2006)
Laramie River, U.S.A (41°N)	0.20	72 h (irradiated)	nd	2681	−597	na	−22	NMD	Brooks et al. (2007)
Chimney Park Wetland, U.S.A (41°N)	0.20	72 h (irradiated)	nd	3610	−666	na	−19	NMD	Brooks et al. (2007)
Sturgeon River waters in Lake Superior (47°N)	0.20	5.5 h (0 m)	nd	2829	−32	na	−1	na	Ma and Green (2004)
Sturgeon River waters in Lake Superior (47°N)	0.20	15.5 (0 m)	nd	2829	−61	na	−2	na	Ma and Green (2004)
Sturgeon River waters in | Lake Superior (47°N)	0.20	5.5 h (6.5 m)	nd	2829	−18	na	−0.6	na	Ma and Green (2004)

(continued)

Table 1 (continued)

Type of samples/Locations	Filtration size/type (μm)	Irradiation time (h, or, day)	Solar intensity (MJm^{-2})	DOC Before irradiation	Changes in DOC		Changes in DOC		References
					Photoirradiation	Microbial	Photoirradiation	Microbial	
				(μM C)	(μM C)		%		
Sturgeon River waters in Lake Superior (47°N)	0.20	15.5 (6.5 m)	nd	2829	−15	na	−0.5	na	Ma and Green (2004)
Sturgeon River waters in Lake Superior (47°N)	0.20	5.5 h (24 m)	nd	2829	−12	na	−0.4	na	Ma and Green (2004)
Sturgeon River waters in Lake Superior (47°N)	0.20	15.5 (24 m)	nd	2829	−25	na	−0.9	na	Ma and Green (2004)
Lakes									
Lake Biwa, 35°N: surface water (2.5 m)	0.10	12 (irradiated)	137	126	−7	na	−6	na	Mostofa KMG et al. (unpublished) (2004)
Lake Biwa, 35°N: surface water (2.5 m)	0.10	12 (dark)	na	126	na	−2	na	−2	Mostofa KMG et al. (unpublished) (2004)
Lake Biwa, 35°N: surface water (70 m)	0.10	12 (irradiated)	137	93	−8	na	−9	na	Mostofa KMG et al. (unpublished) (2004)
Lake Biwa, 35°N: surface water (70 m)	0.10	12 (dark)	na	93	na	−7	na	−8	Mostofa KMG et al. (unpublished) (2004)

(continued)

Table 1 (continued)

Type of samples/Locations	Filtration size/type (µm)	Irradiation time (h, or, day)	Solar intensity (MJm^{-2})	DOC Before irradiation	Changes in DOC		Changes in DOC		References
					Photoirradiation	Microbial	Photoirradiation	Microbial	
				(µM C)	(µM C)		%		
Lake Biwa, 35°N: surface water (2.5 m)	<5 kDa	12 (irradiated)	137	73	−5	na	−11	na	Mostofa KMG et al. (unpublished) (2004)
Lake Biwa, 35°N: surface water (2.5 m)	<5 kDa	12 (dark)	na	73	na	0	na	0	Mostofa KMG et al. (unpublished) (2004)
Lake Biwa, 35°N: surface water (70 m)	<5 kDa	12 (irradiated)	137	63	−10	na	−16	na	Mostofa KMG et al. (unpublished) (2004)
Lake Biwa, 35°N: surface water (70 m)	<5 kDa	12 (dark)	na	63	na	2[a]	na	3[a]	Mostofa KMG et al. (unpublished) (2004)
Lake Lacawac, 41°N: surface water	0.20	7 (irradiated)	nd	400	−80	NMD	−20	NMD	Morris and Hargreaves (1997)

(continued)

Table 1 (continued)

Type of samples/Locations	Filtration size/type (µm)	Irradiation time (h, or, day)	Solar intensity (MJm^{-2})	DOC Before irradiation	Changes in DOC		Changes in DOC		References
					Photoirradiation	Microbial	Photoirradiation	Microbial	
				(µM C)	(µM C)		%		
Lake Waynewood, 41°N: surface water	0.20	7 (irradiated)	nd	440	−75	NMD	−17	NMD	Morris and Hargreaves (1997)
Lake Giles, 41°N: surface water	0.20	7 (irradiated)	nd	91	NPD	NMD	NPD	NMD	Morris and Hargreaves (1997)
Lake Tuscaloosa	0.22	70 (irradiated)	nd	~235	−97	nm	−41	nm	Vähätalo and Wetzel (2004)
Lake Bjän, southern Sweden (58°N)	0.20	75 h (irradiated)	nd	1217	−125	na	−10	na	Bertilsson and Allard (1996)
Lake Bjän, southern Sweden (58°N)	0.20	75 h (irradiated)	nd	1217	−9	na	na	−1	Bertilsson and Allard (1996)
Lake Savojärvi, southwestern Finland	0.45	4 h (irradiated)	nd	1769	−396	na	−22	na	Corin et al. (1996)
Extracted humic acid, Pond water, Norway	0.45	80 h (irradiated)	nd	5500	−1925	−35	−35	na	Corin et al. (1996)
Extracted fulvic acid, Pond water, Norway	0.45	80 h (irradiated)	nd	10417	−2500	−24	−24	na	Corin et al. (1996)
Lake Superior (47°N)	0.20	5.5 h (0 m)	nd	208	−47	na	−22	na	Ma and Green (2004)
Lake Superior (47°N)	0.20	15.5 (0 m)	nd	208	−48	na	−23	na	Ma and Green (2004)

(continued)

Table 1 (continued)

Type of samples/Locations	Filtration size/type (µm)	Irradiation time (h, or, day)	Solar intensity (MJm^{-2})	DOC Before irradiation	Changes in DOC		Changes in DOC		References
					Photoirradiation	Microbial	Photoirradiation	Microbial	
				(µM C)	(µM C)		%		
Lake Superior (47°N)	0.20	5.5 h (6.5 m)	nd	208	−8	na	−23	na	Ma and Green (2004)
Lake Superior (47°N)	0.20	15.5 (6.5 m)	nd	208	−48	na	−24	na	Ma and Green (2004)
Lake Superior (47°N)	0.20	5.5 h (24 m)	nd	208	−51	na	−4	na	Ma and Green (2004)
Lake Superior (47°N)	0.20	15.5 (24 m)	nd	208	−19	na	−9	na	Ma and Green (2004)
Lake Erie (42°N)	0.10	Surface water	nd	583, 625	525, 575	583, 667	(10–8)	0, (+)7	Winter et al. (2007)
Luther Marsh northeast (43°N)	0.10	Surface water	nd	817, 958	533, 792	817, 950	(35–17)	0, −1	Winter et al. (2007)
Mill Creek east of Cambridge (43°N)	0.10	Surface water	nd	825, 875	683, 583	833, 883	(17–30)	(+)1	Winter et al. (2007)
Bannister Lake southwest of Cambridge (43°N)	0.10	Surface water	nd	775, 867	617, 642	758, 867	(20–22)	(+)1, −2	Winter et al. (2007)
Sanctuary Pond (41°N)	0.10	Surface water	nd	917, 992	650, 750	892, 1008	(20–24)	(+)2, −3	Winter et al. (2007)
Aldrich humic acid in deionized water	0.10	Surface water	nd	908, 842	675, 600	808, 817	(26–29)	−(11–3)	Winter et al. (2007)
Seawaters									
Satilla Estuary	0.20	70 (irradiated)	nd	2046	−628	na	−31	na	Moran et al. (2000)
Satilla Estuary	0.20	70 (irradiated)	nd	1972	−706	na	−36	na	Moran et al. (2000)

(continued)

Table 1 (continued)

Type of samples/Locations	Filtration size/type (µm)	Irradiation time (h, or, day)	Solar intensity (MJm^{-2})	DOC Before irradiation	Changes in DOC		Changes in DOC		References
					Photoirradiation	Microbial	Photoirradiation	Microbial	
				(µM C)	(µM C)		%		
Satilla Estuary, control (nonincubated)	0.20	51 (dark incubated)	nd	1886–1946	na	(170–215)	na	(8–11)	Moran et al. (2000)
Satilla Estuary, control (incubated)	0.20	51 (dark incubated)	nd	1881–2004	na	(171–209)	na	(9–10)	Moran et al. (2000)
Satilla Estuary, 12–16 % photobleached	0.20	51 (dark incubated)	nd	1728–1874	na	(227–261)	na	(13–14)	Moran et al. (2000)
Satilla Estuary, 21–25 % photobleached	0.20	51 (dark incubated)	nd	1563–1739	na	(177–261)	na	(11–15)	Moran et al. (2000)
Satilla Estuary, 32–44 % photobleached	0.20	51 (dark incubated)	nd	1498–1548	na	(170–292)	na	(11–19)	Moran et al. (2000)
Satilla Estuary, 59–64 % photobleached	0.20	51 (dark incubated)	nd	1249–1386	na	(194–322)	na	(16–23)	Moran et al. (2000)
Seawater + humic substances (SH)	0.20	16 h (Artificial sunlight)	nd	695	−22	na	−3	na	Miller and Moran (1997)
Seawater + the control addition (SC)	0.20	16 h (Artificial sunlight)	nd	515	−21	na	−4	na	Miller and Moran (1997)
Artificial seawater + the control addition (AC)	0.20	16 h (Artificial sunlight)	nd	241	−7	na	−3	na	Miller and Moran (1997)
Seawater + humic substances (SH)	0.20	14 (Dark incubation)	nd	695	na	−67	na	−10	Miller and Moran (1997)

(continued)

Table 1 (continued)

Type of samples/Locations	Filtration size/type (μm)	Irradiation time (h, or, day)	Solar intensity (MJm^{-2})	DOC Before irradiation	Changes in DOC		Changes in DOC		References
					Photoirradiation	Microbial	Photoirradiation	Microbial	
				(μM C)	(μM C)		%		
Seawater + the control addition (SC)	0.20	14 (Dark incubation)	nd	515	na	−39	na	−8	Miller and Moran (1997)
Artificial seawater + the control addition (AC)	0.20	14 (Dark incubation)	nd	241	na	−13	na	−5	Miller and Moran (1997)
Baltic Sea, BY15, Gotland Deep (57°N)	0.20 (unfiltered)	6	nd	328	−10	nd	−3	nd	Skoog et al. (1996)
Baltic Sea, BY32, Norrköping Deep (58°N)	0.20 (unfiltered)	6	nd	347	−10	nd	−3	nd	Skoog et al. (1996)
Baltic Sea, F15, Sydostbrotten (63°N)	0.20 (unfiltered)	4	nd	331	−23	nd	−7	nd	Skoog et al. (1996)

[a] means an increase in DOC concentration occurred during incubation period

[b] means incubated unfiltered sample filtered before analytical measurements using Ekicrodisc 25 mm syringe filter with 0.45 mm HT-Tuffryn Membrane (PALL, Gelman Laboratory)

(-) means losses in DOC concentration,*na* not applicable; *nm* not exactly mentioned

NPD nosignificant photochemical degradation; *NMD* no significant microbial degradation

From the results of photoinduced degradation of DOM (Table 1), several key phenomena highlighted the DOM photoinduced degradation in natural waters: First, photoinduced degradation is greatly dependent on the initial concentration of DOC: high photo mineralization is observed in waters with low DOC concentration, while mineralization greatly decreases with increasing DOC concentration. Second, photo mineralization of DOM is typically high in source waters (stream waters) and then decreases in downstream rivers or lakes or seawater. Third, photoinduced degradation is a relatively rapid process for mineralization of DOM compared to microbial degradation in natural waters, except for rivers that contain sewage effluents. It is demonstrated that the photoinduced mineralization of DOM is relatively high during the first day of irradiation in experimental observations, and then almost gradually decreases during the irradiation period (Table 1).

The results of photoinduced degradation on molecular size fractions of DOM demonstrate that photo mineralization is approximately 6 % for large molecular fractions (<0.10 μm) in surface lake waters compared to 9 % in deep waters during 12 days irradiation (Table 1). The results also show that photo mineralization of molecular fractions <5 kDa is relatively higher in deeper waters (16 %) than in surface layers (11 %), and it is higher compared to the 0.1 μm fractions of DOM (Table 1). These results can highlight four important features about the photoinduced degradation of DOM. First, molecular fractions <0.1 μm in surface waters composed of approximately 35 % of autochthonously produced DOC during the summer stratification period may not be photolytically susceptible to mineralization (Mostofa et al. 2009a). Second, molecular fraction of <5 kDa are highly susceptible to photoinduced degradation. Third, DOM in deeper layers is highly susceptible to photo mineralization. It can be noted that the DOC in Lake Biwa is autochthounously produced (45 %) during the summer stratification period, as estimated from higher DOC in summer (135 μM C in August) than in winter (~93 μM C in January) samples during the vertical mixing period (Mostofa et al. 2005). The low photodegradative nature of surface DOM appears to be caused by autochthonous production (~45 % in Lake Biwa), thus autochthonous DOM might be resistant to photoinduced mineralization. This result is in agreement with earlier studies where phytoplankton-exudate DOM, which is the major DOM source from bacterial production (Azam and Cho 1987), is resistant to photoinduced degradation by natural sunlight (Thomas and Lara 1995).

The highly photo-reactive nature of DOM in deeper waters than in the surface layer appears to be caused by two phenomena. First, major fractions of DOM in deeper waters belong to low molecular weight substances (Yoshioka et al. 2007), which may be photolytically mineralized. Second, microbial assimilation or respiration of particulate organic matter (POM: ca. algae) can produce the autchthonous DOM, which are highly photosensitive and photodegradable (Mostofa K et al., unpublished; Zhang et al. 2009; Johannessen et al. 2007; Zhang et al. 2009). The experimental study suggests that the algal-derived DOM is photolytically decomposed by natural sunlight, which is a more efficient photoinduced substrate than is the allochthonous DOM (Mostofa K et al., unpublished; Johannessen et al. 2007; Hulatt et al. 2009). The autochthonous organic substances in deeper layers are typically distinguished by a red shift of the fluorescence peak compared to the upper surface layer (Yoshioka et al. 2007; Mostofa et al. 2005; Hayase and Shinozuka 1995). These autochthonous substances are also identical to the organic substances produced experimentally upon photoinduced and microbial assimilations of algae (Mostofa et al. 2009b; Fu et al. 2010). This hypothesis is supported by the features of autochthonous fulvic acid extracted from POM in sea waters or sediment pore waters, which typically show the fluorescence peak at longer wavelength regions (see also chapter "Fluorescent Dissolved Organic Matter in Natural Waters") (Li W et al., unpublished data; Komada et al. 2002; Burdige et al. 2004; Managaki and Takada 2005; Calace et al. 2006; Parlanti et al. 2000). Another possible explanation is that photolabile DOM in the surface water layers is probably quickly mineralized by sunlight, which leaves only the more photolytically refractory substances near the surface, while photolabile DOM in the deeper layers is more protected from mineralization by the lower sunlight intensity. Interestingly, groundwater DOM has been found to be significantly more susceptible to photo mineralization than surface lake water DOM (Vione et al. 2009).

2.2 Microbial Degradation of DOM in Natural Waters

Microbial actions can decompose the DOM, estimated as dissolved organic carbon (DOC) concentration, in natural waters. This has been verified in experiments conducted on waters under dark conditions. Microbial activity can decrease DOC concentrations either slowly or rapidly depending on the DOM sources during the incubation period (Fig. 1g–i). The initial DOC concentration, amount of DOC changes and its percentage (%), as well as other experimental conditions in microbial degradation experiments are presented in Table 1. It is demonstrated that the decrease of DOC concentration because of microbial activity for various natural waters is approximately 0–8 % in stream waters during 12–13 days, 1–85 % in downstream river waters during hours to 10 days, 0–8 % in lake waters during hours to 70 days, 8–23 % in estuarine waters during 51 days, 5–10 % in seawaters during 14 days of incubation period under dark conditions (Table 1) (Mostofa et al. 2007; Moran et al. 2000; Bertilsson and Allard 1996; Mostofa et al. 2005; Miller and Moran 1997; Mostofa and Sakugawa unpublished data ; Borisover et al. 2011; Winter et al. 2007). From the results of microbial degradation (Table 1) it is possible to generalize several key features commonly observed in natural waters: First, downstream DOM, particularly in sewerage-impacted rivers is significantly labile to microbial degradation. Second, upstream DOM is typically recalcitrant to microbial degradation (Fig. 1g). Third, microbial degradation is typically a slow process for the mineralization of DOM in natural waters, except for downstream rivers with sewage effluents. For example, DOC mineralization rapidly occurs in unfiltered and filtered dark samples (32–85 %) of downstream rivers where DOM is mostly fluxed from untreated sewerage effluents near urban areas (Table 1; Fig. 1i) (Mostofa et al. 2007; Mostofa and Sakugawa unpublished data).

The results of microbial degradation on molecular size fractions of DOM demonstrate that DOC mineralization is approximately 2 % for large molecular fractions (<0.10 μm) in surface layers and 8 % in deeper layers (Table 1). However, DOM with molecular fractions of <5 kDa is not altered at all under dark incubation (Table 1). These results can suggest four important features about microbial degradation of DOM in natural waters. First, molecular fractions of <0.1 μm in both lake surface and deeper waters are labile to microbial degradation, but deeper waters are much labile than surface waters. It is also suggested that autochthonous DOM in surface waters, typically produced during the summer stratification period, is less susceptible to microbial processes. It can be noted that the DOC concentration in Lake Biwa waters is autochthounously produced (45 %) during the summer stratification period, as estimated from the summer DOC values (135 μM C in August) that are higher than the winter ones (~93 μM C in January) during vertical mixing (Mostofa et al. 2005). Second, DOM with molecular weight <5 kDa in both surface and deeper layers is not susceptible to microbial degradation.

2.3 *Mechanisms of the Photoinduced Degradation of DOM in Natural Waters*

The $HO^{\bullet}$ radical plays a significant role in photoinduced degradation of DOM in natural waters (Zepp et al. 1992; Southworth and Voelker 2003; Zafiriou et al. 1984; Zika 1981; Voelker et al. 1997). Photoinduced degradation of DOM generally occurs upon direct absorption of UV and visible sunlight by functional groups in DOM, which are optically detected either as chromophores in CDOM or fluorophores in FDOM. Evidence has been provided that an electron transfer from functional groups on DOM can lead to the photoinduced formation of H_2O_2 in aqueous solution (Eqs. 3.13–3.18, see also chapter "Dissolved Organic Matter in Natural Waters") (Mostofa and Sakugawa 2009; Senesi 1990). H_2O_2 subsequently leads to the generation of $HO^{\bullet}$, by direct photochemistry or by Fenton/photo-Fenton/photo-ferrioxalate reaction systems. These processes can be involved into the photo transformation of DOM in natural waters. Therefore, a general mechanistic scheme for photoinduced degradation of DOM can be depicted as follows (Eqs. 2.1–2.4):

$$\mathrm{DOM} + \mathrm{O_2} + \mathrm{H_2O} + \mathrm{H^+} \overset{h\upsilon}{\rightarrow} \mathrm{H_2O_2} + \mathrm{DOM^{\bullet +}} + \mathrm{O_2} + \mathrm{OH^-} \tag{2.1}$$

$$\mathrm{H_2O_2} \overset{h\upsilon}{\rightarrow} 2\mathrm{HO^{\bullet}} \tag{2.2}$$

$$\mathrm{DOM^{\bullet +}} + \mathrm{HO^{\bullet}} \overset{h\upsilon}{\rightarrow} \left[\mathrm{DOM^{\bullet +}HO^{\bullet}}\right]^* \tag{2.3}$$

$$\left[\mathrm{DOM^{\bullet +}HO^{\bullet}}\right]^* \overset{h\upsilon}{\rightarrow} \mathrm{LMWDOM} + \mathrm{DIC} + \mathrm{CO_2} + \text{other byproducts} \tag{2.4}$$

First, H_2O_2 is formed photolytically through production of $O_2^{\bullet -}$ ion by the release of electrons from DOM chromophores or fluorophores, due to solar effects (Eq. 2.1) that have been discussed earlier in chapter "Photoinduced and Microbial Generation of Hydrogen Peroxide and Organic Peroxides in Natural Waters". Subsequent irradiation converts H_2O_2 into $HO^{\bullet}$ either photolytically (Eq. 2.2), or via Fenton and photo-Fenton reactions and the other processes that have been mentioned earlier in chapter "Photoinduced Generation of Hydroxyl Radical in Natural Waters". The generated $HO^{\bullet}$ can rapidly react with the $DOM^{\bullet+}$, initially formed during H_2O_2 production (Eq. 2.1), to form a complex $(DOM^{\bullet+}\ HO^{\bullet})^{*}$ (Eq. 2.3) that is subsequently transformed into low molecular weight DOM (LMWDOM), dissolved inorganic carbon (DIC), CO_2, and other byproducts (Eq. 2.4). It is noted that the sequential photoinduced degradation of functional groups in DOM will be elucidated in the next section.

The described mechanism might be applicable in merely DOM-rich natural waters. However, in iron-rich waters the degradation of DOM might be caused by the $HO^{\bullet}$ radicals mostly generated from Fenton reaction (Fenton 1894; Kang et al. 2000), photo-Fenton reaction (Zepp et al. 1992; Southworth and Voelker 2003; Voelker et al. 1997) and photo-ferrioxalate/H_2O_2 reaction (Safarzadeh-Amiri et al. 1997; Safarzadeh-Amiri et al. 1996; Jeong and Yoon 2005) depending on the concentrations of iron as well as oxalate ions in waters. The mechanisms for $HO^{\bullet}$ production from Fenton, photo-Fenton and photo-ferrioxalate/H_2O_2 reaction have been discussed earlier in chapter "Photoinduced Generation of Hydroxyl Radical in Natural Waters". Another most important pathway of $HO^{\bullet}$ production is the photolysis of NO_2^- and NO_3^-, thereby causing the indirect photodegradation of DOM by NO_2^- and NO_3^- in waters (Zafiriou and True 1979a, b; Takeda et al. 2004; Minella et al. 2011; Arakaki et al. 1999; Mack and Bolton 1999).

Therefore, the photoinduced transformation of DOM may undergo by two major pathways depending on the production of free radicals ($^{\bullet}OR$, R=H or alkyl group) in aqueous solution. First, direct photoinduced reactions of DOM, which take place by $HO^{\bullet}$ or other reactive species that may be photolytically generated from DOM components in natural waters. Second, indirect photoinduced reactions of DOM, which typically occur photolytically by $HO^{\bullet}$ that may be generated from Fenton reaction, photo-Fenton reaction, photo-ferrioxalate/H_2O_2 reaction, as well as NO_2^- and/or NO_3^- photolysis in natural waters. If the direct photoinduced processes dominate, the rates of photoinduced degradation as well as of product formation will be proportional to the amount of light absorbed by DOM components such as FDOM or CDOM (Cooper et al. 1989; Blough and Zepp 1995; Goldstone et al. 2002). The indirect photoinduced processes induce the homogeneous production of $HO^{\bullet}$, which subsequently leads to non-selective photoinduced degradation of all organic moieties in DOM in natural waters (Haag and Hoigné 1985; Zepp et al. 1987; Zhou and Mopper 1990; Nakatani et al. 2004). These results can suggest two important facts that occur in photoinduced reactions: (a) Photobleaching can typically proceed with photoproduction of LMW organic substances via direct mechanisms, especially in waters having high FDOM or CDOM content such as in river, lake and coastal waters, and (b) Photoinduced generation of LMW organic substances can typically proceed via indirect mechanisms. The photoinduced generation rate of $HO^{\bullet}$ in lake water by CDOM/FDOM and other sources was too low to account for the photoinduced mineralization of DOM. The latter process appears to be favoured in Fe-rich waters, and possibly involves the photochemistry of Fe(III)-DOC complexes (Vione et al. 2009).

2.4 Mechanisms for Photoinduced Degradation of DOM Functional Groups by HO$^{\bullet}$

It has been shown that the photoinduced generation of HO$^{\bullet}$ from DOM occurs primarily through H_2O_2 that is produced via photoionization of the most electron-rich organic compounds. The process yields DOM$^{\bullet+}$, which initiates several other reactions (Eqs. 2.1, 2.2). The HO$^{\bullet}$ radical can subsequently react with DOM$^{\bullet+}$ and initiate complex chain reactions (Eq. 2.3). The sequential reactions with HO$^{\bullet}$ yields various end products such as LMWDOM, CO_2, DIC and CO (Eq. 2.4).

The group contribution method (GCM) by Minakata and his co-workers (Minakata et al. 2009) allows the prediction of the aqueous phase HO$^{\bullet}$ rate constants for various functional groups of a given organic compound. It may pave the way to understand the mechanism for the degradation of organic compounds in Advanced Oxidation Processes (AOPs) such as O_3/H_2O_2, UV/H_2O_2 and UV/TiO_2, as well as in natural water photochemistry (Mostofa et al. 2007, 2011; Moran et al. 2000; Minakata et al. 2009; Huber et al. 2003; Rosenfeldt and Linden 2004; Westerhoff et al. 2005; Minakata et al. 2011). The rate constants are discussed in the following section. Photodecarboxylation ($RCOOH + 1/2O_2 + h\upsilon \rightarrow ROH + CO_2$) is one of the important reactions for generating CO_2 by degradation of LMWDOM such as RCOOH in aqueous media (Xie et al. 2004). Another possible pathway could involve phosgene, which is generated photolytically from photosensitive chloroform ($CHCl_3 + O_2 + h\upsilon \rightarrow COCl_2 + HCl$) (Shriner and Cox 1943). The phosgene ($COCl_2$) is highly photosensitive and highly reactive, and it could degrade fluorophores such as the amino groups ($RNH_2 + COCl_2 \rightarrow RN{=}CO + 2\ HCl$) or carboxylic functional groups ($RCO_2H + COCl_2 \rightarrow RC(O)Cl + HCl + CO_2$) (Mostofa et al. 2011; Shriner and Cox 1943). It is noted that macromolecules such as stream fulvic acid and humic acid of vascular plant origin are composed of various functional groups such as –COOH, methoxyl, alcoholic OH, phenolic OH, carbohydrate OH, –C=C–, C=O, aromatic carbon (17–30 %), aliphatic carbon (47–63 %) as well as N, S, and P-atom-containing functional groups (Malcolm 1985; Steelink 2002). Marine DOM of biological origin is composed of amino group in its molecular structure (Midorikawa and Tanoue 1998, 1996). The photoinduced reactions of natural organic matter can lead to the sequential degradation of various functional groups (Mostofa et al. 2011; Xie et al. 2004; Minakata et al. 2009, 2011; Shriner and Cox 1943; Li and Crittenden 2009), of organic molecules bound to fulvic and humic acids (Allard et al. 1994; Amador et al. 1989), and to the sequential decrease in fluorescence intensity of fulvic acid-like substances (peak C and A) with irradiation time (Mostofa et al. 2007, 2011; Moran et al. 2000). The general reaction mechanisms that HO radicals induce are a parent compound → aldehydes and ketones → carboxylic compounds → carbon dioxide and minerals (Bolton and Carter 1994). This reaction mechanism is mostly applicable to fulvic acid and humic acid of plant origin, autochthonous fulvic acid of algal origin, proteins and aromatic amino acids, and of all the compounds that can initiate the reaction through self-generation of HO$^{\bullet}$ via H_2O_2 photo production.

2.4.1 Reaction rate Constants by Functional Group Contribution Method

Recently, it has been possible to determine the aqueous phase HO$^\bullet$ reaction rate constants by the functional GCM, which can be applied to the photoinduced degradation of a given organic compound in aqueous media (Minakata et al. 2009). The GCM is based on Benson's thermochemical group additivity (Benson 1976). Under the principle of group additivity, it is hypothesized that an observed experimental rate constant for a given organic compound is the combined rate of all elementary reactions involving HO$^\bullet$, which can be estimated using Arrhenius activation energy E_a and frequency factor A. Each reaction mechanism defines a base activation energy, $E_a{}^o$, and a functional group contribution of activation energy, $E_a{}^{Ri}$. The latter results from the neighboring (i.e., α-position) and/or the next-nearest neighboring (i.e., β-position) functional group (i.e., Ri). The GCM considers four reaction mechanisms that can be initiated by HO$^\bullet$ in the aqueous phase, which include (1) H-atom abstraction, (2) HO$^\bullet$ addition to C C doble bond(s) on alkenes, (3) HO$^\bullet$ addition to C=C doble bond(s) on aromatic compounds, and (4) HO$^\bullet$ interaction with sulfur (S)-, nitrogen (N)-, or phosphorus (P)-atom-containing compounds (Minakata et al. 2009). Accordingly, an overall reaction rate constant, k_{overall}, can be given by Eq. 2.5

$$k_{\text{overall}} = k_{\text{abs}} + k_{\text{add}-\text{alkene}} + k_{\text{add}-\text{aromatic}} + k_{\text{i}} \tag{2.5}$$

where, k_{abs}, $k_{\text{add-alkene}}$, $k_{\text{add-aromatic}}$, and k_{int} are the rate constants for the aforementioned reaction mechanisms (1)–(4), respectively.

Rate constant for hydrogen-atom abstraction (Minakata et al. 2009): For H-atom abstraction, the active bond is a C–H bond. In general, molecules are categorized based on the number of C–H bond(s) (i.e., CH_3R_1, $CH_2R_1R_2$, and $CHR_1R_2R_3$, where R_i is a functional group ($i = 1-3$)). Each of the fragments corresponds to a partial rate constant $k_{CH_3R_1}$, $k_{CH_2R_1R_2}$, and $k_{CHR_1R_2R_3}$, respectively. The C–H bond itself and adjacent functional group(s) contributes to the overall E_a as the base activation energy, $E_a{}^0$, and group contribution parameter, $E_{a,\text{abs}}$ Ri, due on the functional group R_i, respectively. For example, the base activation energy for H-atom abstraction from one of the primary C–H bonds is $E_{a,\text{prim}}0$. The $E_{a,\text{abs}}$ Ri indicates the electron-donating and—withdrawing ability of the functional group. An electron-donating functional group decreases the E_a and, hence, increases the overall reaction rate constant, and vice versa. Accordingly, the partial rate constant for the fragmented parts such as CH_3R_1, $CH_2R_1R_2$ and $CHR_1R_2R_3$ can be written as below (Eqs. 2.6–2.8)

$$k_{CH_3R_1} = 3A_{\text{prim}}e^{-\frac{E^0_{a,\text{prim}}+E^{R_1}_{a,\text{abs}}}{RT}} \tag{2.6}$$

$$k_{CH_2}R_1R_2 = 2A_{\text{sec}}e^{-\frac{E^0_{a,\text{sec}}+E^{R_1}_{a,\text{abs}}+E^{R_2}_{a,\text{abs}}}{\text{RT}}} \tag{2.7}$$

$$k_{CHR_1R_2R_3} = A_{\text{tert}}e^{-\frac{E^0_{a,\text{tert}}+E^{R_1}_{a,abs}+E^{R_2}_{a,abs}+E^{R_3}_{a,abs}}{RT}} \tag{2.8}$$

where 3 is the amount of primary C–H bonds, A_{prim} denotes the Arrhenius frequency factor for the reaction of HO• with CH_3R_1, R is the universal gas constant, and T denotes absolute temperature. However, for (Eqs. 2.6–2.8), the functional group contribution is ignored for cases where the neighboring functional groups have no effect on the H-atom abstraction (i.e.,$E^{\text{-H}}_{a,\text{abs}}$is zero, where a valence bond of the H-atom is expressed as a line before H).

In (Eqs. 2.6–2.8), the group rate constants, which represent H-atom abstraction from the primary, secondary and tertiary C–H bond are defined as $k^0{}_{\text{prim}}$, $k^0{}_{\text{sec}}$, and $k^0{}_{\text{tert}}$, respectively. They are expressed in (Eqs. 2.9–2.11).

$$k^0_{\text{prim}} = A^0_{\text{prim}} e^{-E^0_{a,\text{prim}} \big/ RT} \tag{2.9}$$

$$k^0_{\text{sec}} = A^0_{\text{sec}} e^{-E^0_{a,\text{sec}} / RT} \tag{2.10}$$

$$k^0_{\text{tert}} = A^0_{\text{tert}} e^{-E^0_{a,\text{tert}} / RT} \tag{2.11}$$

In addition, the group rate constant k_{R4} is defined for the $\text{HO}^\bullet$ interaction with the functional group R_4 (e.g. –OH and –COOH). The group contribution factor, $X_{\text{R}i}$, that represents the influence of functional group R_i can be denoted as (Eq. 2.12)

$$X_{R_i} = e^{-E^{Ri}_{a,abs} \big/ RT} \tag{2.12}$$

The rate constant for H-atom abstraction, k_{abs}, can be written as the sum of the partial rate constants in (Eq. 2.13) because each reaction is independent from one another

$$k_{abs} = 3\sum_{0}^{I} k^0_{\text{prim}} X_{\text{R}_1} + 2\sum_{0}^{J} k^0_{\text{sec}} X_{\text{R}_1} X_{\text{R}_2} + \sum_{0}^{k} k^0_{\text{tert}} X_{\text{R}_1} X_{\text{R}_2} X_{\text{R}_3} + k_{\text{R}_4} \tag{2.13}$$

where, I, J, and K denote the number of the fragments CH_3R_1, CH_2R_2, and $\text{CHR}_1\text{R}_2\text{R}_3$, respectively.

As a typical example the rate constant calculation for 1,2-dichloro-3-bromopropane ($\text{CH}_2\text{Cl–CHCl–CH}_2\text{Br}$) can be written as below (Eq. 2.14)

$$k_{\text{overall}} = 2k^{\text{o}}_{\text{sec}} X_{-\text{Cl}} X_{-\text{CHCl}} + k^{\text{o}}_{\text{tert}} X_{-\text{Cl}} X_{-\text{CH}^2\text{Cl}} X_{-\text{CH}^2\text{Br}} + 2k^{\text{o}}_{\text{sec}} X_{-\text{Br}} X_{-\text{CHCl}-} \tag{2.14}$$

It is shown that group rate constants of $k^{\text{o}}{}_{\text{prim}}$, $k^{\text{o}}{}_{\text{sec}}$, and $k^{\text{o}}{}_{\text{tert}}$ are 1.18×10^8, 5.11×10^8, and $1.99 \times 10^9\ \text{M}^{-1}\ \text{s}^{-1}$, respectively and follow the order $k^{\text{o}}{}_{\text{tert}} > k^{\text{o}}{}_{\text{sec}} > k^{\text{o}}{}_{\text{prim}}$ that is consistent with the radical stability of primary, secondary, and tertiary carbon-centered radicals due to the hyperconjugation. The term k_{R4} is accounted for by the group rate constants $k_{-\text{OH}}$ and $k_{-\text{COOH}}$, respectively (Eq. 2.13). The $k_{-\text{OH}}$ is $1.00 \times 10^8\ \text{M}^{-1}\ \text{s}^{-1}$, representing 33, 8.5, and <5 % of the

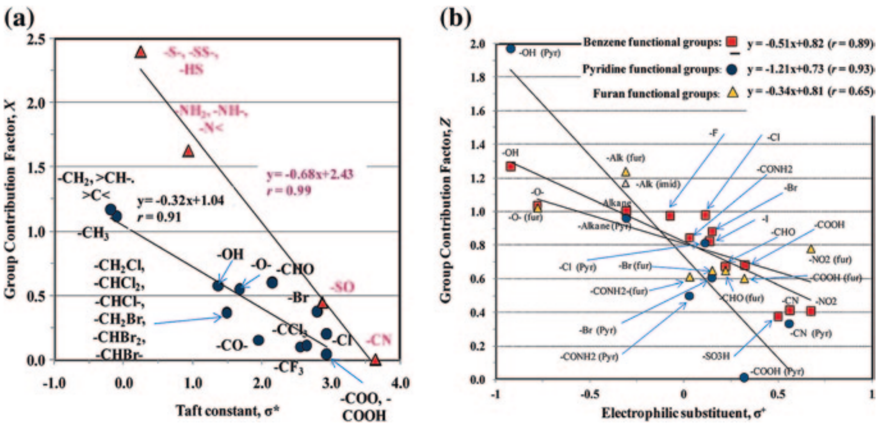

Fig. 2 Comparison of the group contribution factors for H-atom abstraction with the Taft constant, σ^* (a; Karelson 2000) and those for $HO^{\bullet}$ addition to aromatic compounds with electrophilic substituent parameter, σ^+ (Fig. b; Karelson 2000. Group contribution factors include ● alkyl, oxygenated, and halogenated functional groups and ▲ S–, N–, or P-atom-containing functional groups (Fig. a). Group contribution factors for benzene (■), pyridine (●), and furan (▲) compounds (Fig. b). The σ^* of [–$CHCl_2$], [–CO], [–COO, COOH], [–S–, –SS–, HS–], [–NH_2, –NH–, –N <] is an average of [CH_2Cl, CH_2Br, $CHCl_2$, $CHBr_2$], [$COCH_3$, COC_2H_5, $COC(CH_3)_3$, COC_6H_5, COF, COCl], [COOH, $COOC_2H_5$], [SCH_3, SC_2H_5, $SCH(CH_3)_2$], and [$NHCH_3$, $NH(CH_2)_3CH_3$, $N(C_2H_5)_2$], respectively. The σ^* of [–SO] and [–N–CO-] refer to [$S(O)CH_3$] and [$NHCOC_6H_5$], respectively. *Data source* Minakata et al. (2009)

H-atom abstraction from the O–H bond in methanol, ethanol, and other alcohol compounds, respectively, which is comparable with the experimental observations (Asmus et al. 1973). The $k_{\text{–COOH}}$ is 7.0×10^5 M^{-1} s^{-1}, which is consistent with experimental data for oxalic acid (Getoff et al. 1971).

It is demonstrated that the group contribution factors for the H-atom abstraction linearly correlate with the Taft constant, σ^* (Karelson 2000) (Fig. 2). The alkyl functional groups may often weaken the C–H bond with release of the steric compression. The alkyl functional group moves apart to form a planar radical, thereby increasing the $HO^{\bullet}$ reactivity in the H-atom abstraction reactions. Therefore, $X_{\text{–CH3}}$ and $X_{\text{–CH2–}} \approx X_{\text{>CH–}} \approx X_{\text{>C<}}$ values are greater than 1.0, which correspond to negative values of the Taft constant (Fig. 2). In contrast, low values of the group contribution factors for any functional groups indicate their electron-withdrawing ability ($\sigma^* > 0$).

Rate constant for $HO^{\bullet}$ addition to alkenes (Minakata et al. 2009): The detailed mechanisms of $HO^{\bullet}$ addition to alkenes in the aqueous phase are not well documented in earlier studies (Getoff 1991; Billamboz et al. 2010). It is generally considered that π-electrons in alkene compounds (>C=C<) absorb radiation to form an excited state, which then releases electron (e^-) to form H_2O_2 and $>C=C^+<$ (Eq. 2.1; chapter "Photoinduced and Microbial Generation of Hydrogen Peroxide and Organic Peroxides in Natural Waters", Eqs. 2.13–2.18). The $HO^{\bullet}$ then reacts with C^+ to form the reaction intermediates. The excitation of the π-electrons in >C=C< depends on the other functional groups bonded to the alkene.

Except ethylene, alkenes are categorized into six basic structures on the basis of the number of H atoms and their positions, including *cis* and *trans* conformations (i.e., >C=C< , H>C=C< , H_2C=C<, H>C=C<H (*cis*), H>C=C<H (*trans*), and H_2C=C<H). If the base structure is symmetrically associated with the number and position of hydrogen atom(s), the probability of $HO^\bullet$ addition to two unsaturated carbons is considered to be identical, whereas it is different for the asymmetrical base structure. This may reflect the differences in the A resulting from regioselectivity. Accordingly, the group rate constant, $k^{o}_{(\text{structure})\text{-}h}$, and group contribution factor, Y_{Rl}, for $HO^\bullet$ addition to one of the base structures can be written using Arrhenius frequency factor, $A^{o}_{(\text{structure})\text{-}h}$, and group contribution parameter, $E_{\text{a,add-alkene}}Rl$ of the functional group R_l (l denotes the number of functional groups, $l = 1$–4):

$$k^{\text{o}}{}_{(\text{structure})\text{-}h} = A^{\text{o}}{}_{(\text{structure})\text{-}h}\, e^{-\left[E^{\text{o}}{}_{a,(\text{structure})}\right]\Big/ RT} \tag{2.15}$$

$$Y_{R1} = e^{-\left[E_{a,(\text{structure})}R1\right]/\,RT} \tag{2.16}$$

where (structure) represents six base structures, $E^{o}_{\text{a(structure)}}$ denotes a base part of E_{a} for (structure), and h denotes a position for $HO^\bullet$ to add i.e., 1 and 2 for the addition to the left and right carbon, respectively. The rate constant for $HO^\bullet$ addition to alkene, $k_{\text{add-alkene}}$, can be written as below (Eq. 2.17)

$$k_{\text{add-alkene}} = \sum g k^{\text{o}}_{(\text{structure-}h)} Y_{R1} \tag{2.17}$$

where g indicates the 1 or 2 that represents asymmetrical and symmetrical addition, respectively. The rate constant for tetrachloroethylene ($Cl_2C{=}CCl_2$) as a typical example that is shown below (Eq. 2.18):

$$k = 2k^{\text{o}}_{>\text{C=C}<} Y_{-\text{Cl}} Y_{-\text{Cl}} Y_{-\text{Cl}} Y_{-\text{Cl}} \tag{2.18}$$

Few rate constants are reported for the conjugated and unconjugated dienes. It is shown that the group contribution factors do not linearly correlate with the Taft constant. Two reasons can be considered. First, the functional group contribution to the E_{a} does not follow the general inductive effect (i.e., Taft constant). Second, the experimental rate constants do not seem to follow the inductive effect (e.g., vinyl chloride > ethylene > vinyl alcohol) because of experimental errors or the existence of unknown reaction mechanisms. Considering new reaction mechanisms such as the excitation of alkenes by radiation may pave the way for future studies in that regard. Despite the observation of the nonlinear correlation between the group contribution factors and the Taft constant, 79 % of the calibrated rate constants were within the error goal, which might be acceptable for a rate constant estimator.

Rate constants for $HO^\bullet$ Addition to Aromatic Compounds (Minakata et al. 2009): The $HO^\bullet$ addition to the aromatic ring often occurs at rates close to diffusion-control. The electron-donating and -withdrawing functional groups on the aromatic ring can significantly affect the rate constants and the ratio of *ortho*-, *meta*-, *para*-, and *ipso*-addition. For the $HO^\bullet$ addition to aromatic compounds, the following points are considered: (i) Probability for the symmetrical $HO^{\bullet}$ addition to the benzene ring is identical (ii) Addition to the *ipso*-position is negligible for the aromatic compounds with single functional groups (e.g., <8 % for phenol and <1 % for chloro benzene) due to the significant steric effect (Raghavan and Steenken 1980; Merga et al. 1996; Mvula et al. 2001). Therefore, only when all positions on the aromatic ring are filled with functional groups, $HO^{\bullet}$ adds to the *ipso*-position with identical probability for all the available positions.

For the determination of the reaction rate constant, the E_a is a sum of two parts: (i) a base part, E^{o}_{a}, resulting from the $HO^{\bullet}$ addition to the aromatic ring depending on the number(s) and position(s) of the functional groups and (ii) group contribution parameter(s), $E_{a,\text{add-aromatic}}\text{Rm}$, due to the functional group(s), R_m (where m is the number of functional group(s), $m = 1$–6), on the aromatic ring. To reduce the number of group contribution factors to calibrate, it is assumed that A differs not by the type of the functional groups but by their number and position. Accordingly, the group rate constant, $k^{o}_{(\text{i-name})\text{-j}}$, and the group contribution factor, Z_{Rm}, may be expressed as below (Eqs. 2.19, 2.20)

$$k^{o}_{(\text{i-name})\text{-j}} = A^{o}_{(\text{i-name})\text{-j}} e^{-[(E^{o}a(\text{i-name})]/RT} \tag{2.19}$$

$$Z_{\text{Rm}} = e^{-\left(E_{a,\text{add-aromatic}}\text{Rm}\right)/RT} \tag{2.20}$$

where $A^{o}_{(i\text{-name})\text{-}j}$ denotes the Arrhenius frequency factor; $E^{o}_{a(i\text{-name})}$ denotes a base part of E_a; the name (benz, pyr, fur, imid, or triaz) denotes a compound that has a base structure of benzene, pyridine, furan, imidazole, or triazine, respectively; i denotes position(s) of the functional group, and j denotes position(s) for $HO^{\bullet}$ to add. The rate constant for the $HO^{\bullet}$ addition to aromatic compounds can be expressed by (Eq. 2.21)

$$k_{\text{add-aromatic}} = \sum n k^{o}{}_{(\text{i-name})\text{-j}} Z_{\text{Rm}} \tag{2.21}$$

where n indicates the number of available position(s) to add. The rate constant for 1,4-*tert*-butylphenol $[(CH_3)_3C–C_6H_4–OH]$ can be depicted as a typical example (Eq. 2.22)

$$\begin{aligned} k = &\left\{2k^{o}{}_{(1,4\text{-benz})-2,6} + 2k^{o}{}_{(1,4\text{-benz})\text{-}3,5}\right\} Z_{-\text{OH}} Z_{\text{-alkane}} \\ &+ 3 \times 3 \times k_{\text{prim}} X_{>\text{C}<} + k_{-\text{OH}} \end{aligned} \tag{2.22}$$

The group contribution factors for the $HO^{\bullet}$ addition to aromatic compounds, against electrophilic substituent constants σ^{+} are depicted in Fig 2b for benzene ($r = 0.89$), pyridine ($r = 0.93$), and furan ($r = 0.65$) compounds (EPI 2007). The figure shows that the group contribution factors that are empirically derived from the experimental rate constants linearly correlate with the general electron-donating and -withdrawing property. It is shown that a total of 64 % of the rate constants for 64 compounds from the prediction is within the error goal.

Rate constants for $HO^{\bullet}$ interactions with S-, N-, or P-atom containing compounds (Minakata et al. 2009): The $HO^{\bullet}$ radical reacts with the S-, N-, or

P-atom-containing functional groups bonded to a given compound in the aqueous phase forming a $2\sigma/1\sigma^*$ two-center-three-electron (2c–3e) adduct (Bonifačič 1999). These functional groups also affect the H-atom abstraction reaction by donating or withdrawing electrons on the C–H bonds. The group rate constant, k_{R4} (Eq. 2.13) represents the reaction of $HO^\bullet$ with S-, N-, or P-atom-containing compounds. The influence of neighboring functional groups is considered as negligible. The rate constant, k, for $HO^\bullet$ addition to iminodiacetic acid (HOOC–CH_2–NH–CH_2–COOH) as a typical example is expressed below (Eq. 2.23):

$$k = 2 \times 2k^{o}{}_{\mathrm{sec}} X_{-\mathrm{COOH}} X_{-\mathrm{NH}-} + k_{-\mathrm{NH}-} + 2k_{-\mathrm{COOH}} \tag{2.23}$$

It is shown that the group rate constants $k_{-\mathrm{CN}}$ and $k_{-\mathrm{NH2}}$ can be compared with the rate constants for compounds that react with $HO^\bullet$ via only interaction such as cyanogen and thiourea, respectively. The rate constant for thiourea (which has two –NH_2 groups) is approximately twice $k_{-\mathrm{NH2}}$, because the electron positive –CS– functional group does not significantly affect the electron density of the N atom. The reaction of $HO^\bullet$ with urea is presumably different because the two amine functional groups of urea are bonded to the electron-negative functional group, –CO–. Thus, another group rate constant $k_{-\mathrm{N-CO-N}-}$ is considered for methylurea, tetramethyl urea, and 1,3-dimethylurea. The magnitude of most group rate constants for the S-containing compounds is of the same order as for the amine-containing ones, but approximately 1 order of magnitude larger than for the amide-containing compounds. This might be caused by the electronegative –CO– functional group of the amide. The S-, N-, or P-atom-containing group contribution factors apparently play the same role as the functional groups for H-atom abstraction, i.e., $X_{\mathrm{R}i} = e^{-(Ea,\ \mathrm{absR}i)/RT}$. However, it is anticipated that S-, N-, or P-atom-containing functional groups may have different effects on H-atom abstraction. The group contribution factors for –S, –S–S–, and –SH, and –NH_2, –NH–, and –N<, respectively, are assumed to be identical due to the following reasons: (1) limited data availability for single functional group compounds, (2) similar electron inductive ability, and (3) application for the gaseous phase. In addition, the same data sets for the S– and N-atom-containing compounds are used to calibrate the group rate constants, $k_{-\mathrm{S}-}$, $k_{-\mathrm{S-S}-}$, and $k_{-\mathrm{SH}}$, and $k_{-\mathrm{NH2}}$, $k_{-\mathrm{NH}-}$, and $k_{-\mathrm{N}<}$, respectively. These group rate constants are not assumed to be identical because the interaction of $HO^\bullet$ with each functional group might be more significant than the electron donating effects of the functional groups. For similar electron inductive ability, the Taft constant indicates similar values among the S– and N-atom-containing functional groups. For example, the Taft constants for SCH_3, SC_2H_5, and SH are 1.66, 1.44, and 1.52, respectively (Karelson 2000), and those for NH_2, $NHCH_3$, $N(CH_3)_2$, $NH(CH_2)_3CH_3$, and $N(C_2H_5)_2$ are 0.62, 0.94, 1.02, 1.08, and 1.00, respectively (Karelson 2000). These values are well distinguished from 3.61 of $NH_3{}^+$, 4.66 of NO_2, 4.16 of $N^+(CH_3)_3$, and 3.64 of CN. Finally, it is assumed that the group contributed factors for –S–,–S–S–, and –SH, and for –NH_2, –NH–, –N< , –NNO, and –NNO_2 are identical, which successfully predicted the gas-phase $HO^\bullet$ rate constants (Atkinson 1986, 1987; Kwok and Atkinson 1995). A linear correlation between

Table 2 Hydrogenotrophic homoacetogens and methanogens isolated from various environments

Microorganism	Growth temp (ºC)	Optimum temp (ºC)		References
Acetobacterium bakiia	1–30	20	Sediments of a polluted pond	Kotsyurbenko et al. (1995)
Acetobacterium paludosuma	1–30	20	Sediments of a fen	Kotsyurbenko et al. (1995)
Acetobacterium fumetariuma	1–35	30	Manure digested at low temp	Kotsyurbenko et al. (1995)
Acetobacterium tundraeb	1–30	20–25	Tundra wetlands	Simankova et al. (2000)
Methanogenic strain MSB	1–32	25–30	Sediments of a polluted pond	Kotsyurbenko et al. (2001)
Methanogenic strain MSP	4–35	25–30	Sediments of a polluted pond	Kotsyurbenko et al. (2001)
Methanobacterium strain MB4	5–30	25–30	Peat samples	Kotsyurbenko et al. (2007)

the group contribution factors of S-, N-, or P-atom-containing functional groups and the Taft constant, σ^*, is observed ($r = 0.99$) (Fig. 2) (Karelson 2000). The $X_{\mathrm{R}i}$ values for S-, N-, or P-atom-containing functional groups are greater than those of the alkyl, oxygenated, and halogenated functional groups (Fig. 2). This suggests that S-, N-, or P-atom-containing functional groups donate more electrons toward the neighboring C–H bond(s), thereby enhancing the H-atom abstraction by $HO^{\bullet}$.

The GCM includes 66 group rate constants and 80 group contribution factors, which characterize each $HO^{\bullet}$ reaction mechanism with steric effects of the chemical structure groups and impacts of the neighboring functional groups, respectively (Minakata et al. 2009). The group contribution factors for H-atom abstraction and $HO^{\bullet}$ addition to the aromatic compounds linearly correlate with the Taft constants, σ^*, and the electrophilic substituent parameters, σ^+, respectively. The best calibrations for 83 % (257 rate constants) and predictions for 62 % (77 rate constants) of the rate constants are within 0.5–2 times the experimental values. Literature-reported experimental $HO^{\bullet}$ rate constants for 310 and 124 compounds are used for calibration and prediction, respectively.

Although there are a few tools available to determine aqueous phase hydroxyl radical reaction rate constants (Minakata et al. 2011; Herrmann 2003; Monod et al. 2005; Minakata and Crittenden 2011; Herrmann et al. 2010), the GCM is quoted as “The wide application range in combination with the user-friendliness makes it probably the best currently available estimation tool for HO radical reactions in aqueous solution. Overall, the method of Minakata et al. (2009) is currently the most broadly usable method for the prediction of HO radical reaction rates in aqueous solution (Herrmann et al. 2010). The GCM peer-reviewed paper provided both MS Excel spread sheet and compiled Fotran program as supportion information. Any users are able to access these programs and determine the aqueous phase $HO\cdot$ reaction rate constants with inputs of structural information of a compound of interest.

Various functional groups widely differ for their reaction rate constants with $HO^{\bullet}$ (Fig. 2). Similarly, the production rates of H_2O_2 and $HO^{\bullet}$ photolytically formed from different organic compounds are much varied (Table 1: chapter "Photoinduced and Microbial Generation of Hydrogen Peroxide and Organic Peroxides in Natural Waters"; Table 2: chapter "Photoinduced Generation of Hydroxyl Radical in Natural Waters"). Variations in the production rates depend on the chemical nature of the functional groups bonded to each organic compound. Therefore, it can be concluded that the functional groups have an important impact both on the photoinduced production of $HO^{\bullet}$ and on the $HO^{\bullet}$ reaction with organic compounds. Both issues are very significant for the photoinduced processes that involve dissolved organic matter in surface waters.

2.5 Mechanisms of Microbial Degradation of DOM in Natural Waters

The organic matter in wastes and biomass is diagenetically altered by complex microbial processes into various kinds of organic substances such as long-chain fatty acids, C_3 to C_5 organic acids, alcohols, aromatic compounds, humic substances (fulvic and humic acids) of terrestrial plant origin, autochthonous fulvic acid of algal origin, acetate, formate, methanol, CO_2, H_2, as well as minor products. These processes take place in waters, in soil environments or in sediment pore waters of lake and marine systems (Mostofa et al. 2009a; Conrad 1999; Lovley 2006; Li W et al., unpublished data; Burdige et al. 2004; Yang and Guo 1990; Leenheer and Croue 2003).

The functional groups of organic substances and the minor components may be subsequently converted into CO_2, methane and other products by fermentative microorganisms and Fe(III)-reducing microorganisms. These processes take place with simultaneous reduction of an array of electron acceptors, including oxygen, H_2, nitrate, manganese oxides, Fe(III) oxides, sulfate, H_2S, and humic substances in water (Lovley 2006; Lovley et al. 1996; Nagase and Matsuo 1982; Jetten et al. 1992; Coleman et al. 1993; Roden and Wetzel 1996; Pelmenschikov et al. 2002; Keppler et al. 2006; Itoh et al. 2008; Reguera et al. 2005).

Fe(III)-reducing microorganisms, commonly *Geobacter* species in temperate environments (Lovley et al. 2004), and Fe(III)-reducing archaea in warm environments (Kashefi et al. 2004) metabolize the fermentation products and the functional groups in organic substances. They are oxidized to CO_2, with Fe(III) oxides serving as the electron acceptor (Lovley 2006; Lovley et al. 1996). The mechanism for CO_2 formation from Fe(III) oxide in the presence of Geobactor spp. is depicted (Fig. 3) (Lovley et al. 1996):

The general reactions for microbial Fe(III) reduction coupled with the oxidation of fermentation products such as acetate (Eq. 2.24) and hydrogen (Eq. 2.25) are described below (Eqs. 2.24, 2.25) (Coleman et al. 1993; Lovley 1991).

$$4Fe_2O_3 + CH_3COO^- + 7H_2O \rightarrow 8Fe^{2+} + 2HCOL_3{}^- + 15OH^- \quad (2.24)$$

$$Fe_2O_3 + H_2 + H_2O \rightarrow 2Fe^{2+} + 4OH^- \quad (2.25)$$

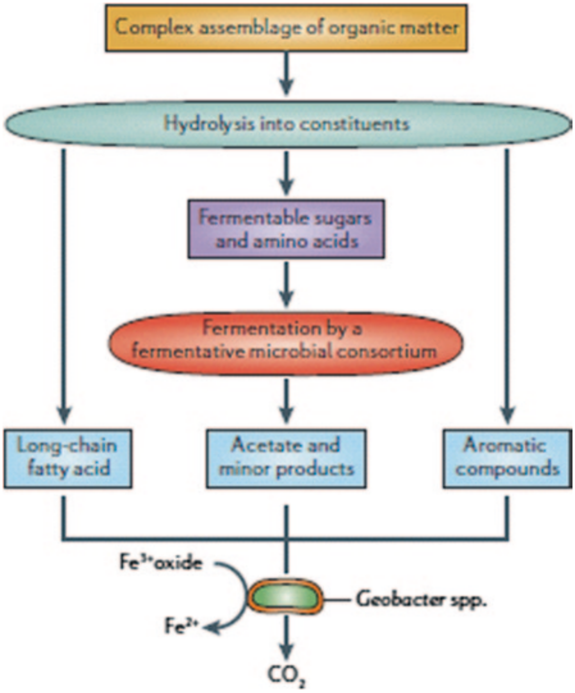

Fig. 3 Generalized pathway for the anaerobic oxidation of organic matter to carbon dioxide with Fe^{3+} oxide serving as an electron acceptor in temperate, freshwater and sedimentary environments. The process is mediated by a consortium of fermentative microorganisms and Geobacter species (ca. *Geobactter metallireducens*). *Data source* Lovley (2006)

$$Fe^{2+} + HCO_3^- + OH^- \rightarrow FeCO_3 + H_2O \quad (2.26)$$

The ferrous iron, hydroxyl ions and bicarbonate, produced together in (Eqs. 2.24, 2.25) can combine to form siderite in aquatic sediment porewaters (Eq. 2.26) (Coleman et al. 1993). Evidences from that research study show that two genera of sulphate-reducing bacteria, *Desulfobacter* and *Desulfovibrio*, can oxidize H_2 and acetate in aquatic sediment waters (Coleman et al. 1993). It is shown that H_2 is the most important electron donor for *Desulfovibrio* (Eq. 2.27), and acetate is the most environmentally significant electron donor for *Desulfobacter* (Eq. 2.28) sulphate reducing bacteria (Coleman et al. 1993):

$$4H_2 + SO_4{}^{2-} \rightarrow S^{2-} + 4H_2O \quad (2.27)$$

$$CH_3COO^- + SO_4{}^{2-} \rightarrow S^{2-} + 2HCO_3^- + H^+ \quad (2.28)$$

The study shows that *Desulfobulbus propionicus* can oxidize S to $SO_4{}^{2-}$ with an electrode serving as the electron acceptor (Lovley 2006). This is an important reaction at the anode surface in sediments, where high concentrations of sulphide can abiotically react with electrodes producing S° (Fig. 4) (Lovley 2006). This abiotic reaction merely yields two out of eight electrons potentially available from sulphide (S^{2-}) oxidation (Fig. 4). Oxidation of S° to $SO_4{}^{2-}$ extracts six electrons and regenerates $SO_4{}^{2-}$ as an electron acceptor for further microbial reduction by microorganisms in the family *Desulfobulbaceae* (Lovley 2006; Holmes et al. 2004).

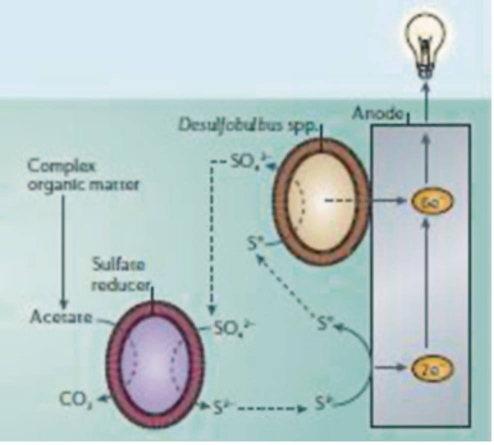

Fig. 4 Mechanism by which sulfate reducer can convert acetate to CO_2 and reduced sulphur compounds to electricity production in sediment microbial fuel cells in sulphide-rich sediments. *Data source* Lovley (2006)

A pure culture of *Desulfovibrio desulfuricans* can readily reduce Fe(III), but *Desulfobacter postgatei and Desulfobactercurvatus* cannot (Coleman et al. 1993). The experimental study showed the occurrence of the metabolism of Fe(III) and sulphate by *D. desulfuricans*; at low concentrations of H_2 in aquatic sediments, Fe(III) might be the predominant electron acceptor (Coleman et al. 1993). It has been evidenced that fermentation or methanogenesis do not metabolize the organics rapidly (Lovley 2006), but can produce a number of minor components such as acetate, formate, methanol, CO_2 and H_2 at the end of the metabolic process (Yang and Guo 1990; Roden and Wetzel 1996; Zeikus et al. 1975; Lovley and Klug 1986; Lovley and Phillips 1987). These products are subsequently used for methane formation.

Methanogenic bacteria are a diverse subgroup of *archaebacteria (Archaea*) that convert CO_2 into methane to provide energy (31 kcal/mol) for the cell (Eq. 2.29) (Thauer et al. 2008; Thauer 1998):

$$CO_2 + 4H_2 \rightarrow CH_4 + 2H_2O \tag{2.29}$$

The conversion of glucose to alcohols and fatty acids during the fermentation allows the utilization of the standard Gibbs free energy content (Conrad 1999; Thauer et al. 1977). The degradation of alcohols and fatty acids to acetate and H_2 caused by syntrophic bacteria is endoergonic under standard conditions (Conrad 1999; Thauer et al. 1977), but it can take place when it is combined with H_2-consuming methanogenesis (Conrad 1999). Hydrogenotrophic and acetotrophic methanogenesis may convert fermentation products or glucose to CH_4 and/or CO_2.

The mechanism for methane formation in methyl-coenzyme *M* reductase (MCR) has been evidenced using the B3LYP hybrid density functional method and chemical models consisting of 107 atoms (Pelmenschikov et al. 2002). In this mechanism, the reaction starts with CoB and methyl-CoM coenzymes and with the active Ni(I) state of the tetrapyrrole F_{430} prosthetic group, which then forms a

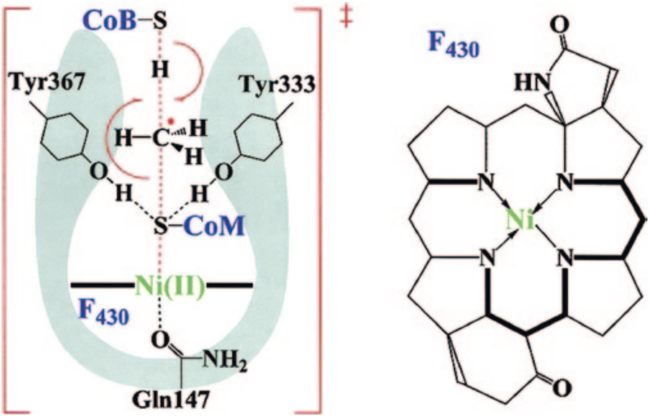

Fig. 5 The mechanism for methane formation in methyl-coenzyme *M* reductase (MCR) in methanogenesis. *Data source* Pelmenschikov et al. (2002)

free methyl radical at the transition state (Fig. 5). A methyl radical is then released from methyl-CoM, induced by the attack of Ni(I) on the methyl-CoM thioether sulfur, which oxidizes the metal center from Ni(I) to Ni(II). The latter forms a strong bond of 38.6 kcal/mol with the sulfur of CoM (Eq. 2.44):

$$\begin{aligned}&\text{CoB-S-H} + \text{CH}_3\text{-S-CoM} + \text{Ni(I)F}_{430} \rightarrow\\&\text{CoB-S-H} + \text{CH}_3^{\bullet} + \text{CoM-S-Ni(II)F}_{430}\end{aligned} \tag{2.44}$$

The resulting methyl radical is rapidly quenched by hydrogen-atom transfer from the CoB thiol group, yielding the CH_4 and the CoB radical. The pathway has activation energy of approximately 20 kcal/mol, leading to stereoinversion at the reactive carbon (Eq. 2.45):

$$\begin{aligned}&\text{CoB-S-H} + \text{CH}_3^{\bullet} + \text{CoM-S-NI(II)F}_{430} \rightarrow\\&\text{CH}_4 + \text{CoB-S}^{\bullet} + \text{CoM-S-NI(II)F}_{430}\end{aligned} \tag{2.45}$$

In the final step, formation of heterodisulfide CoB-S–S-CoM is proposed in which nickel is reduced back to Ni(I) (Eq. 2.46).

$$\text{CoB-S}^{\bullet} + \text{CoM-S-NI(II)F}_{430} \rightarrow \text{CoB-S-S-CoM} + \text{NI(I)F}_{430} \tag{2.46}$$

It can be noted that methyl-coenzyme M is 2-mercaptoethanesulfonic acid that is unique to the methanogens, and coenzyme B is 7-mercaptoheptanoylthreonine phosphate that includes an aliphatic linker of six methylene units between the phosphothreonine head group and the thiol group.

A recent study shows that MCR is the key enzyme in methane formation by methanogenic *Archaea* when it is incubated with the natural substrates

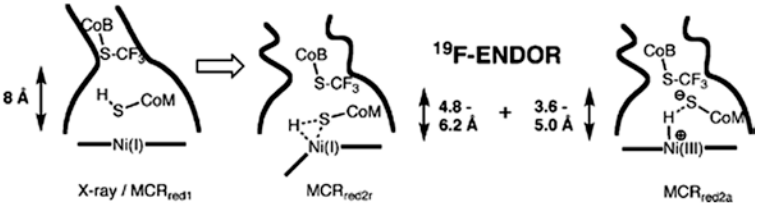

Fig. 6 The mechanism for methane formation in methyl-coenzyme *M* reductase (MCR) in methanogenesis in presence of natural substances. Data source Ebner et al. (2010)

(Ebner et al. 2010). In this mechanism, the enzyme converts the thioether methyl-coenzyme M, and the thiol coenzyme B, into methane and the heterodisulfide of coenzyme M and coenzyme B (Ebner et al. 2010). In the presence of the competitive inhibitor coenzyme M instead of methyl-coenzyme M, addition of coenzyme B to the active Ni(I) state of $\mathrm{MCR_{red1}}$ induces two new species called $\mathrm{MCR_{red2a}}$ and $\mathrm{MCR_{red2r}}$ (Fig. 6). The two $\mathrm{MCR_{red2}}$ signals can also be induced by the *S*-methyl- and the *S*-trifluoromethyl analogs of coenzyme B. It is thus suggested that the protein may undergo a conformational change upon formation of $\mathrm{MCR_{red2}}$ species in the transition from $\mathrm{MCR_{red1}}$, which opens up the possibility that nickel coordination geometries other than square planar, tetragonal pyramidal, or elongated octahedral might occur in intermediates of the catalytic cycle (Ebner et al. 2010).

The degradation of specific aliphatic carbon or functional groups by microbial processes in natural waters may preferentially occur in macromolecules such as fulvic and humic acids of terrestrial plant origin, as well as autochthonous fulvic acid of algal origin. The microbial changes in the functional groups of organic substances are typical phenomena in sediment pore waters, where a decrease of the acidic functional groups as well as an increase of basic and neutral functional groups occurs with depth (Rosenfeld 1979; Burdige and Martens 1988; Wu and Tanoue 2001; Maita et al. 1982; Steinberg et al. 1987). Such changes in functional groups of autochthonous fulvic acid (C-like) can be understood from the vertical increase in fluorescence intensity with depth, identified with excitation and emission matrix (EEM) of pore water samples and their parallel factor (PARAFAC) modeling in the pore waters of lakes (Li W et al., unpublished data). The low values of fluorescence index for autochthonous fulvic acid (C-like) at deeper depth, compared with upper sediment pore water, confirm the changes with depth in the functional groups of that component (Li W et al., unpublished data). Such changes might be a useful indicator for complex microbial processing of the functional groups of autochthonous fulvic acids in the pore waters of lakes. Therefore, it is suggested that microbial degradation may diagenetically alter either the minor components (e.g. acetate) or the functional groups bound to macromolecules, such as fulvic and humic acid from terrestrial plants and autochthonous fulvic acid from algal biomass, generating CO_2, CH_4 and other products.

2.6 *Kinetics of Photoinduced Degradation of DOM*

Photoinduced degradation can decrease the concentration of dissolved organic carbon (DOC) as a function of the integrated solar intensity (Fig. 7) (Mostofa et al. 2005, 2007). The changes in the DOC concentration can be best fit with a first order reaction as reported below (Eq. 2.47):

$$Ln\,(DOC/DOC_o) = -k_1 S \tag{2.47}$$

where k_1 is the reaction rate constant for the photoinduced degradation of DOC, *DOC* is organic carbon concentration after irradiation and DOC_o the initial one, and *S* is the integrated solar intensity or photon energy (MJ m^{-2}) (Fig. 7a) (Mostofa et al. 2007).

Kinetics studies on the photoinduced degradation of DOM can explain several important phenomena in waters (Mostofa et al. 2007). First, stream DOM undergoes rapid photoinduced degradation (1.8–2.6 × 10^{-3} MJ^{-1} m^2 in waters of the Kago and Nishi-Mataya upstreams) (Mostofa et al. 2007). Second, microbial degradation under dark incubation is quite low or negligible for upstream DOM (0.7–4.6 × 10^{-4} MJ^{-1} m^2 for the same upstreams). Third, in rivers that include various sources of DOM the latter can be uniformly degraded both photolytically (9.5 × 10^{-4} MJ^{-1} m^2) and microbiologically (11 × 10^{-4} MJ^{-1} m^2) (Fig. 1c and d).

3 Factors Controlling the Photoinduced Degradation of DOM in Natural Waters

Photoinduced degradation of DOM depends on the sources of waters, concentration level and optical-chemical nature of DOM, time and space. Photoinduced degradation of DOM is an important phenomenon that plays a significant role in the biogeochemistry of the carbon cycle, biological activity and primary and secondary productions in natural waters (Mostofa et al. 2009a; Ma and Green

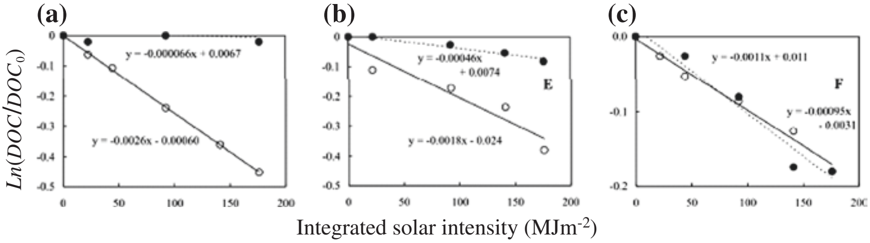

Fig. 7 Relationship between the *Ln*(*DOC*/DOC_0) and the integrated solar intensity (MJm^{-2}) in the Kago upstream (**a**), Nishi-Mataya upstream (**b**), and in the downstream waters of Yasu River (**c**). *Data source* Mostofa et al. (2007)

2004; Vahatalo et al. 2000; Mostofa et al. 2000, 2007; Gao and Zepp 1998; Graneli et al. 1996, 1998; Wu et al. 2005; Mopper et al. 1991; Miller and Zepp 1995; Miller and Moran 1997; Rosenstock et al. 2005; Nieto-Cid et al. 2006). The Photoinduced degradation rate is mostly dependent on several major factors that are greatly related to variable local conditions and to the concentration levels and molecular nature of DOM. The key factors are: (1) Sunlight or solar radiation, (2) Water temperature, (3) Effects of total dissolved Fe and photo-Fenton reaction, (4) Occurrence and quantity of NO_2^- and NO_3^- ions, (5) Molecular nature of DOM, (6) pH and alkalinity of the waters, (7) Dissolved oxygen (O_2), (8) Depth of the water, (9) Physical mixing in the surface mixing zone, (10) Increasing UV-radiation during ozone hole events, (11) Global warming and (12) Salinity.

3.1 Sunlight or Solar Radiation

Solar radiation is the key factor for photoinduced degradation of DOM or organic contaminants in water (Morris and Hargreaves 1997; Reche et al. 1999; Mostofa and Sakugawa 2009; Vahatalo et al. 2000; Mostofa et al. 2007; Moran et al. 2000; Wu et al. 2005; Molot and Dillon 1997; Dobrović et al. 2007). Photoinduced degradation of DOM depends on the spectral wavelengths of solar radiation such as UV-A (315–400 nm), UV-B (280–315 nm), and visible light (400–700 nm) as well as their significant variations after penetration in the water column (Scully et al. 1996; Morris and Hargreaves 1997; Reche et al. 1999; Vahatalo et al. 2000; Graneli et al. 1996, 1998; Lindell et al. 1996; Kieber et al. 1990; Molot and Dillon 1997; de Haan 1993; Herndl et al. 1993; Valentine and Zepp 1993). DOM is typically susceptible to absorb UV radiation in sea and lake waters (Kirk 1994; Morris et al. 1995). The penetration of UV radiation in natural waters is greatly variable, with typical penetration depths in clear ocean water of ~20 m for UV-B and ~50 m for UV-A radiation, 5–10 m for UV-B radiation in oligotrophic oceans and 0.5–3 m in freshwaters (Kirk 1994; Smith and Baker 1981; Waiser and Robarts 2000). It can be expected that the photoinduced degradation of DOM is significantly dependent on the attenuation of downward irradiance in natural waters. It has been shown that the contribution of solar intensity to total photoinduced degradation of DOM in lakes is 39–69 % by UV-A, 9–17 % by UV-B, and 23–44 % by visible light radiation (Vahatalo et al. 2000). Photoinduced mineralization of natural DOC is increased <9 % when the UV-B radiation is doubled in humic lakes (Vahatalo et al. 2000). Control irradiation by wavelengths 254 nm (hereafter UV) and 185 nm (hereafter VUV) on DOM demonstrates that the DOM degradation rate at 185 nm increases approximately ten-fold compared to those at 254 nm. An increase in fluxes of the UV radiation can substantially increase the quantity of the reactive free radicals such as $HO^\bullet$ and H_2O_2 in waters (Qian et al. 2001; Rex et al. 1997; Yocis et al. 2000). Rex et al. 1997; Yocis et al. 2000; During an ozone hole event, the production rates of $HO^\bullet$ are greatly enhanced in Antarctic waters (Qian et al. 2001; Rex et al. 1997). The $HO^\bullet$ is the most powerful oxidizing agent that can be involved into the photoinduced degradation of DOM in waters, although there is evidence that the formation rate of $HO^{\bullet}$ may be insufficient to account for the DOM mineralization (Vione et al. 2009).

Variations in the spectral irradiance penetration among various waters and in the effect of radiation wavelength on DOM transformation might be caused by three factors. First, concentration levels and molecular nature of DOM can modify the absorption spectrum for a variety of waters. Second, contents of total iron, a major factor of $HO^{\bullet}$ production through photo-Fenton reaction and probably also of DOM mineralization through $HO^{\bullet}$-independent processes (Vione et al. 2009), are greatly varied for a variety of waters. Third, depletion of the stratospheric ozone layer may greatly increase the UV-B radiation, thereby enhancing the photoinduced mineralization of DOM by UV-B (Qian et al. 2001; Randall et al. 2005). An effort is still needed to accout for the different results obtained in different studies. On the one hand, a limited increase (~4 %) in DOM photoinduced mineralization has been observed in Brazil compared to Sweden, although the dose of UV-B was three-fold higher in Brazil than in Sweden (Graneli et al. 1998). On the other hand, half of the total photoinduced degradation of DOM was attributable to wavelengths shorter than 360 nm (Vahatalo et al. 2000).

3.2 Water Temperature

Air temperature is greatly varied from 0 to approximately 50 °C in different regions, which might control the water temperature (WT) and its variation in natural waters. A low WT can reduce the movement of the reactants in the aqueous solution, thereby causing a decrease in the reaction kinetics of DOM in waters. WT that is driven by solar intensity is directly related to the photoinduced generation of H_2O_2. The H_2O_2 in river shows a significantly higher production in summer and lower in winter (Mostofa and Sakugawa 2003, 2009). The lower production of H_2O_2 due to low WT and solar irradiance may subsequently decrease the production rate of $HO^{\bullet}$ (Qian et al. 2001) and, as a consequence, the photoinduced degradation rate of DOM in aqueous solution.

3.3 Effects of Total Dissolved Fe and Photo-Fenton Reaction

The concentration of total dissolved Fe is one of the most important factors for the photoinduced degradation of DOM in waters (Vione et al. 2009; Gao and Zepp 1998; Wu et al. 2005; Gennings et al. 2001), through the photo-Fenton reaction (Zepp et al. 1992; Southworth and Voelker 2003; McKnight et al. 1988; Arakaki and Faust 1998); or via $HO^{\bullet}$-independent processes (Vione et al. 2009). The generation rate of $HO^{\bullet}$ is much higher for elevated Fe levels in acidic waters (McKnight et al. 1988; Allen et al. 1996). The oxidation of Fe^{2+} by photo-generated H_2O_2 causes the production of $HO^{\bullet}$ and Fe^{3+}, but Fe^{2+} is regenerated from Fe^{3+} by several pathways via the process of $h\upsilon/H_2O_2/O_2^{\bullet-}$. The regeneration of Fe^{2+} greatly enhances the production of $HO^\bullet$ (Vione et al. 2004) and leads to high photoinduced degradation of DOM in iron-rich waters. Addition to the water of fluoride ion or deferoxamine mesylate (DFOM) can form unreactive Fe^{3+} complexes, inhibiting iron photoreduction and slowing down the photoinduced degradation of DOM (Gao and Zepp 1998; Wu et al. 2005). The photoinduced formation of DIC, CO and NH_4^+ has been greatly affected by the addition of fluoride ion to the water of the River Satilla (Gao and Zepp 1998). Thus, the photo-Fenton reaction plays an important role in natural waters, especially in acidic waters. The photoinduced degradation rate constant of humic acid is significantly decreased by the addition of fluoride, but that of fulvic acid is not affected (Wu et al. 2005). Dissolved Fe is thus thought to play an important role in the photoinduced degradation of humic acid rather than fulvic acid. Due to the higher aromaticity of humic acid as compared to fulvic acid (30–51 % of aromatic carbon vs. 14–20 %) (Malcolm 1985; Gron et al. 1996), humic acid is more susceptible to react with $HO^\bullet$ which is generated from the photo-Fenton reaction ($Fe^{2+} + H_2O_2 \rightarrow HO^\bullet + {}^-OH + Fe^{3+}$) (Zepp et al. 1992; Senesi 1990; Minakata et al. 2009; Chen and Pignatello 1997). Therefore, it is likely that humic acid is the DOM component that undergoes the fastest photoinduced degradation in natural waters.

3.4 *Occurrence and Quantity of NO_2^- and NO_3^- Ions*

Photoinduced degradation of DOM can be affected by the occurrence and concentration levels of NO_2^- and NO_3^- ions, both of which are efficient in the production of $HO^\bullet$ upon photolysis in waters (see also chapter “Photoinduced Generation of Hydroxyl Radical in Natural Waters”) (Zafiriou and True 1979a, b; Takeda et al. 2004; Vione et al. 2006; Mack and Bolton 1999; Nakatani et al. 2004; Chin et al. 2004). Contribution of $HO^\bullet$ production in sewage polluted rivers is 48–80 % from NO_2^- and 2–19 % from NO_3^-, but the contribution is 6–26 % and 1–49 %, respectively, in upstreams and clean rivers (Takeda et al. 2004; Nakatani et al. 2004). In anthropogenically polluted Rhône River Delta (S. France) and Lake Piccolo (NW Italy) the contribution of $HO^\bullet$ production is accounted for by NO_2^- (62–63 %) and NO_3^- (27–38 %), while in the unpolluted and remote Lake Goose and Lake Divide (Wyoming, USA) the contribution of nitrate and nitrite is relatively lower, 0–11 % and <0.5 %, respectively (Minero et al. 2007). In seawater NO_2^- is the major source of $HO^\bullet$ in Seto Inland Sea (7–75 %) and Yellow Sea (10–44 %) compared to NO_3^- (<1 % and 0.4–8 %, respectively) (Takeda et al. 2004). The two anions (NO_2^- and NO_3^-) collectively are dominant sources in both river and seawater, while their role in lake water is less important (Vione et al. 2006). Natural waters that include high concentration levels of NO_2^- and NO_3^- could induce degradation of DOM by photoinduced production of $HO^\bullet$. However, it has been found that the rate of mineralization of DOM in acidified lake water far exceeds that rate of $HO^\bullet$ generation by all the sources, which suggests that $HO^\bullet$-independent processes (tentatively, photolysis of Fe(III)-DOM complexes) may also play an important role in DOM mineralization (Vione et al. 2009).

3.5 Molecular Characteristics of the DOM

Photoinduced degradation of DOM is significantly dependent on the molecular characteristics or the absorbing nature of the organic substances in the chromophoric dissolved organic matter (CDOM) or fluorescent dissolved organic matter (FDOM) in waters (Table 1). Chromophores in CDOM and fluorophores in FDOM are considered to be equivalent components with respect to photosensitization by sunlight. Photoinduced degradation of DOM takes place upon absorption of photons, which is predominantly dependent on the chemical nature of the organic substances present in DOM. The radiation absorption by organic matter increases along the spectrum from visible toward UV regions (Amador et al. 1989; Kieber et al. 1990). High molecular weight (HMW) DOM such as humic substances (fulvic and humic acids), and fluorescent whitening agents (FWAs) or components of detergents (DAS1 and DSBP) can absorb both visible and shorter wavelength regions (Kramer et al. 1996; Kieber et al. 1990; Sadtler 1968; Strome and Miller 1978). Many low molecular weight organic acids photo-generated from large CDOM or FDOM can absorb only in UV-C range, but they do not absorb radiation in the UV-B, UV-A or visible range (Sadtler 1968). For example, acetaldehyde absorbs light at 208–224 nm (Kieber et al. 1990; Mopper et al. 1991; Strome and Miller 1978), acetate at 204–270 nm (Dahlén et al. 1996; Wetzel et al. 1995), formaldehyde at 207–250 nm (Mopper et al. 1991; Mopper and Stahovec 1986), glyoxal at <240 nm (Mopper et al. 1991; Mopper and Stahovec 1986), malonate at 225–240 nm (Dahlén et al. 1996), pyruvate at 200–227 nm (Wetzel et al. 1995; Kieber et al. 1990; Mopper et al. 1991), and propanal at ~230 nm (Mopper and Stahovec 1986).

Fulvic acid absorbs radiation in both the visible and UV ranges (Fig. 1a) (Mostofa et al. 2005). The DOC concentrations varied between upstream (99 μM C, Kago) and downstream rivers (194 μM C, Yasu), but the absorption in the visible region is likely the same in both upstream (Fig. 1a) and downstream waters (Fig. 1b). Such an absorption is usually caused by HMW DOM. Humic acid is degraded more quickly than fulvic acid in water (Wu et al. 2005), probably because of the higher aromaticity (Malcolm 1985; Gron et al. 1996). The absorption of visible light by chromophores or fluorophores in HMW DOM causes decomposition, which is usually more marked in upstream (Fig. 1a) than in downstream waters (Fig. 1b). The following order for DOM photoinduced degradation can be proposed: upstream DOM > downstream rivers > lake > seawaters (Table 1; Fig. 1). Therefore, photoinduced degradation is greatly dependent on the molecular nature of DOM compositions in waters. Interestingly, the residence time of water in lakes and sea is much higher compared to the rivers. Possibly the lower photoinduced lability of the DOM found in lake or sea water is due to the fact that labile DOM in these environment has sufficient time to undergo photoinduced degradation.

3.6 pH and Alkalinity of Waters

Both pH and alkalinity, which can greatly vary among different waters, can influence the photoreaction rates of DOM, its chemical structure and speciation

(Vahatalo et al. 2000; Wu et al. 2005; Gennings et al. 2001; Molot et al. 2005). The photo-Fenton reaction is greatly influenced by pH. A decrease in pH greatly accelerated the photoinduced degradation of DOM in softwater stream (Molot et al. 2005), in Satilla river (Gao and Zepp 1998) as well as in lake water from NW Italy (Vione et al. 2009). The experimental study shows that after 69 hours of artificial irradiation without addition of KI, DOC loss is decreased as pH increases from pH 4 to 9 whilst addition of KI is significantly reduced loss of DOC at pH 4, 5 and 7 but not at pH 9 with the fraction of DOC lost by non-$HO^\bullet$ mechanisms gradually increasing from 58 % to 75 % between pH 4 and 7, and 100 % at pH 9 (Molot et al. 2005). Photoinduced degradation rates of DOC and fluorescence are greatly increased with a decrease in sample pH from 8 to 6 and then to 4 (Wu et al. 2005). Conversely, the production rates of $HO^\bullet$ in the Fenton or photo-Fenton reaction are greatly enhanced with a decrease in pH of natural waters (Zepp et al. 1992; Vione et al. 2009; Goldstone et al. 2002; Moffett and Zika 1987; Millero and Sotolongo 1989).

The apparent mechanism for enhanced photoinduced loss of DOC at low pH is oxidation to dissolved inorganic carbon (DIC) by reaction with $HO^\bullet$ produced via the iron-mediated photo-Fenton pathway (Zepp et al. 1992; Voelker et al. 1997). Therefore, high production rate of $HO^\bullet$ at low pH can accelerate the photoinduced degradation of DOM in waters. However, there is evidence that the production rate of $HO^\bullet$ in acidified lake water is unable to account for the rate of DOM mineralization, which suggests that additional mineralization processes would also be operational (Vione et al. 2009). The major terrestrial alkalinity-producing processes such as ionic exchange, weathering and biological assimilation of nitrate and other anions, mostly depend on the watershed geology, morphology, soil characteristics, and hydrological conditions (Psenner 1988). Watersheds of lakes exported more SO_4^{2-}, NO_3^- and H^+ than they received, and the lakes are the dominant acidity-consuming parts of the whole ecosystem, neutralizing 50–58 % of the H^+ input (Kopacek et al. 2003). Terrestrial fluxes of organic acid anions can also consume H^+ in natural lakes and are thought to be the third major internal alkalinity-producing mechanism after the biochemical reductions of NO_3^- and SO_4^{2-} (Kopacek et al. 2003; Cook et al. 1986; Schindler et al. 1986). An increase in alkalinity in waters can decrease the production of H_2O_2 by slowing the reaction of $O_2^{\bullet -}$ protonation ($2O_2^{\bullet -} + 2H^+ \rightarrow H_2O_2 + O_2$). A decrease in H_2O_2 production can reduce the photoinduced generation of $HO^\bullet$ through photo-Fenton reaction or direct photolysis, thereby decreasing the photoinduced degradation of DOM in natural waters.

3.7 Dissolved Oxygen

Dissolved oxygen (O_2) can enhance the photoinduced degradation of DOM in waters (Vahatalo et al. 2000; Amon and Benner 1996; Obernosterer et al. 2001; Laane et al. 1985; Lindell and Rai 1994; Reitner et al. 1997). Addition of O_2 to photoinduced reaction systems can greatly promote the photoinduced degradation rates (Gao and Zepp 1998; Stumm and Lee 1961; Miles and Brezonik 1981). Stumm and Lee 1961; Miles and Brezonik 1981; In iron-rich waters, the ferrous iron is often oxidized by dissolved O_2 with production of ferric oxide floc (Stumm and Lee 1961). O_2 is consumed at a rate of 0.02–0.09 mg L^{-1} h^{-1} in humic colored waters having pH 3–4 and total iron concentration of 0.1–2.0 mg L^{-1} under irradiation. The consumption rate is slightly lower (0.01–0.04 mg L^{-1} h^{-1}) under dark conditions (Miles and Brezonik 1981). Some standard organic compounds can consume O_2 at rates of 0.01–0.83 mg L^{-1} h^{-1} under irradiation and 0.01–0.70 mg $L^{-}1$ h^{-1} in the dark. These results have been obtained for a concentration of 100 mg L^{-1} of organic compounds in the presence of 6 mg L^{-1} of Fe(III) (Miles and Brezonik 1981). In photoexperiments conducted on Amazon river water samples, the O_2 consumption rate was 3.68 μM O_2 h^{-1} under irradiation and it was twelve times lower (0.30 μM O_2 h^{-1}) in the dark (Amon and Benner 1996). High rates of DOC loss and O_2 consumption are often observed in riverine DOM, with little or no additional production of biologically labile organic compounds. The photoinduced O_2 demand of surface water DOM in the Atlantic Ocean varied from 0.1 to 2.8 μmol O_2 L^{-1} d^{-1} in 12 h irradiation periods (Obernosterer et al. 2001). Rivers usually exhibit a higher O_2 consumption rate than seawaters. The O_2 consumption in waters is hypothesized to contribute to the generation of H_2O_2 through production of superoxide radical ion ($O_2^{\bullet -}$) as intermediate, upon monoelectronic reduction of O_2 by aquated electrons (e^-) produced by DOM (see chapter "Photoinduced and Microbial Generation of Hydrogen Peroxide and Organic Peroxides in Natural Waters"). Photolytically produced H_2O_2 can participate to the production of $HO^\bullet$, by either the photo-Fenton reaction or the direct photolysis, and such processes can contribute to the photoinduced degradation of DOM in waters.

3.8 Depth of the Water Column

The Photoinduced degradation of DOM is significantly dependent on the depth of the water column. Degradation is higher in the upper surface layer and gradually decreases with an increase in the water column depth (Ma and Green 2004; Vahatalo et al. 2000). Solar radiation can mineralize 19 mmol C m^{-3} d^{-1} at a depth of 1 cm, and the rate of mineralization decreases with increasing depth with an attenuation coefficient of 23 m^{-1} (Vahatalo et al. 2000). Most of the photo mineralization takes place in the top 10 cm in lakes (Vahatalo et al. 2000). The presence of low quantity of suspended solids or particulate matter allows for a deeper penetration of light in the water column, which can result into a greater potential for the photoinduced degradation of deeper DOM. Both river and lake DOM have a high potential to undergo photoinduced degradation in the surface layers (0 m), and photoinduced degradation gradually decreases in the deeper layers (6.5 and 24 m), as has been found in an in situ experimental study (Ma and Green 2004). Surface waters with a high level of DOC greatly inhibit the penetration of solar radiation into the deeper layers, whilst penetration of radiation at longer depth of the water column is usually observed in water bodies with low DOC (Morris et al. 1995). UV-B radiation penetrates at a depth of 0.1–5 m, while UV-A penetrates at 0.2–15 m (Farmer et al. 1993). Therefore, UV-A plays a more important role into the photoinduced degradation of DOM in deeper layers compared to UV-B (Piazena and Häder 1994; Blough et al. 1993). It can be concluded that the photoinduced degradation of DOM at any depth of the water column in freshwater systems and in oceans is greatly dependent on the penetration of light intensity.

3.9 Physical Mixing in the Surface Mixing Zone

Physical or turbulent mixing in the surface mixing zone of the water column might be an important factor to enhance the photoinduced degradation of DOM in waters. The mixing process allows the reactants of a chemical reaction to come more frequently in contact, thus accelerating the reaction rate. It has been shown that the production rates of H_2O_2 are higher for both Suwannee River Fulvic Acid (445 nM h^{-1}) and seawater (86 nM h^{-1}) in stirred samples compared to unstirred ones (211 and 51 nM h^{-1}, respectively) (Mostofa K, Sakugawa H unpublished data). These photoexperiments were conducted using a solar simulator . Simultaneously, the fluorescence intensity of fulvic acid is decreased to a higher extent in stirred samples compared to non-stirred ones. Therefore, physical mixing is an essential factor to increase the reaction rate or promote the photoinduced processes in natural surface waters. Moreover, production of H_2O_2 is merely observed in the surface mixing zone, where H_2O_2 is derived from the photoinduced degradation of DOM (Moore et al. 1993; Sikorski and Zika 1993a, b; Sakugawa et al. 2000; Johnson et al. 1989). Furthermore, the fluorescence intensity of fulvic acids is much lower in the surface mixing zone in lake or seawaters due to solar effects (Mostofa et al. 2005; Hayase and Shinozuka 1995). Therefore, physical mixing in the surface mixing zone is an important factor for promoting the photoinduced degradation of DOM in waters. Mixing processes are typically dependent on physical factors such as strong or weak wind, presence of artificial or natural dams, power-dam outfalls, stream riffles, waterfall, and finally water temperature which affects the stratification-stagnant regime of natural waters.

3.10 Increasing UV Radiation During Ozone Hole Events

The ozone hole due to stratospheric ozone depletion because of anthropogenic activities is a well-known phenomenon in the Antarctic (Qian et al. 2001; Jones and Shanklin 1995) and Arctic oceanic regions (Rex et al. 1997; Randall et al. 2005). Moreover, the incident UV-B radiation is increased at a rate of 10–20 % per decade at temperate latitudes (Kerr and McElroy 1993; Madronich 1992). An increase in UV-B radiation may greatly enhance the production of $HO^{\bullet}$ by inducing higher rates of photolysis of NO_2^- and NO_3^-, and of other redox reactions in natural waters (Qian et al. 2001; Randall et al. 2005). The $HO^\bullet$ formation rates from nitrate, as well as DOM plus nitrite are significantly increased during ozone hole conditions, compared to non-ozone hole periods (Qian et al. 2001). Therefore, a higher production of $HO^\bullet$ during ozone hole events can enhance the photoinduced degradation of DOM. UV transparency of the lake water column is also greatly enhanced during the summer season due to photoinduced degradation of DOM in the lake epilimnion (Morris and Hargreaves 1997). Diffuse attenuation coefficients are greatly varied (39–81 %) seasonally at the epilimnion, and minimum values occur during the summer season (Morris and Hargreaves 1997). Thus, an increase in incident UV radiation (280–400 nm) in response to stratospheric ozone depletion can increase the transformation of surface DOM and, by increasing the UV transparency of water, can also induce additional degradation of DOM in the deeper layers (Qian et al. 2001; Randall et al. 2005).

3.11 Global Warming

Global warming may expand the summer season (Huisman et al. 2006; Sarmiento et al. 2004; Schmittner 2005), which might accelerate the photoinduced degradation of DOM. For example, it might lead high production of $HO^\bullet$ because of the increase in water temperature due to global warming. At the same time, there can be an increase in UV radiation during ozone hole events (Qian et al. 2001; Rex et al. 1997). Global warming may also affect (and possibly enhance) the water column transparency, which is modified on a variety of time scales, and the depth of the mixing layer, as well as lead to changes in climatologic factors such as cloud cover, particulate material and total content of column ozone. These factors may influence the incident UV radiation (Morris and Hargreaves 1997; Morris et al. 1995; Scully and Lean 1994). Global warming may affect the seasonal patterns of chlorophyll and nutrient concentrations in the deep chlorophyll maxima (DCM) in waters (Huisman et al. 2006; Mostofa et al. 2009b; Letelier et al. 2004). The combination of global warming and photoinduced degradation may significantly impact on primary production, species composition, global carbon cycle, biological activities, and finally the seasonal modifications of the water column in natural waters (Huisman et al. 2006; Häder et al. 2011). The effects of global warming on photoinduced degradation of DOM are extensively discussed in the global warming chapter (see chapter "Impacts of Global Warming on Biogeochemical Cycles in Natural Waters").

3.12 Salinity

DOM photoreactivity is significantly increased with salinity or addition of salts in natural waters (Osburn et al. 2009; Hernes and Benner 2003; Osburn and Morris 2003; Anastasio and Newberg 2007; Grebel et al. 2009). Controlled laboratory studies demonstrate that the presence of seawater concentrations of chloride and bromide ions can enhance absorbance photobleaching reaction rates by ~40 %, regardless of DOM source or the presence or absence of carbonate ions (Grebel et al. 2009). In another study, a decrease in CDOM photobleaching at 280 nm is detected when humic CDOM is added to an artificial salinity gradient used to mimic coastal mixing (Minor et al. 2006). Dissolved lignin phenols are significantly affected by salinity and at salinities >25 psu, photooxidation is a dominant factor influencing lignin compositions and concentrations (Hernes and Benner 2003).

The mechanism behind the high photoinduced degradation of DOM with salinity apparently involves two factors: first, irradiated CDOM can induce photoinduced production of hydrogen peroxide (H_2O_2) that is a $HO^•$ source via photolysis or the Fenton reaction, and the photoinduced generation of H_2O_2 is enhanced by salinity. Trace metal ions (M) in salinity or sea waters can complex with DOM (M-DOM) forming a strong ϖ–electron bonding system between metal ions and the functional groups in DOM (see chapter "Complexation of Dissolved Organic Matter With Trace Metal Ions in Natural Waters" for in details explanation). This ϖ–electron in M-DOM complex is rapidly excited photolytically, which is responsible for high production of aqueous electrons (e_{aq}^-) and subsequently the high production of superoxide ion ($O_2^{•-}$), H_2O_2 and $HO^•$, respectively. Indeed, photogeneration of H_2O_2 from ultrafiltered river DOM is substantially increased with salinity, from 15 to 368 nM h^{-1} at circumneutral pH (Osburn et al. 2009). Salinity or NaCl salts can substantially increase the aqueous electrons (e_{aq}^-) from DOM components photolytically in aqueous media (Assel et al. 1998; Gopinathan et al. 1972). This effect subsequently can enhance the H_2O_2 production from DOM components in waters (Moore et al. 1993; Mostofa and Sakugawa 2009; Richard et al. 2007; Fujiwara et al. 1993). Recent studies observe that the sea-salt particulate matter extracted from coastal seawaters show substantially high $HO^•$ production (rate: ~2778–27778 M s^{-1}), approximately 3–4 orders of magnitude greater than $HO^•$ photoformation rates in surface seawater (Anastasio and Newberg 2007), which may support the above phenomena.

Second, the reaction of $HO^•$ with halide ions (X^-) can form reactive halogen radicals ($BrX^{•-}$) that can react with electron-rich functional groups within DOM more selectively than $HO^•$ (Goldstone et al. 2002; Grebel et al. 2009; Salinity can significantly affect the CDOM or FDOM properties, which are responsible for their high photoinduced behavior, which are discussed in detail in other chapters (see chapters "Colored and Chromophoric Dissolved Organic Matter in Natural Waters", "Fluorescent Dissolved Organic Matter in Natural Waters" and "Complexation of Dissolved Organic Matter With Trace Metal Ions in Natural Waters").

4 Factors Controlling the Microbial Degradation of DOM in Waters

Microorganisms are generally responsible for catalyzing the oxidation of organic matter and for inducing changes in the functional groups of DOM, either in deeper waters or in soil and sediment pore waters (Mostofa et al. 2007; Moran et al.

2000; Lønborg and Søndergaard 2009; Lovley and Chapelle 1995; Coble 2007; Hopkinson et al. 2002; Koschorreck et al. 2008; Lønborg et al. 2009a, b). An increase in fulvic acid-like (or humic-like) fluorescence either in deeper waters of lakes and oceans or in dark incubated water samples are considered to be the effect of microbial degradation of organic matter and of the related transformation of the functional groups of DOM (Ma and Green 2004; Mostofa et al. 2007a; b; Moran et al. 2000; Hayase and Shinozuka 1995; Coble 2007; Coble 1996). Microbial degradation of DOM depends on several key factors that can be distinguished as: (1) Occurrence and nature of microbes in waters; (2) Sources of DOM and the quantity of its fermentation products; (3) Temperature; (4) pH; and (5) Sediment depths.

4.1 Occurrence and Nature of Microorganisms

Microbial degradation of organic matter and of functional groups of macromolecules depends on the occurrence and nature of microorganisms in waters (Lovley 2006; Uchida et al. 1998; Lovley et al. 1996; Kotsyurbenko et al. 2001; Coleman et al. 1993; Conrad et al. 1989; Conrad et al. 1989; Morvan et al. 1994). Recent studies demonstrated the presence of methanogens belonging to the *Methanomicrobiaceae*, *Methanobacteriaceae*, *Methanococcaceae*, *Methanosarcinaceae*, and *Methanosaetaceae*, as well as new archaeal lineages within the *Euryarchaeota* (Kotsyurbenko et al. 2007; Basiliko et al. 2003; Cadillo-Quiroz et al. 2006; Casper et al. 2003; Galand et al. 2002; Horn et al. 2003; Sizova et al. 2003; Upton et al. 2000; Utsumi et al. 2003). It is shown that methanogenic archaea and homoacetogenic bacteria are the main H_2 consumers in the absence of inorganic electron acceptors such as nitrate, ferric iron and sulfate, which compete for available H_2 in anoxic environments (Kotsyurbenko et al. 2001). Degradation of alcohols and fatty acids is usually enabled by syntrophy between H_2-producing syntrophic bacteria and H_2-consuming methanogenic archaea (Conrad 1999; Schink 1997). The most important reactions for hydrogenotrophic (Eq. 4.1) and acetotrophic methanogenesis (Eq. 4.1) for degradation of glucose can be expressed below (Eqs. 4.1, 4.2) (Conrad 1999; Thauer et al. 1977):

$$C_6H_{12}O_6 \rightarrow \ CH_3COOH + CO_2 + CH_4 \Delta G^{o\prime} = -346.8 \tag{4.1}$$

$$C_6H_{12}O_6 \rightarrow \ 3CO_2 + 3CH_4 \Delta G^{o\prime} = -418.1 \tag{4.2}$$

An experimental study shows that *D. desulfuricans* can reduce the Fe(III) and sulphate simultaneously at rates comparable to Fe(III) and sulphate reduction under non-limiting H_2 concentration, when only one of the electron acceptors is provided (Coleman et al. 1993). On the other hand, H_2 is metabolized by *D. desulfuricans* at lower concentrations with Fe(III) than with sulphate (Coleman et al. 1993). Interestingly, these bacteria do not metabolize H_2 below ~10^{-5} atm partial pressure (Cord-Ruwisch et al. 1988).

4.2 Sources of DOM and its Fermentation Products

The methanogenesis depends on the sources of organic matter such as vascular plants or algal biomass, the fermentation or degradation products of which are greatly varied in soil, peatland or sediment pore waters. For example, the disintegration or fermentation of vascular plant materials by aerobic and anaerobic bacteria can produce humic substances (fulvic and humic acid), structural polysaccharides, polyphenols, proteins, amino acids, carbohydrates and inorganic components in soil environments (Mostofa et al. 2009a; Malcolm 1985; Chefetz 2002; Cadillo-Quiroz et al. 2010; Hur 2011; Peña-Méndez et al. 2005). In contrast, among the DOM components that originated from algal or phytoplankton biomasses, one can find autochthonous fulvic acid, protein, amino sugars and labile polysaccharides (Mostofa et al. 2009a; Zhang et al. 2009; Li W et al., unpublished data; Parlanti et al. 2000; Benner and Kaiser 2003). The changes of the DOM by microbial processes significantly depend on its sources and composition and/or the mixing ratios of the individual original source materials in natural water (Hur 2011).

It is shown that fulvic and humic acids are composed of diverse functional groups such as –COOH, carboxyl, methoxyl, alcoholic OH, carbohydrate OH and phenolic OH. Low aromaticity is observed in fulvic acid (17 % of aromatic C and 63 % of aliphatic C) compared to humic acid (30 % and 47 %, respectively) (Malcolm 1985; Steelink 2002). Carbon distribution by solid-state CPMAS ^{13}C NMR shows about 24 % of C–O, 3 % of anomeric C, 12 % of C=C, 5 % of φ–O (φ = other elements except C), 16 % of COOH, 4 % of C=O. Elemental analysis showed 38 % of O, 0.87 % of N, 0.74 % of S and 0.62 % of P (Malcolm 1985). Although the chemical structure of autochthonous fulvic acid of algal origin is still unclear, the material is likely to be a macromolecule because of the similarity of its EEM spectra to standard Suwannee River Fulvic Acid (Fig. 1d,e, and f) (Mostofa et al. 2009b). This might be the reason of the effective degradation of the autochthonous fulvic acid of algal origin, which is observed in the EEM images in the lake sediment pore waters Li W et al. (unpublished data). Therefore, it is not surprising that functional groups bound to either fulvic and humic acids of terrestrial origin or autochthonous fulvic acid of algal origin are affected by microbial processes in the sediment waters.

Depending on the presence of either terrestrial plant material or algal or phytoplankton biomass, different fermentation products can be found in a variety of sediment waters. In a similar way, the contribution of H_2 to CH_4 production in different methanogenic sediments is quite variable: 32–46 % in Kichier Lake, 36–46 % in Lake Mendota, 15–39 % in Lake Washington, 17–31 % in anoxic paddy soil, 8 % in Colne Pt. Salt marsh, 4 % in Knaack Lake, 0 % in Lake Constance, 97 % in Kuznechika lake, 74–86 % in Octopus Spring mat, 76–82 % in Blelham Tarn, 71–80 % in Cape Lookout Bight, 100 % in Kings Lake Bog, 95–97 % in Bunger Hills (Antarctica), and 99–100 % in Lake Baikal deep sediments (Schulz and Conrad 1996; Ivanov et al. 1976; Winfrey and Zeikus 1979; Sandbeck and Ward 1981; Jones et al. 1982; Banat et al. 1983; Crill and Martens 1983; Phelps and Zeikus 1984; Kuivila et al. 1989; Lansdown et al. 1992; Rothfuss and Conrad 1992; Galchenko 1994; Namsaraev et al. 1995). It is shown that different types of plant material lead to different rates of acetate formation. There is also a stronger substrate-based coupling of root surface and methanogens in oligotrophic (bog) than in minerotrophic (fen) sites (Cadillo-Quiroz et al. 2010; Ström et al. 2003; Öquist and Svensson 2002). Seasonal algal or phytoplankton blooms might be responsible for formation of acetate and CH_4 in the sediments of deep lakes (Schulz and Conrad 1995). The acetate concentration profiles show maxima (~100 μM in 2 or 4 cm depth) in summer and minima (~5 μM over the entire depth) in winter, when the respective CH_4 concentrations are ~750 μM in summer and ~120 μM in winter (Schulz and Conrad 1995).

It is evidenced that gas bubbles contain about 60–70 % CH_4 with an average $\delta^{13}C$ of –56.2 % and δD of –354 %, and 2 % CO_2 with an average $\delta^{13}C$ of –14.1 % (Thebrath et al. 1993). These data indicate that CH_4 is produced from methyl carbon, *i.e.* mainly using acetate as fermentative substrate (Thebrath et al. 1993). In anoxic paddy soil, interspecies H_2 transfer within methanogenic bacterial associations (MBA) account for 95–97 % of the conversion of $^{14}CO_2$ to $^{14}CH_4$, and only 3–5 % of the $^{14}CH_4$ is produced from the turnover of dissolved H_2 (Conrad et al. 1989a, b). An experimental study demonstrates that the ratio of Fe(II) production to CO_2 production (3.9) is similar to that expected (4.0) for organic carbon oxidation coupled to Fe(III) oxide reduction (Fig. 8) (Roden and Wetzel 1996). The study also shows that the rates of CH_4 production are low during the Fe(III) reduction in oxidized sediments, but increase when the Fe(III) oxides are depleted to background levels (Fig. 8a). The rates of CO_2 and CH_4 production are about

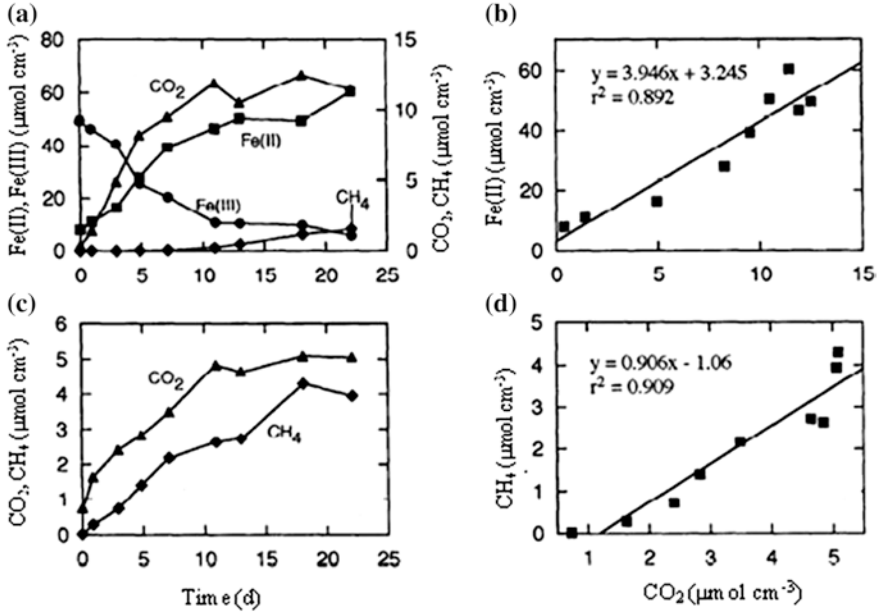

Fig. 8 Fe(III) reduction, CO_2 production, and CH_4 production in oxidized (**a**, **b**) and reduced (**c**, **d**) Talladega wetland sediment slurries. *Data source* Roden and Wetzel (1996)

equal during the incubation of reduced sediments (Fig. 8c,d) (Roden and Wetzel 1996). Therefore, the occurrence and the nature of organic matter and its fermentation or disintegration products are key factors for the production of CO_2, CH_4 and other end products in the aquatic environments.

4.3 Temperature

The growth of homoacetogenic bacteria and methanogenic archaea significantly depends on the ambient temperature (Table 2) (Kotsyurbenko et al. 2001; Kotsyurbenko et al. 2007; Thebrath et al. 1993; Westermann 1994; Kotsyurbenko et al. 1995; Simankova et al. 2000; Zinder 1990). It is shown that the microbial function is typically much higher at low temperature (5.0–7.0 °C), showing maximum bacterial abundance (3.9–7.9 $\times 10^5$ cells ml^{-1}, mean = 6.4) and biomass (4.0–6.7 μg C L^{-1}, mean = 5.2). Lower values (1.3–2.5 $\times 10^5$ cells ml^{-1}, mean = 1.8; and 1.3–2.4 μg C L^{-1}, mean = 1.7, respectively) have been found at higher temperature (7.5–11.1 °C) in open water in Lake La Caldera (Carrillo et al. 2002). Homoacetogenic bacteria and methanogenic archaea can consume H_2 over a temperature range of 1–35 °C, but their optimum temperature is often high (~20–30 °C, Table 2). Homoacetogenic *A. bakii, A. tundrae* and the methanogenic strain MSB have shown the largest temperature range for optimal H_2 consumption, which is extending at least from 4 to 30 °C (Kotsyurbenko et al. 2001). However, *A. fimetarium*, *A. paludosum* and strain MSP become less efficient toward H_2 consumption when the temperature decreases below 10 °C (Kotsyurbenko et al. 2001). Low temperatures are often favorable for acetogenesis, which becomes a quantitatively important process in anaerobic environments (Nozhevnikova et al. 1994; Kotsyurbenko et al. 1993).

At low temperature, homoacetogenic bacteria outcompetes methanogens for H_2 in laboratory experiments (Conrad et al. 1989; Kotsyurbenko et al. 1993). According to kinetic estimations, homoacetogens have a much higher growth rate at low temperature than methanogens (Kotsyurbenko et al. 1996). It is also shown that the contribution of methanogenic bacterial associations (MBA) to H_2-dependent methanogenesis is enhanced (it reaches 99 %) when the temperature is shifted from 30 to 17 °C, or when the soil is planted with rice (Conrad et al. 1989a, b). This enhancement is partially due to an increased utilization of dissolved H_2 by chloroform-insensitive non-methanogenic bacteria, most probably homoacetogens, so that CH_4 production is almost completely restricted to H_2-syntrophic MBA. Acetate is the precursor of approximately two-thirds of the methane produced in mesophilic (30–40 °C) and thermophilic (45–65 °C) anaerobic bioreactors (Zinder 1990). Increasing the incubation temperature of two swamp slurries from 2 to 37 °C resulted in a 8- to 18-fold increase in the H_2 partial pressure (Westermann 1994). The study also shows that the concentration of volatile fatty acids remained fairly constant except for butyrate, which decreased with increasing temperature.

Despite the constant low temperature (4 °C) during the summer and winter seasons in lake sediment pore waters, high variations in methane production in summer compared to winter are suggested to be caused by algal biomass blooms in surface waters (Schulz and Conrad 1995). In this case, the effect of temperature would not be significant in the microbial formation of methane from acetate in the sediment pore waters. The effect of temperature on methanogenesis mostly depends on the nature of organic sediments, presence of microorganisms and the fermentation or degradation products in water.

4.4 pH

The pH is an important factor that influences the rate of methanogenesis as well as the CH_4 production pathway and the methanogenic archaeal community in sediment waters. The methanogenesis is typically inhibited at low pH, where microbial turnover rates are slower, although significant methane production is still observed in acidic peat lands (Kotsyurbenko et al. 2007; Horn et al. 2003; Dunfield et al. 1993; Hornibrook et al. 2000; Goodwin and Zeikus 1987; Bräuer et al. 2004, 2006). Acetate as a major carbon source for methanogenesis may be unavailable to the methanogens at low pH because of the inhibitory effect of non-dissociated acetate toward methanogenesis (Fukuzaki et al. 1990). Low pH conditions may also reduce the microbial processes of H_2 production and consumption in anaerobic environments (Goodwin et al. 1988). An isolate from a landfill is able to grow at pH 5 (Lapado and Barlaz 1997) and an isolate from a peat land grows at pH 5.3 but generates some methane down to pH 3.1 (Williams and Crawford 1985). Acidotolerant hydrogenotrophic methanogenic consortia have been enriched from a peat bog at pH 4 (Sizova et al. 2003), and molecular analysis of an acidic peat bog reveals the presence of *Methanomicrobiaceae* and *Methanosarcinaceae* at pH 4.5 (Kotsyurbenko et al. 2004).

In acidic mining lakes, sulfate reduction often occurs when the pH in the sediment is almost neutral (Meier et al. 2004). An increase with depth of pH from 2.6 up to 6 enhanced the production of CH_4 and CO_2 in the sediment cores of Lake Caviahue (Koschorreck et al. 2008). In the most acidic surface layer of the sediment ($pH < 4$), methanogenesis is inhibited as suggested by a linear CH_4 concentration profile. In contrast, methanogenesis is highly active below 40 cm depth at high pH (>4). The carbon isotope composition of CH_4 is between –65 and –70 ‰, which is indicative of the biological origin of methane in Lake Caviahue. Therefore, it is suggested that the high biomass content of the sediment may induce high rates of sulfate reduction, which presumably raises the pH and creates favorable conditions for methanogens in deeper sediment layers (Koschorreck et al. 2008). On the other hand, the ratio of $\delta^{13}CO_2$ to $\delta^{13}CH_4$ increases from 1.053 at pH 6 up to 1.072 at pH 3.8, indicating a relative increase of hydrogenotrophic methanogenesis at low pH values (Hornibrook et al. 2000; Whiticar 1999). The genus *Methanobacterium* contains two alkaliphilic and one moderate acidophilic species, and collectively they have the widest growth ranges over a pH variation from 3.8 to 9.9 (Kotelnikova et al. 1998; Worakit et al. 1986; Patel et al. 1990). The pH is thus one of the important factors that can control the methanogenesis in sediment.

4.5 Sediment Depths

It is shown that the degradation of organic matter is mostly occurring in the upper sediment layer (1–10 cm depths) in lakes or in soil (Nakane et al. 1997; Li et al. unpublished data; Roden and Wetzel 1996; Schulz and Conrad 1995). However, the methanogenesis may also occur in deeper sediment layers under favorable conditions, either in peatlands or in sediment pore waters (Koschorreck et al. 2008; Nakagawa et al. 2002; Galand et al. 2005). In the sediments of Lake Caviahue the CH_4 concentration is steadily increased from 0 to 6.0 mM from 1 to 30 cm sediment depths (Fig. 9) (Koschorreck et al. 2008). The concentration of CH_4 typically reaches saturation (~1 mM) at 3–40 cm below the top few centimeters in unvegetated sediments. In vegetated sediments CH_4 concentrations are very low (0.0–0.1 mM) until 20 cm, after which they increase at ~1 mM level at 40 cm (Roden and Wetzel 1996). In humic bog lakes the deeper parts of the water column favor microdiversification of methanogens, whilst the periodically disturbed water column of shallower dimictic lakes promotes genetically more diverse methanogen communities (Milferstedt et al. 2010). In peatlands, hydrogenotrophic methanogenesis is the predominant pathway of CH_4 formation, accounting for 50 to 100 % of total CH_4 production, particularly in the deeper layers (Nakagawa et al. 2002; Galand et al. 2005). Therefore, sediment depths play an important role in the production of methane in sediment waters.

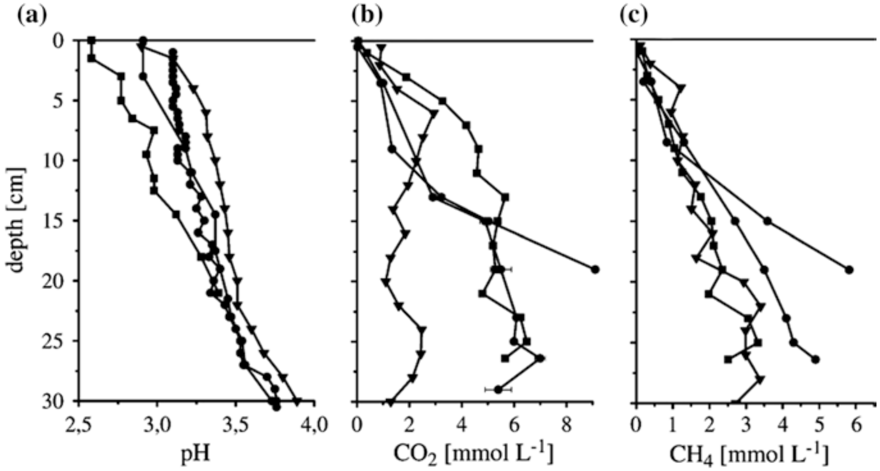

Fig. 9 Vertical profiles of pH (**a**), dissolved gases CO_2 (**b**) and CH_4 (**c**) in different sediment cores from Lake Caviahue. The pH is measured in KCl extracts during the field work in 2003 (■ 2001, ● 2003, ▼ 2004). *Data source* Koschorreck et al. (2008)

5 Photoproducts of DOM and Their Significance on Biogeochemical Cycles in Natural Waters

Photoinduced degradation of DOM in natural waters generally occurs by the sequential degradation of high molecular weight substances, producing low molecular weight compounds and ending up in mineralization yielding CO_2, CO, DIC, COS, and so on (Table 3) (Reche et al. 1999; Ma and Green 2004; Graneli et al. 1996, 1998; Xie et al. 2004; Mopper et al. 1991; Miller and Zepp 1995; Bertilsson and Tranvik 2000; Fujiwara et al. 1995; Bushaw et al. 1996; Miller and Moran 1997; Stiller and Nissenbaum 1999; White et al. 2010; Valentine and Zepp 1993; Mostofa K et al., unpublished data; Francko and Heath 1982; Fang 2004; Chen et al. 2001; Karl and Tien 1997; Jones 1991; Jones and Amador 1993). Photoinduced degradation on DOM can typically lead to a variety of photo products, which can be distinguished in: (1) Hydrogen peroxide and organic peroxides; (2) Low molecular weight organic substances; (3) Aromatic mono- and dibasic acids; (4) Microbiologically labile organic photoproducts; (5) Carbon-gas end photoproducts; (6) Nitrogenous compounds (e.g. NH_4^+); (7) Phosphate; and (8) Release of energy to the water ecosystem.

5.1 Photoinduced Formation of Hydrogen Peroxide and Organic Peroxides

The formation of hydrogen peroxide (H_2O_2) and organic peroxides (ROOH) is the primary step of the photoinduced processes involving DOM in waters. The concentration levels of H_2O_2 are significantly different for a variety of waters, ranging from 4 to 3200 nM in rivers, 10–800 nM in lakes, and 0–1700 nM in seawaters as mentioned in chapter "Photoinduced and Microbial Generation of Hydrogen Peroxide and Organic Peroxides in Natural Waters". The concentration levels of ROOH compounds are also highly variable in natural waters, showing low concentrations in rivers (0–200 nM) and relatively higher levels in seawater (1–389 nM). H_2O_2 and ROOH may form free radicals ($HO^\bullet$, $RO^\bullet$, R = H or alkyl group), either directly upon photolysis or indirectly by photo-Fenton reactions. The reactive radicals thus generated contribute to the degradation of the organic substances that make up DOM.

5.2 Photoinduced Formation of Low Molecular Size Organic Substances

Photoinduced degradation can convert the high molecular weight DOM into low molecular size organic substances in natural waters (Table 3) (Moran and Zepp 1997; Biddanda and Benner 1997; Kramer et al. 1996; Allard et al. 1994; Yoshioka et al. 2007;

Table 3 Concentration levels and photoproduction rates of various end products generated from photochemical degradation of dissolved organic matter in natural waters and in photoexperiments conducted conducted on natural waters as well as on standard organic subsatnces

Samples/Sources of water	Source of light/Natural level	H_2O_2 (nM)	ROOHs (nM)	LMW compounds (nM h^{-1})	DIC (nM h^{-1})	CO_2(nM or nM h^{-1})	CO (nM or nM h^{-1})	Hydrocarbons (nM)	Ammonium (nM or nM h^{-1})	COS (ng L^{-1})	PO_4^{3-} (µg L^{-1})	DOC (µM C)	DON (µM)	References
Rivers														
Suwannee River, FL (29°N)	Xe lamp	–	–	–	80–630	–	4.1–5.1	–	–	–	–	4100–5150	–	Miller and Zepp (1995)
Suwannee River, FL (29°N)	Xe lamp	–	–	–	–	–	41–1500	–	–	–	–	2250–3917	–	Valentine and Zepp (1993)
Sturgeon River (47°N)	Sunlight (0 m)	–	–	–	2424	–	–	–	–	–	–	2798	–	Ma and Green (2004)
Sturgeon River (47°N)	Sunlight (6.5 m)	–	–	–	606	–	–	–	–	–	–	2873	–	Ma and Green (2004)
Sturgeon River (47°N)	Sunlight (24 m)	–	–	–	2727	–	–	–	–	–	–	2818	–	Ma and Green (2004)
Sturgeon River (47°N)	Dark	–	–	–	99970	–	–	–	–	–	–	2798	–	Ma and Green (2004)
Houghton Marsh (47°N)	Xe lamp	–	–	–	–	–	120–1330	–	–	–	–	2000–3083	–	Valentine and Zepp (1993)
Okefenokee Swamp (31°N)	Xe lamp	–	–	–	–	–	1200	–	–	–	–	3083	–	Valentine and Zepp (1993)
Jordan River (31°N), East African Rift Valley	Natural level	–	–	–	–	–	–	–	20588	–	8.8–85	–	–	Stiller and Nissenbaum (1999)
En Feshkha (31°N), East African Rift Valley	Natural level	–	–	–	–	–	–	–	<588	–	0–6	–	–	Stiller and Nissenbaum (1999)

(continued)

Table 3 (contniued)

Samples/Sources of water	Source of light/Natural level	H_2O_2 (nM)	ROOHs (nM)	LMW compounds (nM h^{-1})	DIC (nM h^{-1})	CO_2(nM or nM h^{-1})	CO (nM or nM h^{-1})	Hydrocarbons (nM)	Ammonium (nM or nM h^{-1})	COS (ng L^{-1})	PO_4^{3-} (μg L^{-1})	DOC (μM C)	DON (μM)	References
Nahal David (31°N), East African Rift Valley	Natural level	–	–	–	–	–	–	–	1176	–	<5	–	–	Stiller and Nissenbaum (1999)
Ein Noit (31°N), East African Rift Valley	Natural level	–	–	–	–	–	–	–	50588	–	<5	–	–	Stiller and Nissenbaum (1999)
Suwannee River, whole	Xe lamp	–	–	–	–	–	–	–	360	–	–	ND	74	Bushaw et al. (1996)
Boreal Pond, whole (July)	Xe lamp	–	–	–	–	–	–	–	80–150	–	–	3000	55	Bushaw et al. (1996)
Okefenokee swamp, whole	Xe lamp	–	–	–	–	–	–	–	40–340	–	–	3840	86	Bushaw et al. (1996)
Rivers	Natural level	4 –3200	0–200	–	–	–	–	–	–	–	–	–	–	Table 1 (Photoinduced and Microbial Generation of Hydrogen Peroxide and Organic Peroxides in Natural Waters)
Satilla River: Air-saturation	Xe lamp	–	–	–	–	22950	–	–	–	–	–	1570	–	Xie et al. (2004)

(continued)

Table 3 (contniued)

Samples/Sources of water	Source of light/Natural level	H_2O_2 (nM)	ROOHs (nM)	LMW compounds (nM h^{-1})	DIC (nM h^{-1})	CO_2(nM or nM h^{-1})	CO (nM or nM h^{-1})	Hydrocarbons (nM)	Ammonium (nM or nM h^{-1})	COS (ng L^{-1})	PO_4^{3-} (µg L^{-1})	DOC (µM C)	DON (µM)	References
Satilla River: O_2-saturation	Xe lamp	–	–	–	–	26450	–	–	–	–	–	1620	–	Xie et al. (2004)
Satilla River: air-saturation + DFOM**	Xe lamp	–	–	–	–	5950	–	–	–	–	–	1588	–	Xie et al. (2004)
Satilla River: O_2-saturation + DFOM	Xe lamp	–	–	–	–	7150	–	–	–	–	–	1545	–	Xie et al. (2004)
Satilla River: N_2-saturation	Xe lamp	–	–	–	–	1913	–	–	–	–	–	1574	–	Xie et al. (2004)
Altamaha River: air-saturation	Xe lamp	–	–	–	–	13150	–	–	–	–	–	1442	–	Xie et al. (2004)
Altamaha River: O_2-saturation	Xe lamp	–	–	–	–	18325	–	–	–	–	–	1430	–	Xie et al. (2004)
Altamaha River: air-saturation + DFOM	Xe lamp	–	–	–	–	5428	–	–	–	–	–	1441	–	Xie et al. (2004)
Altamaha River: O_2-saturation + DFOM	Xe lamp	–	–	–	–	5622	–	–	–	–	–	1406	–	Xie et al. (2004)
Lakes														
Lake Superior (47°N)	Sunlight (0 m)	–	–	–	10606	–	–	–	–	–	–	161	–	Ma and Green (2004)
Lake Superior (47°N)	Sunlight (6.5 m)	–	–	–	10909	–	–	–	–	–	–	160	–	Ma and Green (2004)

(continued)

Table 3 (contniued)

Samples/Sources of water	Source of light/Natural level	H_2O_2 (nM)	ROOHs (nM)	LMW compounds (nM h^{-1})	DIC (nM h^{-1})	CO_2(nM or nM h^{-1})	CO (nM or nM h^{-1})	Hydrocarbons (nM)	Ammonium (nM or nM h^{-1})	COS (ng L^{-1})	PO_4^{3-} (μg L^{-1})	DOC (μM C)	DON (μM)	References
Lake Superior (47°N)	Sunlight (24 m)	–	–	–	3182	–	–	–	–	–	–	200	–	Ma and Green (2004)
Lake Superior (47°N)	Dark	–	–	–	175485	–	–	–	–	–	–	``	–	Ma and Green (2004)
38 Lakes (55 –71°N)	Artificial	–	–	2500–44200	1300–158500	–	–	–	–	–	–	167 –1833	–	Bertilsson and Tranvik (2000)
Kinoshe Lake (51°N)	Xe lamp	–	–	–	–	–	260	–	–	–	–	1250	–	Valentine and Zepp (1993)
5 Lakes (57°N)	Natural sunlight	–	–	–	800–3400	–	–	–	–	–	–	325–1617	–	Graneli et al. (1996)
10 Lakes (57°N in Sweden and 3–22°S in Brazil)	Natural sunlight	–	–	–	25833–1612833	–	–	–	–	–	–	242–3483	–	Graneli et al. (1998)
24 Lakes, Wisconsin and Michigan, U.S.A	Natural level	–	–	–	–	–	–	–	–	–	8.5–129.3	308–1792	–	Reche et al. (1999)
Crazy Eddie Bog, northeastern Ohio	Natural level	–	–	–	–	–	–	–	–	–	2.0–24.0	–	–	Francko and Heath (1982)
Lake Biwa, Japan, 35°N: 0.5 m	Natural level	–	–	–	–	–	–	–	–	–	0.003–0.011	–	–	Mostofa K et al. (unpublished)
Lake Biwa, Japan, 35°N: 10 m	Natural level	–	–	–	–	–	–	–	–	–	0.005–0.009	–	–	Mostofa K et al. (unpublished)

(continued)

Table 3 (contniued)

Samples/Sources of water	Source of light/Natural level	H_2O_2 (nM)	ROOHs (nM)	LMW compounds (nM h^{-1})	DIC (nM h^{-1})	CO_2(nM or nM h^{-1})	CO (nM or nM h^{-1})	Hydrocarbons (nM)	Ammonium (nM or nM h^{-1})	COS (ng L^{-1})	PO_4^{3-} (µg L^{-1})	DOC (µM C)	DON (µM)	References
Lake Biwa, Japan, 35°N: 20 m	Natural level	–	–	–	–	–	–	–	–	–	0.004–0.009	–	–	Mostofa K et al. (unpublished)
Lake Biwa, Japan, 35°N: 40 m	Natural level	–	–	–	–	–	–	–	–	–	0.003–0.008	–	–	Mostofa K et al. (unpublished)
Lake Biwa, Japan, 35°N: 80 m	Natural level	–	–	–	–	–	–	–	–	–	0.005–0.023	–	–	Mostofa K et al. (unpublished)
Lakes	Natural level	10–800	–	–	–	–	–	–	–	–	–	–	–	Table 1 (Photoinduced and Microbial Generation of Hydrogen Peroxide and Organic Peroxides in Natural Waters)
Estuaries and sea waters														
Ohta River Estuary (34°N), Japan	Natural (July)	–	–	–	–	–	–	–	–	54.4	–	~80–290	–	Fujiwara et al. (1995)
Ohta River Estuary (34°N), Japan	Natural (December)	–	–	–	–	–	–	–	–	23.9	–	"	–	Fujiwara et al. (1995)
Delaware estuary	Xe lamp	–	–	–	–	83–625	–	–	–	–	–	–	–	White et al. (2010)

(continued)

Table 3 (contniued)

Samples/Sources of water	Source of light/Natural level	H_2O_2 (nM)	ROOHs (nM)	LMW compounds (nM h^{-1})	DIC (nM h^{-1})	CO_2(nM or nM h^{-1})	CO (nM or nM h^{-1})	Hydrocarbons (nM)	Ammonium (nM or nM h^{-1})	COS (ng L^{-1})	PO_4^{3-} (µg L^{-1})	DOC (µM C)	DON (µM)	References
Seto Inland Sea (34°N), Japan (surface: 0–5 m)	Natural	–	–	–	–	–	–	–	–	~5–17	–	“	–	Fujiwara et al. (1995)
Seto Inland Sea (34°N), Japan (deeper: 20 m)	Natural	–	–	–	–	–	–	–	–	~3–5	–	“	–	Fujiwara et al. (1995)
Coastal waters (31°N), East African Rift Valley	Natural level	–	–	–	–	–	–	–	82353–2047059	–	5 –63	–	–	Stiller and Nissenbaum (1999)
East China Sea, 24–30°N, China	Natural level	–	–	–	–	–	–	–	–	–	1.6–96.3	–	–	Fang (2004)
East China Sea, 24–30°N, China	Natural level (summer)	–	–	–	–	–	–	–	–	–	2.6–22.7	–	–	Chen et al. (2001)
East China Sea, 24–30°N, China	Natural level (winter)	–	–	–	–	–	–	–	–	–	3.5–23.4	–	–	Chen et al. (2001)
North Pacific Ocean, Station ALOHA (22°N)	Natural level (0–150 m)	–	–	–	–	–	–	–	–	–	~0.3–9.6	–	–	Karl and Tien (1997)

(continued)

Table 3 (contniued)

Samples/Sources of water	Source of light/Natural level	H_2O_2 (nM)	ROOHs (nM)	LMW compounds (nM h^{-1})	DIC (nM h^{-1})	CO_2(nM or nM h^{-1})	CO (nM or nM h^{-1})	Hydrocarbons (nM)	Ammonium (nM or nM h^{-1})	COS (ng L^{-1})	PO_4^{3-} (μg L^{-1})	DOC (μM C)	DON (μM)	References
Intracoastal Waterway, caostal waters (30°N)	Xe lamp	–	–	–	–	–	110	–	–	–	–	267	–	Valentine and Zepp (1993)
Live Oak, Gulf coast of Florida (30°N)	Xe lamp	–	–	–	–	–	90	–	–	–	–	642	–	Valentine and Zepp (1993)
Sargasso Sea (photic zone)	Natural	–	–	–	–	–	5.8	–	–	–	–	–	–	Jones (1991)
Sargasso Sea (aphotic zone)	Natural	–	–	–	–	–	0.1	–	–	–	–	–	–	Jones (1991)
Sapelo Island Marsh, GA (31°N)	Natural	–	–	–	40–1280	–	3.3–4.9	–	–	–	–	500	–	Miller and Zepp (1995)
Gulf of Mexico (28°N)	Natural	–	–	–	120–400	–	15.8–24.8	–	–	–	–	170	–	Miller and Zepp (1995)
Seawater + humic substances (SH)	Artificial sunlight	–	–	–	2300	–	147	–	–	–	–	695	–	Miller and Moran (1997)
Seawater + the control addition (SC)	Artificial sunlight	–	–	–	1600	–	104	–	–	–	–	515	–	Miller and Moran (1997)
Artificial seawater + the control addition (AC)	Artificial sunlight	–	–	–	300	–	40	–	–	–	–	241	–	Miller and Moran (1997)

(continued)

Table 3 (contniued)

Samples/Sources of water	Source of light/Natural level	H_2O_2 (nM)	ROOHs (nM)	LMW compounds (nM h^{-1})	DIC (nM h^{-1})	CO_2(nM or nM h^{-1})	CO (nM or nM h^{-1})	Hydrocarbons (nM)	Ammonium (nM or nM h^{-1})	COS (ng L^{-1})	PO_4^{3-} (µg L^{-1})	DOC (µM C)	DON (µM)	References
Sargasso Sea waters (1–20 m)	Sunlight	–	–	4.1	–	–	4.1	–	–	–	–	–	–	Mopper et al. (1991)
Sargasso Sea waters (20–150 m)	Sunlight	–	–	3.3	–	–	9.6	–	–	–	–	–	–	Mopper et al. (1991)
Sargasso Sea waters (500–4000 m)	Sunlight	–	–	10.6	–	–	16.1	–	–	–	–	–	–	Mopper et al. (1991)
Southeastern Caribbean Sea & Gulf of Paria	Natural level (Spring)	–	–	–	–	–	0.9–6.3	–	–	–	–	–	–	Jones and Amador (1993)
Southeastern Caribbean Sea & Gulf of Paria	Natural level (Fall)	–	–	–	–	–	0.6–31.6	–	–	–	–	–	–	Jones and Amador (1993)
Seawater	Natural level	0–1700	1–389	–	–	–	–	–	–	–	–	–	–	Table 1 ("Photoinduced and Microbial Generation of Hydrogen Peroxide and Organic Peroxides in Natural Waters")

(continued)

Table 3 (contniued)

Samples/Sources of water	Source of light/Natural level	H_2O_2 (nM)	ROOHs (nM)	LMW compounds (nM h^{-1})	DIC (nM h^{-1})	CO_2(nM or nM h^{-1})	CO (nM or nM h^{-1})	Hydrocarbons (nM)	Ammonium (nM or nM h^{-1})	COS (ng L^{-1})	PO_4^{3-} (μg L^{-1})	DOC (μM C)	DON (μM)	References
Standard and extracted organic substances						–								
Fluka humic	Xe lamp	–	–	–	–	–	1500	–	–	–	–	2500	–	Valentine and Zepp (1993)
Contech fulvic	Xe lamp	–	–	–	–	–	1600	–	–	–	–	4333	–	Valentine and Zepp (1993)
Oyster River fulvic (43°N)	Xe lamp	–	–	–	–	–	3200	–	–	–	–	4667	–	Valentine and Zepp (1993)
Soil fulvic (43°N)	Xe lamp	–	–	–	–	–	3330	–	–	–	–	4667		Valentine and Zepp (1993)
Oyster River, fulvic acid	Xe lamp	–	–	–	–	–	–	–	320	–	–	2840	36	Bushaw et al. (1996)
Fluka, humic acid	Xe lamp	–	–	–	–	–	–	–	230	–	–	1942	51	Bushaw et al. (1996)
Boreal Pond, fulvic acid (August)	Xe lamp	–	–	–	–	–	–	–	65	–	–	1133	24	Bushaw et al. (1996)
Boreal Pond, inlet, fulvic acid (June)	Natural	–	–	–	–	–	–	–	370	–	–	895	–	Bushaw et al. (1996)
Satilla River estuary, fulvic acid	Natural	–	–	–	–	–	–	–	50	–	–	787	20	Bushaw et al. (1996)

* Rate estimated using the deduction of initial values (0 h) from the nearest detected values (2, 8, and 24 h) for Satilla River and (4 and 18 h) for Altamaha River waters

** DFOM indicates the deferoxamine mesylate that is a strong Fe(III)-complexing ligand that forms nearly photo-inert complexes

Amador et al. 1989; Malcolm 1990; Mopper et al. 1991; Bertilsson and Tranvik 2000; Chen et al. 1978; Corin et al. 1996; de Haan 1993; Sun et al. 1993; Hongve 1994; Peuravuori and Pihlaja 1997). The major low molecular size substances examined are polysaccharides, N-acetylamino sugars, polypeptides, lipids, proteins, n-C_{16} and n-C_{18} fatty acid methyl esters, etc. The conversion rate of DOM into identifiable organic photoproducts is 20 % of the bleaching rate of the DOM, leaving a vast unidentified pool of bleached organic matter in natural waters (Miller and Zepp 1995). The unidentified bleached DOM would account for a large proportion of the total biologically available photoproducts (Miller and Moran 1997).

Photoinduced degradation of DOM can produce a variety of low molecular weight (LMW) aliphatic organic compounds which are considered to be microbiologically labile in the aquatic environment (Moran and Zepp 1997; Dahlén et al. 1996; Wetzel et al. 1995; Corin et al. 1996). The most common labile LMW organic compounds include formaldehyde, formic acid, formate, acetaldehyde, acetate, acetic acid, hydroxyacetic acid, hydroxyacetate, acetone, propanal, oxalic acid, oxalate, citric acid, citrate, glyoxal, methylglyoxal, glyoxylic acid, glyoxylate, ketomalonic acid, malonic acid, malonate, levulinic acid, levulinate, succinic acid, succinate, pyruvic acid and pyruvate. Nine organic peroxides (ROOH) such as methyl hydroperoxide, hydroxymethyl hydroperoxide, ethyl hydroperoxide, 1-hydroxyethyl hydroperoxide, 2-hydroxyethyl hydroperoxide, 1-hydroxypropyl hydroperoxide, 2-hydroxypropyl hydroperoxide, 3-hydroxypropyl hydroperoxide, and bis(hydroxymethyl)peroxide are observed in air and rainwaters (Hellpointner and Gäb 1989; Hewitt and Kok 1991; Jackson and Hewitt 1996). Precipitation is a potential source of these peroxides into surface waters, where they are microbiologically labile in natural waters (Mostofa 2005). A rapid decrease of peracetic acid added to unfiltered river waters was detected in dark controlled samples, suggesting that the organic peroxides are microbiologically labile (Mostofa 2005).

Some long-chain aliphatic organic acids, such as 2-hydroxy propanoic acid, 3-oxobutanoic acid, 4-oxopentanoic acid, hexanoic acid, pentanedioic acid, octanoic acid, nonanoic acid, and decanoic acid, are produced by the Photoinduced degradation of humic substances extracted from lakes (Corin et al. 1996). The production of keto acids such as 3-oxobutanoic acid and 4-oxopentanoic acid is greatly enhanced by an increase of the UV-dose. They are mostly produced from fulvic acid rather than humic acid (Corin et al. 1996), probably because of the higher percentage of aliphatic carbon bound to fulvic acid (63 %) compared to humic acid (47 %) (Malcolm 1985). Carboxylic acids (oxalic, malonic, formic, acetic) are usually major products of the photoinduced degradation of DOM (25–34.4 %) (Ma and Green 2004; Bertilsson et al. 1999; Bertilsson and Tranvik 2000).

The total production rate of LMW organic substances is much higher in lakes (2500–44200 nM h^{-1}) than in seawater (3.3–10.6 nM h^{-1}) (Table 3). Variations of the photolytically produced LMW carboxylic acids in different lakes are linked to the presence of fulvic and humic acids in DOM (Bertilsson and Tranvik 1998). The LMW organic substances undergo a rather fast disappearance in natural waters, probably because of two major pathways. First of all, the LMW organic compounds can be rapidly assimilated by natural microorganisms or bacterial populations and thus participate to the food chains for the growth of microbes in natural waters. Moreover, the LMW organic compounds can be photolytically mineralized into final end photoproducts such as CO or CO_2, which can take part to the global carbon cycle (Miller and Zepp 1995; Kieber et al. 2001).

5.3 Photoinduced Formation of Aromatic Mono- and Dibasic Acids

Photoinduced degradation reactions can convert the high molecular weight DOM into a variety of aromatic mono- and dibasic acids, phenolic compounds, aromatic aldehydes and ketones in waters (Kramer et al. 1996; Wetzel et al. 1995; Chen et al. 1978; Corin et al. 1996; Leenheer and Croue 2003; Peuravuori and Pihlaja 1997; Haan et al. 1979; Choudhry 1981; Langvik et al. 1994; Schmitt-Kopplin et al. 1998). The aromatic compounds most commonly identified as photo products are 4-hydroxy- and 4-hydroxy-3-methoxybenzaldehyde, benzoic acid and its derivatives such as 2-hydroxy-, 3-hydroxy-, 4-hydroxy-, 2,4-dihydroxy-, 3,4-dihydroxy-, 3-methoxy- and 4-hydroxy-3-methoxy-benzoic acid, 1,2-, 1,3- and 1,4-benzenedicarboxylic acid, benzene-di, -tri-, tetra-, penta-, and -hexa-carboxylic acids, decanoic acid and its derivatives such as tetra-, hexa- and octa-decanoic acid, acetophenone and its derivatives, methoxybenzene and its derivatives, methoxytoluenes, methoxystyrene, phenols, methoxylated phenols and hydroxyfuran. Most of the LMW aromatic acids are formed from humic and fulvic acids during the first 2 h irradiation of the natural humic waters. Prolonged irradiation may lead to a decrease of their concentrations due to further mineralization to end products (Corin et al. 1996).

5.4 Photoinduced Formation of Carbon-Gas End Photoproducts Including DIC

The photo mineralization of DOM leads to the formation of carbon-gas end photoproducts, which include CO, CO_2, dissolved inorganic carbon (DIC, usually defined as the sum of an equilibrium mixture of dissolved CO_2, H_2CO_3, HCO_3^-, and CO_3^{2-}: (Eq. 5.1) and carbonyl sulfide (COS) in natural waters (Table 3) (Reche et al. 1999; Ma and Green 2004; Graneli et al. 1996, 1998; Clark et al. 2004; Xie et al. 2004; Borges et al. 2008; Kujawinski et al. 2009; Tranvik et al. 2009; Omar et al. 2010; Ballaré et al. 2011; Zepp et al. 2011; Mopper et al. 1991; Miller and Zepp 1995; Bertilsson and Tranvik 2000; Fujiwara et al. 1995; Bushaw et al. 1996; Miller and Moran 1997; White et al. 2010; Cai 2011; Johannessen et al. 2007; Valentine and Zepp 1993; Molot et al. 2005; Francko and Heath 1982; Fang 2004; Chen et al. 2001; Karl and Tien 1997; Jones 1991; Jones and Amador 1993; Cai and Wang 1998; Zepp et al. 1998; Cai et al. 1998, 1999; Fichot and

Fig. 10 Relationship between DOC concentration and DIC (Fig. a) or CO (Fig. b) photoproducts generated in photo experiments conducted on different sources of natural waters. *Data source* Table 4 and references therein

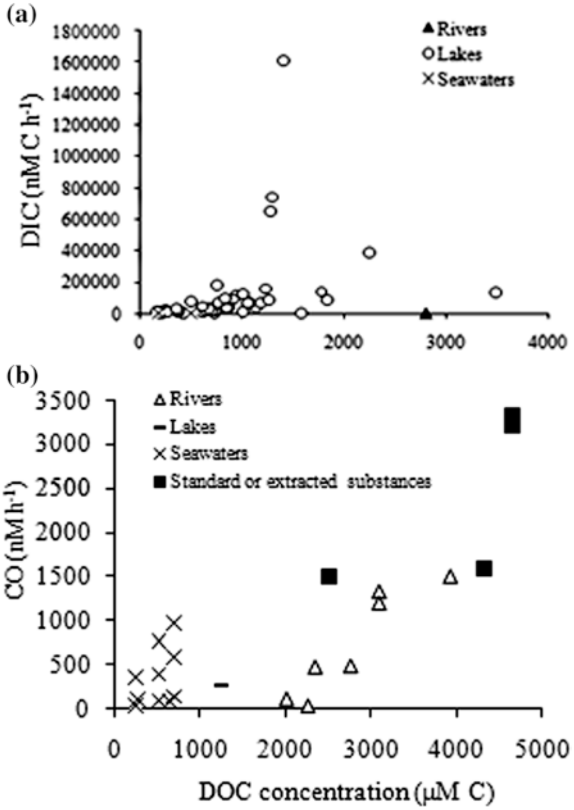

Miller 2010; Liu et al. 2010; Lohrenz et al. 2010). It is shown that gaseous CO_2 is rapidly dissolved in waters, which can be presented as (Eq. 5.1) (Liu et al. 2010):

$$CO_2 + H_2O \leftrightarrow H_2CO_2 \leftrightarrow H^+ + HCO_3{}^- \leftrightarrow 2H^+ + CO_3{}^{2-} \tag{5.1}$$

where the reaction (Eq. 5.1) is an equilibrium mixture of dissolved carbondioxide, carbonic acid, bicarbonate and carbonate ions. The proportion of each species depends on pH whereas at high pH the reaction shifts to the right hand side of (Eq. 5.1) and bicarbonate ($HCO_3{}^-$) at pH between 7 and 9 dominates, approximately 95 % of the carbon in the water. At high pH > 0.5, carbonate predominates (Dreybrodt 1988). DIC is also derived remarkably by carbonate dissolution with uptake of CO_2 in soil water (Eq. 5.2), and weathering as well as dissolution of silicate minerals (Eq. 5.3) (Liu et al. 2010; Dupré et al. 2003; Mortatti and Probst 2003).

$$CaCO_3 + CO_2 + H_2O = Ca^{2+} + 2HCO_3^- \tag{5.2}$$

$$2CO_2 + 3H_2O + CaSiO_3 + 2HCO_3^- + H_4SiO_4 \tag{5.3}$$

The concentration levels of carbon-gas photoproducts are highly variable among rivers, lakes and seawaters studied under light and dark conditions (Table 3;

Fig. 10). The production rate of DIC in irradiated samples is 80–2420 nM h^{-1} in rivers, 3180–1612800 nM h^{-1} in lakes and 40–13200 nM h^{-1} in seawaters. Under dark incubation the production rates are 99970 nM h^{-1} in rivers, 175500 nM h^{-1} in lakes, and 300–2300 nM h^{-1} in seawaters (Table 3).

The production rate of CO_2 in irradiated freshwater two coastal rivers is significantly high in air-saturation (13.2–23.0 μM h^{-1}) and O_2-saturation (18.3–26.5 μM h^{-1}), which are substantially decreased under air-saturation plus DFOM (5.4–6.0 μM h^{-1}), O_2-saturation plus DFOM (5.6–7.2 μM h^{-1}), and N_2-saturation (1.9 μM h^{-1}, measured for one river sample only) (Table 3) (Xie et al. 2004). Note that DFOM is the deferoxamine mesylate that is a strong Fe(III)-complexing ligand that forms nearly photo-inert complexes (Gao and Zepp 1998). The CO_2 production rate in the N_2-saturation river water is only ca. 10 % and 20 % of those in the O_2-saturation and air-saturation samples, respectively (Xie et al. 2004). This study observes that although CO_2 production in the O_2-saturation and DFOM samples is consistently higher than in the air-sat and DFOM samples, the difference between the two seldom exceeded 10 %, which indicates that in the presence of DFOM, iron rather than O_2 is the limiting factor for CO_2 production (Table 3) (Xie et al. 2004). These results suggest that although, O_2 and iron both can play very important roles in CO_2 production, photoinduced processes without the involvement of O_2 and iron (particularly the iron independent processes) can also contribute to CO_2 production in natural waters (Xie et al. 2004). CO_2 photoproduction rate is ~0.08–0.63 μM h^{-1} in estuarine water showing high production rate (~0.63 nM h^{-1}) in low salinity than in high salinity waters ~0.08 μM h^{-1} (White et al. 2010). Studies therefore observe that CO_2 is the largest carbon-containing product of DOM photodegradation in natural waters (Xie et al. 2004; Miller and Zepp 1995).

It is shown that the lakes produce DIC to a higher extent compared to rivers and seawaters (Fig. 10a). The DIC photoproducts in lakes are well correlated with DOC concentration, but no correlation was observed in rivers and seawaters (Fig. 10a). The high production of DIC in lakes could originate from the higher presence of low molecular weight organic substances (54–79 % in the <5 kDa range), which are mostly originated from fulvic and humic acids (Waiser and Robarts 2000; Yoshioka et al. 2007; Wu and Tanoue 2001). The photo production rate of DIC is higher in the upper surface layers (2.42 μM h^{-1} at 0 m), it then gradually decreases (0.60 μM h^{-1} at 6.5 m) and then increases again (2.73 μM h^{-1} at 24 m) in the deeper layers, but they are greatly lower than those of dark incubation samples (100.0 μM h^{-1}) in photoexperiments conducted on river water samples keeping in situ at different vertical depths in lake environment (Ma and Green 2004). For lake waters the production rates of DIC are gradually decreased from the surface (10.6–10.9 μM h^{-1} at 0–6 m) to deeper layers (3.2 μM h^{-1} at 24 m). However, under dark incubation the production rate is 175.5 μM h^{-1}, much higher than the rate of photoproduction. An increase in the DIC production rate of river waters kept in situ in the deeper layer of lakes (24 m depth) is likely caused by the much lower sunlight intensity that makes this set-up equivalent to dark incubation. Therefore, high production of DIC under dark incubation allows the hypothesis that microbial degradation plays a significant and probably a major role in DOM mineralization in natural waters, especially in deeper lake or oceanic environments. The study shows that the global annual rate of photoinduced production of DIC (10^{14}–10^{15} mol DIC per year) (Johannessen 2000) might be on the same order of magnitude as that of sequestration of DIC by new production (~10^{15} mol DIC per year) (Liu et al. 2000).

CO production upon photoinduced degradation of DOM is highly variable for a variety of waters (Table 3). Production rates are 0.004–1.5 μM h^{-1} in rivers, 0.26 μM h^{-1} in lakes, 0.004–1.0 μM h^{-1} in seawaters, and 1.5–3.3 μM h^{-1} in standard dissolved fulvic and humic acids (Table 3). It is estimated that >95 % of the total water-column CO photoproduction occurs within the mixed layer on a global, yearly basis (Fichot and Miller 2010). It has been shown that the production rates of CO are almost linearly correlated with the concentration of DOC and of standard organic substances (Fig. 10b). The photoproduction of CO in the ocean is induced mainly by the UV component of solar radiation (Zepp et al. 1998; Atlas et al. 1994). Quantum yields (the quantum yield is the fraction of absorbed radiation that results in photoreaction) for CO production at wavelengths greater than 297 nm are highest in the UV-B region (Zepp et al. 1998). Turnover times for CO are in the order of hours, and they are generally lower (3–98 h) in fall and higher (2–108 h) in spring samples in the Caribbean Sea (Jones 1991; Jones and Amador 1993). The CO oxidation rate is lower in spring samples (20–340 pmol L^{-1} h^{-1} except one sample, 980 pmol L^{-1} h^{-1}) than in fall samples (20–660 pmol L^{-1} h^{-1} except one sample, 810 pmol L^{-1} h^{-1}). The concentration levels of CO are variable: 1–6 nM in spring and 0.6–32 nM in fall. The variations in the oxidation rates appear to be linked with two important phenomena. First, nitrifying and carboxydobacteria are both thought to have a role in oxidizing CO in the oceans (Conrad and Seiler 1980). Second, high concentrations of CO are able to inhibit marine nitrifying bacteria in natural waters (Jones and Amador 1993; Jones and Morita 1984).

In the estuary of River Ohta, the concentration of carbonyl sulfide (COS) was highest (54.4 ng L^{-1}) in the late afternoon (17:00) during the summer season (July), and lowest (23.9 ng L^{-1}) soon after noontime (14:00) during the winter season (December) (Table 3) (Fujiwara et al. 1995). In Seto Inland Sea the COS concentration was higher (~5–17 ng L^{-1}) in the surface layer (0–5 m), whilst it was lower (~3–5 ng L^{-1}) in the deeper layer (20 m) (Fujiwara et al. 1995). An increase in COS concentrations is often linked with an increase of solar radiation, lower concentrations being detected at night time and in the early morning. Moreover, higher concentrations are found in surface seawater than in the deeper layers, suggesting that COS is photolytically produced in natural waters.

Photo products such as H_2O_2, ROOH and CO_2, simultaneously generated during the photoinduced degradation of DOM, can be photosynthetically transformed into carbohydrates during the summer season in natural surface waters. The relevant processes can be depicted as follows (Eqs. 5.4, 5.5) (Mostofa et al. 2009a; Komissarov 1994, 1995, 2003):

$$\mathrm{DOM} + h\upsilon \rightarrow \mathrm{H_2O_2} + \mathrm{CO_2/CO/DIC} + \mathrm{LOWDOM} + \mathrm{E}\ (\pm) \tag{5.4}$$

$$\mathrm{x\,CO_{2(air)}} + \mathrm{y\,H_2O_{2(H_2O)}} + h\upsilon \rightarrow \mathrm{C_x\,(H_2O)_y} + (\mathrm{x} + \mathrm{y}/2)\ \mathrm{O_2} + \mathrm{E}\ (\pm) \tag{5.5}$$

This mechanism may help in the understanding of the production of autochthonous DOM, particularly carbohydrate compounds, during the summer season in natural waters. The new reaction mechanim for photosynthesis (Eq. 4.2) has been discussed in details in photosynthesis chapter (see chapter "Photosynthesis in Nature: A New Look").

5.5 Photoinduced Formation of Nitrogenous Compounds

Nitrogenous photoproducts include the ammonium (NH_4^+) and nitrate/nitrite (NO_3^-/NO_2^-) that are released by photoinduced degradation of humic substances and degradation of dissolved organic nitrogen (DON) in waters (Table 3) (Mostofa et al. 2011; Li et al. 2008; Bushaw et al. 1996; Mack and Bolton 1999; Carlsson et al. 1993; Stedmon et al. 2007). Ammonium is produced by transformation of aquatic dissolved organic matter in waters, and the production rates are 40–370 nM for 895–3840 μM C of DOC and 20–86 μM of dissolved organic nitrogen (Bushaw et al. 1996). DON concentrations are 7–26 μM in Lake Hongfeng and 14–47 μM in Lake Baihua (Li et al. 2008), approximately 8.35 μM in the epilimnion of Lake Biwa (Kim et al. 2006), and approximately 10 μM in coastal waters (Bronk 2002). The high concentrations of NO_2^- and NH_4^+ in Lakes Hongfeng and Baihua during the summer stratification period suggest the regeneration of inorganic nitrogen (NO_2^- and NH_4^+) in lakes (Li et al. 2008). Photoinduced respiration or assimilation of lake algae under natural sunlight can release NH_4^+ in waters, suggesting that autochthonous organic matter is a major source of NH_4^+ in natural waters Mostofa K et al. (unpublished). DOM in coastal waters derives from terrestrial humic substances (Carlsson et al. 1993). This leads to an increase of the nitrogen availability, which subsequently stimulates the rates of primary and secondary production. The uptake of inorganic nitrogen by bacteria during a phytoplankton bloom can be observed, particularly in lake or coastal waters where the inputs of terrestrial humic substances are much higher (Kirchman et al. 1991; Amon and Benner 1994). Photolytically produced ammonium can be assimilated by bacterial populations, which can lead to an increase in the production of autotrophic and heterotrophic biomass in planktonic environments. Photo release of inorganic nitrogen from DOM is an important source of nitrogen availability in several aquatic ecosystems, such as nitrogen-limited and high-latitude environments, and coastal waters where high primary and secondary production are usually occurring.

5.6 Photoinduced Formation of Phosphate

Photoinduced degradation of DOM can lead to the release of phosphate (PO_4^{3-}) in natural surface waters (Table 3) (Reche et al. 1999; Mostofa et al. 2011; Zhang et al. 2004; Fang 2004; Chen et al. 2001; Karl and Tien 1997; Suzumura and Ingall

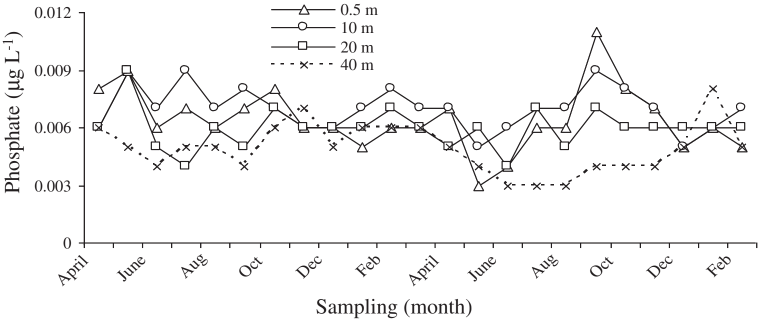

Fig. 11 Variation of phosphate concentration (month by month) during the period of April 1999 to February 2001 in the waters of Lake Biwa. *Data sources* Mostofa KMG et al. (unpublished) and Shiga prefecture office, Japan)

2004). Phosphate concentration in waters of Lake Biwa is often higher in the surface layer during the summer season, compared to other seasons or the deeper layer (Fig. 11) (Mostofa KMG et al., unpublished). This finding suggests that phosphate may be produced by photoinduced degradation processes in the surface waters of Lake Biwa. Indeed, the inorganic phosphorus is increased in the surface layer, whilst the organic phosphorus concentration is decreased and the surface concentration of organic phosphorus is lower compared to the deeper layers (Fang 2004). Therefore, the inorganic phosphorus may be produced from the decomposition of dissolved organic phosphorus in surface waters. The concentration levels of soluble reactive phosphorus were highest in the upper surface layers (0–30 m) in North Pacific Ocean (Karl and Tien 1997). Concentration levels of dissolved hydrophobic phosphorus were much higher in the surface layers (6.6–18 nM) and gradually decreased with depth (5–10 nM at below 400 m) (Suzumura and Ingall 2004). Total dissolved phosphorus (TDP) in coastal waters was much higher in surface waters (3.51–7.12 dpm m^{-3}) than in the deeper layers (0.83–2.0 dpm m^{-3}), and the surface concentrations at inshore stations (5.09–7.12 dpm m^{-3}) were significantly higher than at the offshore stations (3.51 dpm m^{-3}) (Zhang et al. 2004). From these data it can be inferred that inorganic phosphate might be an important photoproduct of DOM photoinduced degradation in surface waters.

5.7 *Photoinduced and Microbial Processes for the Release of Energy and of End Products to the Water Ecosystem*

Photoinduced degradation of DOM generally takes place through redox reactions in waters which can lead to energy changes (±) such as supply (+) or consumption (−) of energy in the aquatic environment. Energy changes also occur during photosynthesis in natural waters (Komissarov 1994, 1995, 2003). DOM with its content of organic

C and N is a thermodynamic anomaly that provides a major source of energy to drive aquatic and terrestrial ecosystems (Salonen et al. 1992; Wetzel 1984, 1992; Hedges et al. 2000; Tranvik 1992). Therefore, any changes in energy during the photoinduced degradation of DOM are thermodynamically vital for all the living organisms and for the natural water ecosystem. Photoinduced degradation of DOM in natural waters is thus interlinked with production of free radicals, microbial processes, photosynthesis, autochthonous DOM, nutrients, end photoproducts and their utilization as food for microorganisms. A conceptual schematic diagram for the photoinduced and microbial processes of DOM and POM, photoproducts and their importance in the aquatic environment is reported below (Fig. 12):

Finally, it can be concluded that most of the changes that take place in the natural ecosystem are closely interlinked.

6 Interactions Between Photoinduced and Microbial Processes in Natural Waters

The understanding of the interactions between photoinduced and microbial degradation of DOM has required a proper elucidation of the photoinduced processes. It is now considered that microbial degradation takes place at the same time as the photoinduced degradation process (Kopacek et al. 2003; Moran

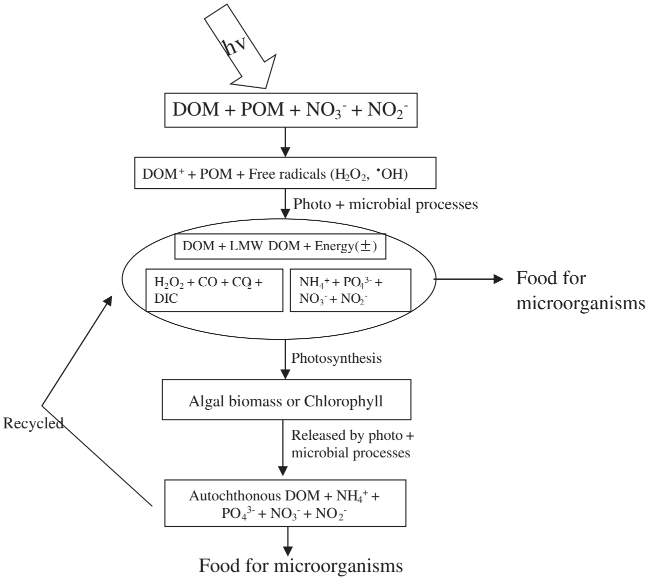

Fig. 12 Conceptual model on photoinduced degradation of DOM and its consecutive effects on key biogeochemical processes in natural waters. [*Data source* with modifications Mostofa et al. (2009b)

et al. 2000; Amon and Benner 1996; Vähätalo and Wetzel 2004; Miller and Moran 1997). In essence, during the photoinduced process various species among which are the superoxide radical ion ($O_2^{\bullet -}$), the $HO^{\bullet}$ and peroxides (H_2O_2 and ROOH) are generated either in surface waters or in aqueous solutions during laboratory irradiation experiments (Takeda et al. 2004; Moore et al. 1993; Mostofa and Sakugawa 2009; Southworth and Voelker 2003; Goldstone et al. 2002). The photogenerated reactive species are involved into the photoinduced degradation of DOM in waters. Simultaneously, these species can inhibit or deactivate the activity of catalase, peroxidase and superoxide dismutase associated with bacterial cells, particulate organic matter and DOM (Moffett and Zafiriou 1990; Tanaka et al. 1985; Serban and Nissenbaum 1986; Zepp et al. 1987). Bacterial cells can protect themselves from harmful oxidizing species such as H_2O_2, $O_2^{\bullet -}$ and $HO^{\bullet}$ by adjusting the level of their enzymes (Chance et al. 1979). Therefore, microbial degradation is expected to take place to a negligible extent during the photoinduced degradation of DOM in aqueous media.

The bacterial growth shows seasonal variations, reaching the maximum during spring to early summer and decreasing greatly during the summer season when the water temperature exceeds 25.5 °C in lakes (Zhao et al. 2003; Darakas 2002). Natural sunlight or UV-exposure can decrease the bacterial production by 15–80 %, which considerably inhibits the formation and biodegradation of DOM in natural surface waters (Amon and Benner 1996; Bertilsson and Tranvik 1998; Benner and Ziegler 1999; Naganuma et al. 1996; Tranvik and Kokalj 1998). However, other studies have found that solar exposure can enhance the bacterial growth by about 35–200 % (Lindell et al. 1996; Wetzel et al. 1995; Bushaw et al. 1996; Miller and Moran 1997; Herndl et al. 1993; Lindell and Rai 1994; Reitner et al. 1997; Jørgensen et al. 1998; Moran and Hodson 1994). Moreover, bacterial growth is usually observed in deeper waters (Benner and Ziegler 1999). The increase or the decrease of bacterial growth by sunlight depends on two key factors: (i) The production of reactive species (H_2O_2, ROOH, $HO^{\bullet}$) and of mineralization products such as CO_2, CO and DIC; (ii) The concentration level and molecular nature of DOM, the concentration of total dissolved iron for photo-Fenton reaction, water temperature, dissolved oxygen, physical mixing etc. Water temperature during the summer season is merely regulated by natural solar radiation, which can lead to high generation of free radicals and mineralization products in natural waters (Moore et al. 1993; Mostofa and Sakugawa 2009; Zafiriou et al. 1984; Zika 1981; Obernosterer et al. 2001; Fujiwara et al. 1993; Sakugawa et al. 2000). The free radicals, as strong oxidants and depending on their concentration, may have several deadly impacts on many stages of cell metabolism, including those involved into the induction of programmed cell death (Samuilov et al. 2001). This hypothesized effect is supported by the observation of an inhibition by UV radiation of the activity of microorganisms in water (Herndl et al. 1993; Lund and Hongve 1994; Karentz et al. 1994), and of the deadly impact of UV radiation on bacterial cells or microorganisms in the aquatic environment (Qian et al. 2001; Randall et al. 2005). Qian et al. 2001; Sunlight often affects bacterial growth merely in the upper surface waters, and UV-B radiation inhibited bacterial production by 39–82 % in a high mountain lake (Carrillo et al. 2002). Therefore, microbial activity may be less efficient during the photoinduced degradation of DOM in natural waters.

7 Scope of Future Challenges

Photoinduced and microbial degradation of DOM is an important research subject in the photochemistry of the aquatic environment. Till now, a few researches have been conducted on the degradation of bulk DOM in natural waters. Photoinduced and microbial degradation of organic substances such as standard fulvic acid, humic acid, fluorescent whitening agents (DAS1 and DSBP) and chlorophyll was seldom conducted to examine their end photoproducts in the aquatic environments. For a better elucidation of the degradation processes of DOM in natural waters, it is vital to conduct an extensive study on streams, rivers, lakes, coastal and seawaters. The photolytically produced low molecular weight (LMW) organic substances are microbiologically important, but in some cases they might be toxic. Till now only a few researches have been conducted to identify the LMW organic compounds in the aquatic environment. The effects of water temperature and pH on the coupled photoinduced and microbial degradation of DOM and of standard organic compounds have not been studied so far. Obviously, variation in water temperature and pH might have a significant role on degradation processes and on the concentration levels of the end photoproducts. Therefore, a number of important research needs for future challenges can be distinguished as: (i) Photoinduced and microbial degradation of various molecular size fractions of DOM for a variety of waters. (ii) An extensive study on the microbial degradation of DOM for a variety of waters, and the development of the mechanism for microbial degradation of DOM. (iii) Effect of temperature and pH on photoinduced and microbial degradation of DOM for a variety of waters and for standard organic substances. (iv) Interactions between photoinduced and microbial degradation of DOM, and its impact on microorganisms in the aquatic ecosystem. (v) Investigation on LMW organic substances produced from photoinduced and microbial degradation of DOM in natural waters and from standard HMW organic substances. (vi) Elucidation of the microbiological changes involving the macromolecules (fulvic acid, humic acid and autochthonous fulvic acid) under dark incubation. (vii) Understanding of the mechanisms of the photoinduced degradation of the macromolecules (fulvic acid, humic acid, and autochthonous fulvic acid) by natural sunlight in aqueous media. The mechanism depicted in this chapter may pave the way for future directions in the field. (viii) Refinement of the group contribution method (GCM) to predict $HO^\bullet$ reaction rate constants. Because of the limited data availability for the rate constants of various compounds in the aqueous phase, the GCM still has many gaps and its implementation should be the focus for future research (Minakata et al. 2009).

It is expected that new research works can focus on the combined photoinduced and microbial degradation of DOM and of the photoproducts of the process, to understand a whole feature of the biogeochemical process of DOM in the aquatic environment.

8 Nomenclature

DFOM	Deferoxamine mesylate
DOC	Dissolved organic carbon
DOM	Disscolved organic matter
DIC	Dissolved inorganic carbon ($CO_2 + H_2CO_3 + HCO_3^- + CO_3^{-2}$)
GCM	Group contribution method
H_2O_2	Hydrogen peroxide
LMW	Low molecular weight
$HO^\bullet$	Hydroxyl radical
SS PM	Sea-salt particulate matter

Problems

(1) Describe the various biogeochemical functions of DOM for photoinduced and microbial processes in natural waters

(2) Explain why the photoinduced degradation of DOM varies for a variety of natural waters.

(3) Explain the theoretical model for photoinduced degradation process in aqueous media.

(4) Explain the mechanism of the photoinduced degradation of DOM in natural waters.

(5) Explain the mechanism for the photoinduced degradation by $HO^\bullet$ of functional groups bonded to DOM and explain the group contribution method (GCM) to predict the $HO^\bullet$ reaction rate constants.

(6) What is the methanogenesis? Explain the chemical reactions that are involved in the formation of CH_4 from methyl-coenzyme *M* reductase.

(7) What are the controlling factors for the photoinduced degradation of DOM? Describe four important factors that can regulate the DOM Photoinduced degradation in aqueous solution.

(8) What are the controlling factors for the microbial degradation of DOM? Describe two of the important factors.

(9) List the various end photo products generated from the photoinduced degradation of DOM in natural waters. Explain what end products are vital for microbial processes in the aquatic environments.

(10) What is the new reaction for photosynthesis? Explain how photo processes can affect photosynthesis in waters.
(11) Explain the flow diagram on how photoinduced and microbial processes work together for the degradation of DOM and POM in natural waters.
(12) What are the key interactions between photoinduced and microbial processes in natural waters?

Acknowledgments We thank Mr. Cui Lifeng of Institute of Geochemistry, Chinese Academy of Sciences, China for his generous assistance. This work was financially supported jointly by the National Natural Science Foundation of China (Grant Nos.40525011, 1314765) and the Chinese Academy of Sciences (KZCX2-YW-102). This work was partly supported by Brook Byers Institute for Sustainable Systems, Georgia Institute of Technology, United States and National Science Foundation of the United States award 0854416; University Turin, Italy; Chinese Research Academy of Environmental Sciences, China; Northwest Missouri State University, USA; Kyoto University, Japan; and Hiroshima University, Japan. This study acknowledges the reprinted (adapted) with permission from Minakata D, Li K, Westerhoff P, Crittenden J, Development of a group contribution method to predict aqueous phase hydroxyl radical (HO•) reaction rate constants, Environ Sci Technol, 43(16), 6220–6227. Copyright (2009) American Chemical Society; reprinted by permission from Macmillan Publishers Ltd: [Nature Rev Microbiol] (Lovley DR, Bug juice: harvesting electricity with microorganisms, 4, 497–508), copyright (2006); reprinted (adapted) with permission from Pelmenschikov V, Blomberg MRA, Siegbahn PEM, Crabtree RH, A Mechanism from Quantum Chemical Studies for Methane Formation in Methanogenesis, JACS, 124, 4039–4049. Copyright (2002) American Chemical Society; reprinted (adapted) with permission from Ebner S, Jaun B, Goenrich M, Thauer RK, Harmer J, Binding of coenzyme B induces a major conformational change in the active site of methyl-coenzyme M reductase, JACS, 132, 567–575. Copyright (2010) American Chemical Society; reprinted from Journal of Volcanology and Geothermal Research, 178 (2), Koschorreck M, Wendt-Potthoff K, Scharf B, Richnow HH, Methanogenesis in the sediment of the acidic Lake Caviahue in Argentina, 197–204. Copyright (2008), with permission from Elsevier; Copyright (1996) by the Association for the Sciences of Limnol Oceanogr, Inc.; Copyright (2000) by the Association for the Sciences of Limnol Oceanogr, Inc.; Copyright (2011) by The Geochemical Society of Japan; and Shiga prefecture office, Japan.

References

Allard B, Boren H, Pettersson C, Zhang G (1994) Degradation of humic substances by UV irradiation. Environ Int 20:97–101

Allen JM, Lucas S, Allen SK (1996) Formation of hydroxyl radical (· OH) in illuminated surface waters contaminated with acidic mine drainage. Environ Toxicol Chem 15:107–113

Amador JA, Alexander M, Zika RG (1989) Sequential photochemical and microbial degradation of organic molecules bound to humic acid. Appl Environ Microbiol 55:2843–2849

Amon RMW, Benner R (1994) Rapid cycling of high-molecular-weight dissolved organic matter in the ocean. Nature 369:549–552

Amon R, Benner R (1996) Photochemical and microbial consumption of dissolved organic carbon and dissolved oxygen in the Amazon River system. Geochim Cosmochim Acta 60:1783–1792

Anastasio C, Newberg JT (2007) Sources and sinks of hydroxyl radical in sea-salt particles. J Geophys Res 112:D10306. doi:10.1029/2006JD008061

Arakaki T, Faust BC (1998) Sources, sinks, and mechanisms of hydroxyl radical (•OH) photoproduction and consumption in authentic acidic continental cloud waters from Whiteface mountain, New York: The role of the Fe (r)(r = II, III) photochemical cycle. J Geophys Res 103:3487–3504

Arakaki T, Miyake T, Shibata M, Sakugawa H (1999) Photochemical formation and scavenging of hydroxyl radical in rain and dew waters. Nippon Kagaku Kaishi 5:335–340 (In Japanese)

Arundhati Pal AKP (2008) Microbial extracellular polymeric substances: central elements in heavy metal bioremediation. Ind J Microbiol 48:49–64

Asmus K-D, Bonifačič M (1999) Sulfur-centered reactive intermediates as studied by radiation chemical and complementary techniques. In: Alfassi ZB (Ed), S-centered radicals, the chemistry of free radicals. John Wiley & Sons Ltd, Chichester. Chapter 5, pp 141–191

Asmus K, Möckel H, Henglein A (1973) Pulse radiolytic study of the site of hydroxyl radical attack on aliphatic alcohols in aqueous solution. J Phys Chem 77:1218–1221

Assel M, Laenen R, Laubereau A (1998) Ultrafast electron trapping in an aqueous NaCl-solution. Chem Phys Lett 289:267–274

Atkinson R (1986) Kinetics and mechanisms of the gas-phase reactions of the hydroxyl radical with organic compounds under atmospheric conditions. Chem Rev 86:69–201

Atkinson R (1987) A structure-activity relationship for the estimation of rate constants for the gas-phase reactions of OH radicals with organic compounds. Int J Chem Kinet 19:799–828

Atlas E, Lueb R, Madronich S, Prezelin B, Smith R (1994) Dissolved trace gas measurements and UV effects near the Antarctic Peninsula during ICECOLORS'93. EOS Trans AGU 75:377

Azam F, Cho B (1987) Bacterial utilization of organic matter in the sea. In: Fletcher M, Gray TRG, Jones JG (Eds), Ecology of microbial communities, Cambridge University Press, Cambridge, pp 261–281

Baker A, Inverarity R (2004) Protein-like fluorescence intensity as a possible tool for determining river water quality. Hydrol Process 18:2927–2945

Ballaré CL, Caldwell MM, Flint SD, Robinson S, Bornman JF (2011) Effects of solar ultraviolet radiation on terrestrial ecosystems. Patterns, mechanisms, and interactions with climate change. Photochem Photobiol Sci 10:226–241

Banat IM, Nedwell DB, Balba MT (1983) Stimulation of methanogenesis by slurries of saltmarsh sediment after the addition of molybdate to inhibit sulphate-reducing bacteria. J Gen Microbiol 129:123–129

Barbiero RP, Tuchman ML (2004) The deep chlorophyll maximum in lake superior. J Great Lakes Res 30:256–268

Basiliko N, Yavitt JB, Dees P, Merkel S (2003) Methane biogeochemistry and methanogen communities in two northern peatland ecosystems, New York State. Geomicrobiol J 20:563–577

Benner R, Biddanda B (1998) Photochemical transformations of surface and deep marine dissolved organic matter: effects on bacterial growth. Limnol Oceanogr 43:1373–1378

Benner R, Kaiser K (2003) Abundance of amino sugars and peptidoglycan in marine particulate and dissolved organic matter. Limnol Oceanogr 48:118–128

Benner R, Ziegler S (1999) Do photochemical transformations of dissolved organic matter produce biorefractory as well as bioreactive substrates? Microbial Biosystems: New Frontiers Procee 8th Int Sym On Microb Ecol In: Bell CR, Brylinsky M, Johnson-Green P (Ed) Atlantic Canada Soc for Micrb Ecol Halifax, Canada

Benson SW (1976) Thermochemical kinetics: methods for the estimation of thermochemical data and rate parameters. 2nd Edn,Wiley, Now York

Bertilsson S, Allard B (1996) Sequential photochemical and microbial degradation of refractory dissolved organic matter in a humic freshwater system. Ergebn Limnol 48:133–141

Bertilsson S, Tranvik LJ (1998) Photochemically produced carboxylic acids as substrates for freshwater bacterioplankton. Limnol Oceanogr 43:885–895

Bertilsson S, Tranvik LJ (2000) Photochemical transformation of dissolved organic matter in lakes. Limnol Oceanogr 45:753–762

Bertilsson S, Stepanauskas R, Cuadros-Hansson R, Granéli W, Wikner J, Tranvik L (1999) Photochemically induced changes in bioavailable carbon and nitrogen pools in a boreal watershed. Aquat Microb Ecol 19:47–56

Biddanda B, Benner R (1997) Carbon, nitrogen, and carbohydrate fluxes during the production of particulate and dissolved organic matter by marine phytoplankton. Limnol Oceanogr 42:506–518

Billamboz N, Grivet M, Foley S, Baldacchino G, Hubinois JC (2010) Radiolysis of the polyethylene/water system: studies on the role of hydroxyl radical. Radiat Phys Chem 79:36–40

Blokhina O, Virolainen E, Fagerstedt KV (2003) Antioxidants, oxidative damage and oxygen deprivation stress: a review. Ann Botany 91:179–194

Blough NV, del Vecchio R (2002) Chromophoric DOM in the coastal environment. In: Hansell DA, Carlson CA (eds) Biogeochemistry of marine dissolved organic matter. Elsevier Science, USA, p 774

Blough NV, Zepp RG (1995) Reactive oxygen species in natural waters. In: Valentine JS, Foote CS (eds) Active oxygen in chemistry. Blackie Academic and Professional, New York, pp 280–333

Blough N, Zafiriou O, Bonilla J (1993) Optical absorption spectra of waters from the Orinoco River outflow: terrestrial input of colored organic matter to the Caribbean. J Geophys Res 98:2271–2278

Bolton J, Carter S (1994) Homogeneous photodegradation of pollutants in contaminated water: An introduction. In: Helz G, Zepp R, Crosby D (Eds), Aquatic and Surface Photochemistry. CRC press, Boca Raton. Chap 33

Borges A, Ruddick K, Schiettecatte LS, Delille B (2008) Net ecosystem production and carbon dioxide fluxes in the Scheldt estuarine plume. BMC Ecol 8:15

Borisover M, Laor Y, Saadi I, Lado M, Bukhanovsky N (2011) Tracing organic footprints from industrial effluent discharge in recalcitrant riverine chromophoric dissolved organic matter. Water Air Soil Pollut 222:255–269

Bräuer S, Yavitt J, Zinder S (2004) Methanogenesis in McLean Bog, an acidic peat bog in upstate New York: stimulation by H_2/CO_2 in the presence of rifampicin, or by low concentrations of acetate. Geomicrob J 21:433–443

Bräuer SL, Cadillo-Quiroz H, Yashiro E, Yavitt JB, Zinder SH (2006) Isolation of a novel acidiphilic methanogen from an acidic peat bog. Nature 442:192–194

Brezonik PL, Fulkerson-Brekken J (1998) Nitrate-induced photolysis in natural waters: controls on concentrations of hydroxyl radical photo-intermediates by natural scavenging agents. Environ Sci Technol 32:3004–3010

Bronk DA (2002) Dynamics of DON. Biogeochemistry of marine dissolved organic matter. In: Hansell DA, Carlson CA (eds) Biogeochemistry of marine dissolved organic matter. Academic Press, San Diego, pp 153–249

Brooks ML, Meyer JS, McKnight DM (2007) Photooxidation of wetland and riverine dissolved organic matter: altered copper complexation and organic composition. Hydrobiology 579:95–113

Burdige DJ, Martens CS (1988) Biogeochemical cycling in an organic-rich coastal marine basin: 10. The role of amino acids in sedimentary carbon and nitrogen cycling. Geochim Cosmochim Acta 52:1571–1584

Burdige DJ, Kline SW, Chen W (2004) Fluorescent dissolved organic matter in marine sediment pore waters. Mar Chem 89:289–311

Bushaw KL, Zepp RG, Tarr MA, Schulz-Jander D, Bourbonniere RA, Hodson RE, Miller WL, Bronk DA, Moran MA (1996) Photochemical release of biologically available nitrogen from aquatic dissolved organic matter. Nature 381:404–407

Cadillo-Quiroz H, Bräuer S, Yashiro E, Sun C, Yavitt J, Zinder S (2006) Vertical profiles of methanogenesis and methanogens in two contrasting acidic peatlands in central New York State, USA. Environ Microbiol 8:1428–1440

Cadillo-Quiroz H, Yavitt JB, Zinder SH, Thies JE (2010) Diversity and community structure of Archaea inhabiting the rhizoplane of two contrasting plants from an acidic bog. Microb Ecol 59:757–767

Cai WJ (2011) Coastal ocean carbon paradox: CO_2 sinks or sites of terrestrial carbon incineration. Annu Rev Mar Sci 3:123–1453

Cai WJ, Wang Y (1998) The chemistry, fluxes, and sources of carbon dioxide in the estuarine waters of the Satilla and Altamaha Rivers, Georgia. Limnol Oceanogr 43:657–668

Cai WJ, Wang Y, Hodson RE (1998) Acid-base properties of dissolved organic matter in the estuarine waters of Georgia, USA. Geochim Cosmochim Acta 62:473–483

Cai WJ, Pomeroy LR, Moran MA, Wang Y (1999) Oxygen and carbon dioxide mass balance for the estuarine-intertidal marsh complex of five rivers in the southeastern US. Limnol Oceanogr 44:639–649

Calace N, Palmieri N, Mirante S, Petronio B, Pietroletti M (2006) Dissolved and particulate humic substances in water channels in the historic centre of Venice. Water Res 40:1109–1118

Call D, Logan BE (2008) Hydrogen production in a single chamber microbial electrolysis cell lacking a membrane. Environ Sci Technol 42:3401–3406

Carlsson P, Segatto AZ, Graneli E (1993) Nitrogen bound to humic matter of terrestrial origin-a nitrogen pool for coastal phytoplankton? Mar Ecol Prog Ser 97:105–116

Carpenter SR, Cole JJ, Kitchell JF, Pace ML (1998) Impact of dissolved organic carbon, phosphorus, and grazing on phytoplankton biomass and production in experimental lakes. Limnol Oceanogr 43:73–80

Carrillo P, Medina-Sánchez JM, Villar-Argaiz M (2002) The interaction of phytoplankton and bacteria in a high mountain lake: importance of the spectral composition of solar radiation. Limnol Oceanogr 47:1294–1306

Casper P, Chim Chan O, Furtado ALS, Adams DD (2003) Methane in an acidic bog lake: The influence of peat in the catchment on the biogeochemistry of methane. Aquat Sci 65:36–46

Chance B, Sies H, Boveris A (1979) Hydroperoxide metabolism in mammalian organs. Physiol Rev 59:527–605

Chaudhuri SK, Lovley DR (2003) Electricity generation by direct oxidation of glucose in mediatorless microbial fuel cells. Nature Biotechnol 21:1229–1232

Chefetz B (2002)

Chen RZ, Pignatello JJ (1997) Role of quinone intermediates as electron shuttles in Fenton and photo assisted Fenton oxidations of aromatic compounds. Environ Sci Technol 31:2399–2406

Chen Y, Khan S, Schnitzer M (1978) Ultraviolet irradiation of dilute fulvic acid solutions. Soil Sci Soc Am J 42:292–296

Chen JH, Lion LW, Ghiorse WC, Shuler ML (1995) Mobilization of adsorbed cadmium and lead in aquifer material by bacterial extracellular polymers. Water Res 29:421–430

Chen YL, Chen HY, Lee WH, Hung CC, Wong GTF, Kanda J (2001) New production in the East China Sea, comparison between well-mixed winter and stratified summer conditions. Contin Shelf Res 21:751–764

Cheng S, Logan BE (2007) Sustainable and efficient biohydrogen production via electrohydrogenesis. Proc Natl Aca Sci 104:18871

Chin YP, Miller PL, Zeng L, Cawley K, Weavers LK (2004) Photosensitized degradation of bisphenol A by dissolved organic matter. Environ Sci Technol 38:5888–5894

Choudhry GG (1981) Humic substances Part II†: photophysical, photochemical and free radical characteristics. Toxicol Environ Chem 4:261–295

Clark CD, Hiscocka WT, Millero FJ, Hitchcock G, Brand L, Miller WL, Ziolkowski L, Chen RF, Zika RG (2004) CDOM distribution and CO2 production on the Southwest Florida Shelf. Mar Chem 89:145–167

Coble PG (1996) Characterization of marine and terrestrial DOM in seawater using excitation-emission matrix spectroscopy. Mar Chem 51:325–346

Coble PG (2007) Marine optical biogeochemistry: the chemistry of ocean color. Chem Rev 107:402–418

Coleman ML, Hedrick DB, Lovley DR, White DC, Pye K (1993) Reduction of Fe(III) in sediments by sulphate-reducing bacteria. Nature 361:436–438

Conrad R (1999) Contribution of hydrogen to methane production and control of hydrogen concentrations in methanogenic soils and sediments. FEMS Microbiol Ecol 28:193–202

Conrad R, Seiler W (1980) Photooxidative production and microbial consumption of carbon monoxide in seawater. FEMS Microbiol Lett 9:61–64

Conrad R, Bak F, Seitz H, Thebrath B, Mayer H, Schütz H (1989a) Hydrogen turnover by psychrotrophic homoacetogenic and mesophilic methanogenic bacteria in anoxic paddy soil and lake sediment. FEMS Microbiol Lett 62:285–293

Conrad R, Mayer HP, Wüst M (1989b) Temporal change of gas metabolism by hydrogen-syntrophic methanogenic bacterial associations in anoxic paddy soil. FEMS Microbiol Lett 62:265–273

Cook R, Kelly C, Schindler D, Turner M (1986) Mechanisms of hydrogen ion neutralization in an experimentally acidified lake. Limnol Oceanogr 31:134–148

Cooper WJ, Zika RG, Petasne RG, Plane JMC (1988) Photochemical formation of hydrogen peroxide in natural waters exposed to sunlight. Environ Sci Technol 22:1156–1160

Cooper WJ, Zika RG, Petasne RG, Fischer AM (1989) Sunlight-induced photochemistry of humic substances in natural waters: major reactive species. Adv Chem Ser 219:333–362

Cord-Ruwisch R, Seitz HJ, Conrad R (1988) The capacity of hydrogenotrophic anaerobic bacteria to compete for traces of hydrogen depends on the redox potential of the terminal electron acceptor. Arch Microbiol 149:350–357

Corin N, Backlund P, Kulovaara M (1996) Degradation products formed during UV-irradiation of humic waters. Chemosphere 33:245–255

Crill PM, Martens CS (1983) Spatial and temporal fluctuations of methane production in anoxic coastal marine sediments. Limnol Oceanogr 28:1117–1130

Cuny P, Marty JC, Chiavérini J, Vescovali I, Raphel D, Rontani JF (2002) One-year seasonal survey of the chlorophyll photodegradation process in the northwestern Mediterranean Sea. Deep Sea Res Part II 49:1987–2005

Dahlén J, Bertilsson S, Pettersson C (1996) Effects of UV-A irradiation on dissolved organic matter in humic surface waters. Environ Int 22:501–506

Darakas E (2002) E. coli kinetics-effect of temperature on the maintenance and respectively the decay phase. Environ Monitor Assess 78:101–110

de Haan H (1993) Solar UV-light penetration and photodegradation of humic substances in peaty lake water. Limnol Oceanogr 38:1072–1076

del Vecchio R, Blough NV (2002) Photobleaching of chromophoric dissolved organic matter in natural waters: kinetics and modeling. Mar Chem 78:231–253

Deshmukh AP, Chen Y, Tarchitzky J, Chefetz B, Hatcher PG (2002) Structural characterization of soil organic matter and humic acids in particle-size fractions of an agricultural soil. Soil Sci Soc Am J 66:129–141

Dobrović S, Juretić H, Ružinski N (2007) Photodegradation of natural organic matter in water with UV irradiation at 185 and 254 nm: importance of hydrodynamic conditions on the decomposition rate. Sep Sci Technol 42:1421–1432

Dreybrodt W (1988) Processes in karst systems, physics, chemistry, and geology

Dunfield P, Dumont R, Moore TR (1993) Methane production and consumption in temperate and subarctic peat soils: response to temperature and pH. Soil Biol Biochem 25:321–326

Dupré B, Dessert C, Oliva P, Goddéris Y, Viers J, François L, Millot R, Gaillardet J (2003) Rivers, chemical weathering and Earth's climate. CR Geosci 335:1141–1160

Ebner S, Jaun B, Goenrich M, Thauer R, Harmer J (2010) Binding of coenzyme B induces a major conformational change in the active site of methyl-coenzyme M reductase. JACS 132:567–575

EPI (2007) Science advisory board review of the estimation programs interface (EPI) suite; office of the administrator science advisory board (SAB). U.S. Environmental Protection Agency, Washington

Fang TH (2004) Phosphorus speciation and budget of the East China Sea. Contin Shelf Res 24:1285–1299

Farmer CT, Moore CA, Zika RG, Sikorski RJ (1993) Effects of low and high orinoco river flow on the underwater light field of the Eastern Caribbean basin. J Geophys Res 98:2279–2288

Fenton HJ (1894) Oxidation of tartaric acid in presence of iron. J Chem Soc 65:899–910

Fichot CG, Miller WL (2010) An approach to quantify depth-resolved marine photochemical fluxes using remote sensing: Application to carbon monoxide (CO) photoproduction. Remote Sens Environ 114:1363–1377

Francko DA, Heath RT (1982) UV-sensitive complex phosphorus: association with dissolved humic material and iron in a bog lake. Limnol Oceanogr 27:564–569

Fu P, Mostofa KMG, Wu F, Liu CQ, Li W, Liao H, Wang L, Wang J, Mei Y (2010) Excitation-emission matrix characterization of dissolved organic matter sources in two eutrophic lakes (Southwestern China Plateau). Geochem J 44:99

Fujiwara K, Ushiroda T, Takeda K, Kumamoto YI, Tsubota H (1993) Diurnal and seasonal distribution of hydrogen peroxide in seawater of the Seto Inland Sea. Geochem J 27:103–115

Fujiwara K, Takeda K, Kumamoto Y (1995) Generations of carbonyl sulfide and hydrogen peroxide in the Seto Inland Sea—Photochemical reactions progressing in the coastal seawater. In: Sakai H, Nozaki Y (eds) Biogeochemical processes and Ocean flux in the Western Pacific. TERRAPUB, Tokyo, pp 101–127

Fukuzaki S, Nishio N, Nagai S (1990) Kinetics of the methanogenic fermentation of acetate. Appl Environ Microbiol 56:3158–3163

Galand PE, Saarnio S, Fritze H, Yrjälä K (2002) Depth related diversity of methanogen Archaea in Finnish oligotrophic fen. FEMS Microbiol Ecol 42:441–449

Galand P, Fritze H, Conrad R, Yrjälä K (2005) Pathways for methanogenesis and diversity of methanogenic archaea in three boreal peatland ecosystems. Appl Environ Microbiol 71:2195–2198

Galchenko V (1994) Sulfate Reduction, methane production, and methane oxidation in various water bodies of Banger-Hills Oasis of Antarctica. Microbiology 63:388–396

Gao H, Zepp RG (1998) Factors influencing photoreactions of dissolved organic matter in a coastal river of the southeastern United States. Environ Sci Technol 32:2940–2946

Gennings C, Molot LA, Dillon PJ (2001) Enhanced photochemical loss of organic carbon in acidic waters. Biogeochemistry 52:339–354

Getoff N (1991) Radiation-and photoinduced degradation of pollutants in water. A comparative study. Radiat Phys Chem 37:673–680

Getoff N, Schwoerer F, Markovic V, Sehested K, Nielsen SO (1971) Pulse radiolysis of oxalic acid and oxalates. J Phys Chem 75:749–755

Goldstone J, Pullin M, Bertilsson S, Voelker B (2002) Reactions of hydroxyl radical with humic substances: bleaching, mineralization, and production of bioavailable carbon substrates. Environ Sci Technol 36:364–372

Goodwin S, Zeikus JG (1987) Ecophysiological adaptations of anaerobic bacteria to low pH: analysis of anaerobic digestion in acidic bog sediments. Appl Environ Microbiol 53:57–64

Goodwin S, Conrad R, Zeikus J (1988) Influence of pH on microbial hydrogen metabolism in diverse sedimentary ecosystems. Appl Environ Microbiol 54:590–593

Gopinathan C, Damle P, Hart EJ (1972) Gamma-Ray irradiated sodium chloride as a source of hydrated electrons. J Phys Chem 76:3694–3698

Graneli W, Lindell M, Tranvik L (1996) Photo-oxidative production of dissolved inorganic carbon in lakes of different humic content. Limnol Oceanogr 41:698–706

Graneli W, Lindell M, de Faria B, de Assis EF (1998) Photoproduction of dissolved inorganic carbon in temperate and tropical lakes-dependence on wavelength band and dissolved organic carbon concentration. Biogeochemistry 43:175–195

Grebel JE, Pignatello JJ, Song W, Cooper WJ, Mitch WA (2009) Impact of halides on the photo bleaching of dissolved organic matter. Mar Chem 115:134–144

Gron C, Wassenaar L, Krog M (1996) Origin and structures of groundwater humic substances from three Danish aquifers. Environ Int 22:519–534

Guildford SJ, Hecky RE (2000) Total nitrogen, total phosphorus, and nutrient limitation in lakes and oceans: Is there a common relationship? Limnol Oceanogr 45:1213–1223

Haag WR, Hoigné J (1985) Photo-sensitized oxidation in natural water via OH radicals. Chemosphere 14:1659–1671

Haan H, Boer T, Halma G (1979) Curie point pyrolysis mass-spectrometry of fulvic acids from Tjeukemeer, The Netherlands. Freshwater Biol 9:315–317

Häder DP, Helbling E, Williamson C, Worrest R (2011) Effects of UV radiation on aquatic ecosystems and interactions with climate change. Photochem Photobiol Sci 10:242–260

Harvey HR, Tuttle JH, Bell JT (1995) Kinetics of phytoplankton decay during simulated sedimentation: Changes in biochemical composition and microbial activity under oxic and anoxic conditions. Geochim Cosmochim Acta 59:3367–3377

Hayase K, Shinozuka N (1995) Vertical distribution of fluorescent organic matter along with AOU and nutrients in the equatorial Central Pacific. Mar Chem 48:283–290

Hedges J, Eglinton G, Hatcher P, Kirchman D, Arnosti C, Derenne S, Evershed R, Kögel-Knabner I, De Leeuw J, Littke R (2000) The molecularly-uncharacterized component of non-living organic matter in natural environments. Org Geochem 31:945–958

Hellpointner E, Gäb S (1989) Detection of methyl, hydroxymethyl and hydroxyethyl hydroperoxides in air and precipitation. Nature 337:631–634

Henrichs SM, Doyle AP (1986) Decomposition of 14 C-labeled organic substances in marine sediments. Limnol Oceanogr 31:765–778

Herndl GJ, Müller-Niklas G, Frick J (1993) Major role of ultraviolet-B in controlling bacterio plankton growth in the surface layer of the ocean. Nature 361:717–719

Hernes PJ, Benner R (2003) Photochemical and microbial degradation of dissolved lignin phenols: Implications for the fate of terrigenous dissolved organic matter in marine environments. J Geophys Res 108:3291–3299

Herrmann H (2003) Kinetics of aqueous phase reactions relevant for atmospheric chemistry. Chem Rev 103:4691–4716

Herrmann H, Hoffmann D, Schaefer T, Bräuer P, Tilgner A (2010) Tropospheric aqueous-phase free-radical chemistry: radical Sources, spectra, reaction kinetics and prediction tools. Chem Phys Chem 11:3796–3822

Hewitt CN, Kok GL (1991) Formation and occurrence of organic hydroperoxides in the troposphere: laboratory and field observations. J Atmos Chem 12:181–194

Holmes D, Bond D, O'neil R, Reimers C, Tender L, Lovley D (2004) Microbial communities associated with electrodes harvesting electricity from a variety of aquatic sediments. Microb Ecol 48:178–190

Hongve D (1994) Sunlight degradation of aquatic humic substances. Acta Hydrochim Hydrobiol 22:117–120

Hopkinson CS, Vallino JJ, Nolin A (2002) Decomposition of dissolved organic matter from the continental margin. Deep Sea Res Part II 49:4461–4478

Horn MA, Matthies C, Küsel K, Schramm A, Drake HL (2003) Hydrogenotrophic methanogenesis by moderately acid-tolerant methanogens of a methane-emitting acidic peat. Appl Environ Microbiol 69:74–83

Hornibrook ERC, Longstaffe FJ, Fyfe WS (2000) Evolution of stable carbon isotope compositions for methane and carbon dioxide in freshwater wetlands and other anaerobic environments. Geochim Cosmochim Acta 64:1013–1027

Huber MM, Canonica S, Park GY, von Gunten U (2003) Oxidation of pharmaceuticals during ozonation and advanced oxidation processes. Environ Sci Technol 37:1016–1024

Huisman J, Thi NNP, Karl DM, Sommeijer B (2006) Reduced mixing generates oscillations and chaos in the oceanic deep chlorophyll maximum. Nature 439:322–325

Hulatt CJ, Thomas DN, Bowers DG, Norman L, Zhang C (2009) Exudation and decomposition of chromophoric dissolved organic matter (CDOM) from some temperate macroalgae. Estuar Coast Shelf Sci 84:147–153

Hur J (2011) Microbial changes in selected operational descriptors of dissolved organic matters from various sources in a watershed. Water Air Soil Pollut 215:465–476

Itoh M, Ohte N, Koba K, Sugimoto A, Tani M (2008) Analysis of methane production pathways in a riparian wetland of a temperate forest catchment, using δ^{13}C of pore water CH_4 and CO_2. J Geophys Res 113:G03005

Ivanov M, Belyaev S, Laurinavichus K (1976) Methods of quantitative investigation of microbiological production and utilization of methane. In: Schlegel HG, Gottschalk G, Pfennig N (eds) Microbial production and utilization of gases. E Goltze, Göttingen, pp 63–67

Jackson A, Hewitt CN (1996) Hydrogen peroxide and organic hydroperoxide concentrations in air in a eucalyptus forest in central Portugal. Atmos Environ 30:819–830

Jeong J, Yoon J (2005) pH effect on OH radical production in photo/ferrioxalate system. Water Res 39:2893–2900

Jetten MSM, Stams AJM, Zehnder AJB (1992) Methanogenesis from acetate: a comparison of the acetate metabolism in Methanothrix soehngenii and Methanosarcina spp. FEMS Microbiol Lett 88:181–197

Johannessen SC (2000) A photochemical sink for dissolved organic carbon in the ocean (176). PhD Thesis, Oceanography, Dalhousie University

Johannessen SC, Peña MA, Quenneville ML (2007) Photochemical production of carbon dioxide during a coastal phytoplankton bloom. Estuar Coast Shelf Sci 73:236–242

Johnson KS, Willason SW, Wiesenburg DA, Lohrenz SE, Arnone RA (1989) Hydrogen peroxide in the western Mediterranean Sea: A tracer for vertical advection. Deep Sea Res Part I 36:241–254

Jones RD (1991) Carbon monoxide and methane distribution and consumption in the photic zone of the Sargasso Sea. Deep Sea Res Part I 38:625–635

Jones RD, Amador JA (1993) Methane and carbon monoxide production, oxidation, and turnover times in the Caribbean Sea as influenced by the Orinoco River. J Geophys Res 98:2353–2359

Jones R, Morita R (1984) Effect of several nitrification inhibitors on carbon monoxide and methane oxidation by ammonium oxidizers. Can J Microbiol 30:1276–1279

Jones A, Shanklin J (1995) Continued decline of total ozone over Halley, Antarctica, since 1985. Nature 376:409–411

Jones JG, Simon BM, Gardener S (1982) Factors affecting methanogenesis and associated anaerobic processes in the sediments of a stratified eutrophic lake. J Gen Microbiol 128:1

Jørgensen NOG, Tranvik L, Edling H, Granéli W, Lindell M (1998) Effects of sunlight on occurrence and bacterial turnover of specific carbon and nitrogen compounds in lake water. FEMS Microbiol Ecol 25:217–227

Kaiser E, Sulzberger B (2004) Phototransformation of riverine dissolved organic matter (DOM) in the presence of abundant iron: effect on DOM bioavailability. Limnol Oceanogr 49:540–554

Kang SF, Liao CH, Po ST (2000) Decolorization of textile wastewater by photo-Fenton oxidation technology. Chemosphere 41:1287–1294

Karelson M (2000) Molecular descriptors in QSAR/QSPR. John Wiley & Sons, Inc: New York

Karentz D, Bothwell M, Coffin R, Hanson A, Herndl G, Kilham S, Lesser M, Lindell M, Moeller R, Morris D (1994) Impact of UV-B radiation on pelagic freshwater ecosystems: report of working group on bacteria and phytoplankton. Ergebn Limnol 43:31–31

Karl DM, Tien G (1997) Temporal variability in dissolved phosphorus concentrations in the subtropical North Pacific Ocean. Mar Chem 56:77–96

Kashefi KK, Holmes DE, Lovley DR, Tor JM (2004) In: (Wilcock WS, DeLong EF, Kelley DS, Baross JA, Cary SC (Ed), The subseafloor biosphere at mid-ocean ridges, American Geophysical Union, Washington pp 199–211

Keppler F, Hamilton JTG, Braß M, Röckmann T (2006) Methane emissions from terrestrial plants under aerobic conditions. Nature 439:187–191

Kerr J, McElroy C (1993) Evidence for large upward trends of ultraviolet-B radiation linked to ozone depletion. Science 262:1032–1034

Kieber DJ, McDaniel J, Mopper K (1989) Photochemical source of biological substrates in sea water: Implications for carbon cycling. Nature 341:637–639

Kieber RJ, Zhou X, Mopper K (1990) Formation of carbonyl compounds from UV-induced photodegradation of humic substances in natural waters: Fate of riverine carbon in the sea. Limnol Oceanogr 35:1503–1515

Kieber D, Mopper K, Qian J, Zafiriou O (2001) Photochemical formation of dissolved inorganic carbon in seawater and its impact on the marine carbon cycle. Paper presented at the Session 2: Photochemical reactions in surface waters ASLO 2001, Albuquerque, February 12–16

Kim DJ, Kim SH (2006) Effect of nitrite concentration on the distribution and competition of nitrite-oxidizing bacteria in nitratation reactor systems and their kinetic characteristics. Water Res 40:887–894

Kim C, Nishimura Y, Nagata T (2006) Role of dissolved organic matter in hypolimnetic mineralization of carbon and nitrogen in a large, monomictic lake. Limnol Oceanogr 51:70–78

Kirchman DL, Suzuki Y, Garside C, Ducklow HW (1991) High turnover rates of dissolved organic carbon during a spring phytoplankton bloom. Nature 352:612–614

Kirk J (1994) Optics of UV-B radiation in natural waters. Ergebn Limnol 43:1–16

Komada T, Schofield OME, Reimers CE (2002) Fluorescence characteristics of organic matter released from coastal sediments during resuspension. Mar Chem 79:81–97

Komissarov G (1994) Photosynthesis: a new look. Sci Russia 5:52–55

Komissarov G (1995) Photosynthesis as a Physicochemical Process. Khim Fiz 14:20–28

Komissarov G (2003) Photosynthesis: the physical-chemical approach. J Adv Chem Phys 2:28–61

Kopacek J, Hejzlar J, Kana J, Porcal P, Klementova S (2003) Photochemical, chemical, and biological transformations of dissolved organic carbon and its effect on alkalinity production in acidified lakes. Limnol Oceanogr 48:106–117

Koschorreck M, Wendt-Potthoff K, Scharf B, Richnow HH (2008) Methanogenesis in the sediment of the acidic Lake Caviahue in Argentina. J Volcanol Geothermal Res 178:197–204

Kotelnikova S, Macario AJL, Pedersen K (1998) Methanobacterium subterraneum sp. nov., a new alkaliphilic, eurythermic and halotolerant methanogen isolated from deep granitic groundwater. Int J Syst Bacteriol 48:357–367

Kotsyurbenko O, Nozhevnikova A, Zavarzin G (1993) Methanogenic degradation of organic matter by anaerobic bacteria at low temperature. Chemosphere 27:1745–1761

Kotsyurbenko O, Simankova M, Nozhevnikova A, Zhilina T, Bolotina N, Lysenko A, Osipov G (1995) New species of psychrophilic acetogens: *Acetobacterium bakii* sp. nov., *A. paludosum* sp. nov., *A. fimetarium* sp. nov. Arch Microbiol 163:29–34

Kotsyurbenko O, Nozhevnikova A, Soloviova T, Zavarzin G (1996) Methanogenesis at low temperatures by microflora of tundra wetland soil. Antonie Van Leeuwenhoek 69:75–86

Kotsyurbenko OR, Glagolev MV, Nozhevnikova AN, Conrad R (2001) Competition between homoacetogenic bacteria and methanogenic archaea for hydrogen at low temperature. FEMS Microbiol Ecol 38:153–159

Kotsyurbenko OR, Chin KJ, Glagolev MV, Stubner S, Simankova MV, Nozhevnikova AN, Conrad R (2004) Acetoclastic and hydrogenotrophic methane production and methanogenic populations in an acidic West-Siberian peat bog. Environ Microbiol 6:1159–1173

Kotsyurbenko O, Friedrich M, Simankova M, Nozhevnikova A, Golyshin P, Timmis K, Conrad R (2007) Shift from acetoclastic to H2-dependent methanogenesis in a West Siberian peat bog at low pH values and isolation of an acidophilic Methanobacterium strain. Appl Environ Microbiol 73:2344–2348

Kramer JB, Canonica S, Hoigné J, Kaschig J (1996) Degradation of fluorescent whitening agents in sunlit natural waters. Environ Sci Technol 30:2227–2234

Kuivila K, Murray J, Devol A, Novelli P (1989) Methane production, sulfate reduction and competition for substrates in the sediments of Lake Washington. Geochim Cosmochim Acta 53:409–416

Kujawinski EB, Longnecker K, Blough NV, Vecchio RD, Finlay L, Kitner JB, Giovannoni SJ (2009) Identification of possible source markers in marine dissolved organic matter using ultrahigh resolution mass spectrometry. Geochim Cosmochim Acta 73:4384–4399

Kulovaara M (1996) Light-induced degradation of aquatic humic substances by simulated sunlight. Int J Environ Anal Chem 62:85–95

Kwok ESC, Atkinson R (1995) Estimation of hydroxyl radical reaction rate constants for gas-phase organic compounds using a structure-reactivity relationship: an update. Atmos Environ 29:1685–1695

Laane R, Gieskes W, Kraay G, Eversdijk A (1985) Oxygen consumption from natural waters by photo-oxidizing processes. Neth J Sea Res 19:125–128

Langvik VA, Akerback N, Holmbom B (1994) Characterization of aromatic structures in humic and fulvic acids. Environ Int 20:61–65

Lansdown J, Quay P, King S (1992) CH_4 production via CO_2 reduction in a temperate bog: a source of $\delta^{13}C$-depleted CH_4. Geochim Cosmochim Acta 56:3493–3503

Lapado JA, Barlaz MA (1997) Isolation and characterization of refuse methanogens. J Appl Microbiol 82:751–758

Laurion I, Ventura M, Catalan J, Psenner R, Sommaruga R (2000) Attenuation of ultraviolet radiation in mountain lakes: Factors controlling the among-and within-lake variability. Limnol Oceanogr 45:1274–1288

Lee HS, Rittmann BE (2009) Evaluation of metabolism using stoichiometry in fermentative biohydrogen. Biotechnol Bioeng 102:749–758

Lee HS, Rittmann BE (2010) Characterization of energy losses in an upflow single-chamber microbial electrolysis cell. International J Hydrogen Energy 35:920–927

Lee HS, Salerno MB, Rittmann BE (2008) Thermodynamic evaluation on H_2 production in glucose fermentation. Environ Sci Technol 42:2401–2407

Leenheer J, Croue JP (2003) Characterizing aquatic dissolved organic matter. Environ Sci Technol 37:18–26

Lehmann MF, Bernasconi SM, Barbieri A, McKenzie JA (2002) Preservation of organic matter and alteration of its carbon and nitrogen isotope composition during simulated and in situ early sedimentary diagenesis. Geochim Cosmochim Acta 66:3573–3584

Letelier RM, Karl DM, Abbott MR, Bidigare RR (2004) Light driven seasonal patterns of chlorophyll and nitrate in the lower euphotic zone of the North Pacific Subtropical Gyre. Limnol Oceanogr 49:508–519

Li K, Crittenden J (2009) Computerized pathway elucidation for hydroxyl radical-induced chain reaction mechanisms in aqueous phase advanced oxidation processes. Environ Sci Technol 43:2831–2837

Li C, Fang HHP (2007) Fermentative hydrogen production from wastewater and solid wastes by mixed cultures. Crit Rev Environ Sci Technol 37:1–39

Li W, Wu F, Liu C, Fu P, Wang J, Mei Y, Wang L, Guo J (2008) Temporal and spatial distributions of dissolved organic carbon and nitrogen in two small lakes on the Southwestern China Plateau. Limnology 9:163–171

Lindell MJ, Rai H (1994) Photochemical oxygen consumption in humic waters. Ergebn Limnol 43:145–145

Lindell M, Granéli W, Tranvik L (1996) Impact of solar (UV)-radiation on bacterial growth in lakes. Aquat Microb Ecol 11:135–141

Liu K, Atkinson L, Chen C, Gao S, Hall J, Macdonald R, Talaue L (2000) Exploring continental margin carbon fluxes on a global scale. Eos Trans AGU 81(52):641. doi:10.1029/EO081i052p00641-01

Liu Z, Dreybrodt W, Wang H (2010) A new direction in effective accounting for the atmospheric CO_2 budget: Considering the combined action of carbonate dissolution, the global water cycle and photosynthetic uptake of DIC by aquatic organisms. Earth Sci Rev 99:162–172

Logan BE, Regan JM (2006) Electricity-producing bacterial communities in microbial fuel cells. TRENDS in Microbiol 14:512–518

Lohrenz SE, Cai WJ, Chen F, Chen X, Tuel M (2010) Seasonal variability in air-sea fluxes of CO_2 in a river-influenced coastal margin. J Geophys Res 115:C10034

Lønborg C, Søndergaard M (2009) Microbial availability and degradation of dissolved organic carbon and nitrogen in two coastal areas. Estuar Coast Shelf Sci 81:513–520

Lønborg C, Álvarez-Salgado XA, Davidson K, Miller AEJ (2009a) Production of bioavailable and refractory dissolved organic matter by coastal heterotrophic microbial populations. Estuar Coast Shelf Sci 82:682–688

Lønborg C, Davidson K, Álvarez-Salgado XA, Miller AEJ (2009b) Bioavailability and bacterial degradation rates of dissolved organic matter in a temperate coastal area during an annual cycle. Mar Chem 113:219–226

Lovley D (1991) Dissimilatory Fe(III) and Mn(IV) reduction. Microbiol Rev 55:259–287

Lovley DR (2006) Bug juice: harvesting electricity with microorganisms. Nature Rev Microbiol 4:497–508

Lovley DR, Chapelle FH (1995) Deep subsurface microbial processes. Rev Geophys 33:365–381

Lovley D, Klug M (1986) Model for the distribution of sulfate reduction and methanogenesis in freshwater sediments. Geochim Cosmochim Acta 50:11–18

Lovley DR, Phillips EJP (1987) Competitive mechanisms for inhibition of sulfate reduction and methane production in the zone of ferric iron reduction in sediments. Appl Environ Microbiol 53:2636–2641

Lovley DR, Coates JD, Blunt-Harris EL, Phillips EJP, Woodward JC (1996) Humic substances as electron acceptors for microbial respiration. Nature 382:445–448

Lovley DR, Holmes DE, Nevin KP (2004) Dissimilatory Fe(III) and Mn(IV) reduction. Adv Microb Physiol 49:219–286

Lund V, Hongve D (1994) Ultraviolet irradiated water containing humic substances inhibits bacterial metabolism. Water Res 28:1111–1116

Ma X, Green SA (2004) Photochemical transformation of dissolved organic carbon in lake superior–an in situ experiment. J Great Lakes Res 30:97–112

Mack J, Bolton JR (1999) Photochemistry of nitrite and nitrate in aqueous solution: a review. J Photochem Photobiol, A 128:1–13

Maddigapu P, Minella M, Vione D, Maurino V, Minero C (2011) Modeling phototransformation reactions in surface water bodies: 2, 4-dichloro-6-nitrophenol as a case study. Environ Sci Technol 45:209

Madronich S (1992) Implications of recent total atmospheric ozone measurements for biologically active ultraviolet radiation reaching the Earth's surface. Geophys Res Lett 19:37–40

Maita Y, Montani S, Ishii J (1982) Early diagenesis of amino acids in Okhotsk Sea sediments. Deep Sea Res Part A 29:485–498

Malcolm R (1985) Geochemistry of stream fulvic and humic substances

Malcolm RL (1990) The uniqueness of humic substances in each of soil, stream and marine environments. Analyt Chim Acta 232:19–30

Managaki S, Takada H (2005) Fluorescent whitening agents in Tokyo Bay sediments: molecular evidence of lateral transport of land-derived particulate matter. Mar Chem 95:113–127

McKnight D, Kimball B, Bencala K (1988) Iron photoreduction and oxidation in an acidic mountain stream. Science 240:637–640

Meier J, Babenzien H-D, Wendt-Potthoff K (2004) Microbial cycling of iron and sulfur in sediments of acidic and pH-neutral mining lakes in Lusatia (Brandenburg, Germany). Biogeochemistry 67:135–156

Merga G, Schuchmann HP, Rao BSM, von Sonntag C (1996) $^{\cdot}$OH radical-induced oxidation of chlorobenzene in aqueous solution in the absence and presence of oxygen. J Chem Soc, Perkin Trans 2:1097–1103

Midorikawa T, Tanoue E (1996) Extraction and characterization of organic ligands from oceanic water columns by immobilized metal ion affinity chromatography. Mar Chem 52:157–171

Midorikawa T, Tanoue E (1998) Molecular masses and chromophoric properties of dissolved organic ligands for copper (II) in oceanic water. Mar Chem 62:219–239

Miles CJ, Brezonik PL (1981) Oxygen consumption in humic-colored waters by a photochemical ferrous-ferric catalytic cycle. Environ Sci Technol 15:1089–1095

Milferstedt K, Youngblut ND, Whitaker RJ (2010) Spatial structure and persistence of methanogen populations in humic bog lakes. ISME J 4:764–776

Miller WL (1998) Effects of UV radiation on aquatic humus: photochemical principles and experimental considerations. In: Hessen DO, Tranvik LJ (eds) Aquatic humic substances. Springer, Berlin, pp 125–144

Miller WL, Moran MA (1997) Interaction of photochemical and microbial processes in the degradation of refractory dissolved organic matter from a coastal marine environment. Limnol Oceanogr 42:1317–1324

Miller WL, Zepp RG (1995) Photochemical production of dissolved inorganic carbon from terrestrial organic matter: significance to the oceanic organic. Geophys Res Lett 22:417–420

Millero FJ, Sotolongo S (1989) The oxidation of Fe(II) with H_2O_2 in seawater. Geochim Cosmochim Acta 53:1867–1873

Minakata D, Crittenden J (2011) Linear free energy relationships between aqueous phase Hydroxyl radical reaction rate constants and free energy of activation. Environ Sci Technol 45:3479–3486

Minakata D, Li K, Westerhoff P, Crittenden J (2009) Development of a group contribution method to predict aqueous phase hydroxyl radical ($HO^{\bullet}$) reaction rate constants. Environ Sci Technol 43:6220–6227

Minakata D, Song W, Crittenden J (2011) Reactivity of aqueous phase hydroxyl radical with halogenated carboxylate anions: experimental and theoretical studies. Environ Sci Technol 45:6057–6065

Minella M, Rogora M, Vione D, Maurino V, Minero C (2011) A model approach to assess the long-term trends of indirect photochemistry in lake water. The case of Lake Maggiore (NW Italy). Sci Total Environ 409:3463–3471

Minero C, Chiron S, Falletti G, Maurino V, Pelizzetti E, Ajassa R, Carlotti ME, Vione D (2007) Photochemincal processes involving nitrite in surface water samples. Aquat Sci 69:71–85

Minor E, Pothen J, Dalzell B, Abdulla H, Mopper K (2006) Effects of salinity changes on the photodegradation and ultraviolet-visible absorbance of terrestrial dissolved organic matter. Limnol Oceanogr 51:2181–2186

Moffett J, Zafiriou O (1990) An investigation of hydrogen peroxide chemistry in surface waters of Vineyard Sound with H218O2 and 18O2. Limnol Oceanogr 35:1221–1229

Moffett JW, Zika RG (1987) Reaction kinetics of hydrogen peroxide with copper and iron in seawater. Environ Sci Technol 21:804–810

Molot LA, Dillon PJ (1997) Photolytic regulation of dissolved organic carbon in northern lakes. Global Biogeochem Cy 11:357–365

Molot LA, Hudson JJ, Dillon PJ, Miller SA (2005) Effect of pH on photo-oxidation of dissolved organic carbon by hydroxyl radicals in a coloured, softwater stream. Aquat Sci 67:189–195

Monod A, Poulain L, Grubert S, Voisin D, Wortham H (2005) Kinetics of OH-initiated oxidation of oxygenated organic compounds in the aqueous phase: new rate constants, structure–activity relationships and atmospheric implications. Atmos Environ 39:7667–7688

Moore CA, Farmer CT, Zika RG (1993) Influence of the Orinoco river on hydrogen peroxide distribution and production in the eastern Caribbean. J Geophys Res 98:2289–2298

Mopper K, Stahovec WL (1986) Sources and sinks of low molecular weight organic carbonyl compounds in seawater. Mar Chem 19:305–321

Mopper K, Zhou X (1990) Hydroxyl radical photoproduction in the sea and its potential impact on marine processes. Science 250:661–664

Mopper K, Zhou X, Kieber RJ, Kieber DJ, Sikorski RJ, Jones RD (1991) Photochemical degradation of dissolved organic carbon and its impact on the oceanic carbon cycle. Nature 353:60–62

Moran MA, Hodson RE (1994) Support of bacterioplankton production by dissolved humic substances from three marine environments. Mar Ecol Prog Ser 110:241–241

Moran MA, Zepp RG (1997) Role of photoreactions in the formation of biologically labile compounds from dissolved organic matter. Limnol Oceanogr 42:1307–1316

Moran MA, Sheldon WM Jr, Zepp RG (2000) Carbon loss and optical property changes during long-term photochemical and biological degradation of estuarine dissolved organic matter. Limnol Oceanogr 45:1254–1264

Morris DP, Hargreaves BR (1997) The role of photochemical degradation of dissolved organic carbon in regulating the UV transparency of three lakes on the Pocono Plateau. Limnol Oceanogr 42:239–249

Morris DP, Zagarese H, Williamson CE, Balseiro EG, Hargreaves BR, Modenutti B, Moeller R, Queimalinos C (1995) The attenuation of solar UV radiation in lakes and the role of dissolved organic carbon. Limnol Oceanogr 40:1381–1391

Mortatti J, Probst JL (2003) Silicate rock weathering and atmospheric/soil CO_2 uptake in the Amazon basin estimated from river water geochemistry: seasonal and spatial variations. Chem Geol 197:177–196

Morvan B, Dore J, Rieu-Lesme F, Foucat L, Fonty G, Gouet P (1994) Establishment of hydrogen-utilizing bacteria in the rumen of the newborn lamb. FEMS Microbiol Lett 117:249–256

Mostofa K (2005) Dynamics, characteristics and photochemical processes of fluorescent dissolved organic matter and peroxides in river water. Ph D Thesis September 2005, Hiroshima University, Japan

Mostofa KMG, Sakugawa H (2003) Spatial and temporal variation of hydrogen peroxide in stream and river waters: Effect of photo-bio-physio-chemical processes of aquatic matters. Abs 13th Ann VM Goldschmidt Conf, Kurashiki, Japan. Geochim Cosmochim Acta 67(18S):A309. In, 2003

Mostofa KMG, Sakugawa H (2009) Spatial and temporal variations and factors controlling the concentrations of hydrogen peroxide and organic peroxides in rivers. Environ Chem 6:524–534

Mostofa KMG, Honda Y, Sakugawa H (2005a) Dynamics and optical nature of fluorescent dissolved organic matter in river waters in Hiroshima Prefecture, Japan. Geochem J 39:257–271

Mostofa KMG, Yoshioka T, Konohira E, Tanoue E, Hayakawa K, Takahashi M (2005b) Three-dimensional fluorescence as a tool for investigating the dynamics of dissolved organic matter in the Lake Biwa watershed. Limnology 6:101–115

Mostofa KMG, Yoshioka T, Konohira E, Tanoue E (2007a) Dynamics and characteristics of fluorescent dissolved organic matter in the groundwater, river and lake water. Water Air Soil Pollut 184:157–176

Mostofa KMG, Yoshioka T, Konohira E, Tanoue E (2007b) Photodegradation of fluorescent dissolved organic matter in river waters. Geochem J 41:323–331

Mostofa K, Wu F, Yoshioka T, Sakugawa H, Tanoue E (2009a) Dissolved organic matter in the aquatic environments. In: Wu F, B X (eds) Natural organic matter and its significance in the environment. Science press, Beijing pp 3–66

Mostofa K, Liu C, Wu F, Fu P, Ying W, Yuan J (2009b) Overview of key biogeochemical functions in Lake Ecosystem: Impacts of organic matter pollution and global warming. Paper presented at the Proceedings of the 13th World Lake Conf Wuhan, Wuhan, China 1–5 Nov 2009

Mostofa KMG, Wu F, Liu CQ, Fang WL, Yuan J, Ying WL, Wen L, Yi M (2010) Characterization of Nanming river (Southwestern China) sewerage-impacted pollution using an excitation-emission matrix and PARAFAC. Limnology 11:217–231

Mostofa KMG, Wu F, Liu CQ, Vione D, Yoshioka T, Sakugawa H, Tanoue E (2011) Photochemical, microbial and metal complexation behavior of fluorescent dissolved organic matter in the aquatic environments. Geochem J 45:235–254

Mvula E, Schuchmann MN, von Sonntag C (2001) Reactions of phenol-OH-adduct radicals. Phenoxyl radical formation by water elimination vs. oxidation by dioxygen. J Chem Soc, Perkin Trans 2:264–268

Naganuma T, Konishil S, Nakane TIT (1996) Photodegradation or photoalteration? Microbial assay of the effect of UV-B on dissolved organic matter. Mar Ecol Prog Ser 135:309–310

Nagase M, Matsuo T (1982) Interactions between amino-acid-degrading bacteria and methanogenic bacteria in anaerobic digestion. Biotechnol Bioeng 24:2227–2239

Nakagawa F, Yoshida N, Nojiri Y, Makarov VN (2002) Production of methane from alasses in eastern Siberia: implications from its 14C and stable isotopic compositions. Global Biogeochem Cy 16:1041

Nakane K, Kohno T, Horikoshi T, Nakatsubo T (1997) Soil carbon cycling at a black spruce (Picea Mariana) forest stand in Saskatchewan, Canada. J Geophys Res 102:28785–28793

Nakatani N, Hashimoto N, Sakugawa H (2004) An evaluation of hydroxyl radical formation in river water and the potential for photodegradation of bisphenol A. In: Hill RJ, Leventhal J, Aizenshtat Z, Baedecker MJ, Claypool G, Eganhouse R, Goldhaber M, Peters K, (Eds), The Geochemical society special publication series 9, Geochemical investigations in earth and space Science: A Tribute to Isaac R Kaplan Elsevier, Amsterdam, pp 233–242

Namsaraev B, Dulov L, Sokolova E (1995) Bacterial methane production in the bottom sediments of Lake Baikal. Mikrobiologiya 64:411–412

Nieto-Cid M, Alvarez-Salgado X, Pérez F (2006) Microbial and photochemical reactivity of fluorescent dissolved organic matter in a coastal upwelling system. Limnol Oceanogr 51:1391–1400

Nozhevnikova A, Kotsyurbenko O, Simankova M (1994) Acetogenesis at low temperature. In: Drake H (ed) Acetogenesis. Chapman and Hall, New York, pp 416–431

Obernosterer I, Ruardij P, Herndl GJ (2001) Spatial and diurnal dynamics of dissolved organic matter (DOM) fluorescence and H_2O_2 and the photochemical oxygen demand of surface water DOM across the subtropical Atlantic Ocean. Limnol Oceanogr 46:632–643

Omar A, Olsen A, Johannessen T, Hoppema M, Thomas H, Borges A (2010) Spatiotemporal variations of fCO_2 in the North Sea. Ocean Sci 6:77–89

Öquist M, Svensson B (2002) Vascular plants as regulators of methane emissions from a subarctic mire ecosystem. J Geophys Res 107:4580

Osburn CL, Morris DP (2003) Photochemistry of chromophoric dissolved organic matter in natural waters. UV Eff Aquat Org Ecosyst 1:185–217

Osburn CL, O'Sullivan DW, Boyd TJ (2009) Increases in the longwave photobleaching of chromophoric dissolved organic matter in coastal waters. Limnol Oceanogr 54:145–159

O'Sullivan DW, Neale PJ, Coffin RB, Boyd TJ, Osburn CL (2005) Photochemical production of hydrogen peroxide and methylhydroperoxide in coastal waters. Mar Chem 97:14–33

Palenik B, Morel F (1988) Dark production of H_2O_2 in the Sargasso Sea. Limnol Oceanogr 33:1606–1611

Parlanti E, Wörz K, Geoffroy L, Lamotte M (2000) Dissolved organic matter fluorescence spectroscopy as a tool to estimate biological activity in a coastal zone submitted to anthropogenic inputs. Org Geochem 31:1765–1781

Patel G, Sprott G, Fein J (1990) Isolation and characterization of Methanobacterium espanolae sp. nov., a mesophilic, moderately acidiphilic methanogen. Int J Syst Bacteriol 40:12–18

Pelmenschikov V, Blomberg MRA, Siegbahn PEM, Crabtree RH (2002) A mechanism from quantum chemical studies for methane formation in methanogenesis. JACS 124:4039–4049

Peña-Méndez EM, Havel J, Patočka J (2005) Humic substances–compounds of still unknown structure: applications in agriculture, industry, environment, and biomedicine. J Appl Biomed 3:13–24

Peuravuori J, Pihlaja K (1997) Pyrolysis electron impact mass spectrometry in studying aquatic humic substances. Analyt Chim Acta 350:241–247

Phelps T, Zeikus J (1984) Influence of pH on terminal carbon metabolism in anoxic sediments from a mildly acidic lake. Appl Environ Microbiol 48:1088–1095

Piazena H, Häder DP (1994) Penetration of solar UV irradiation in coastal lagoons of the southern Baltic Sea and its effect on phytoplankton communities. Photochem Photobiol 60:463–469

Premier G, Kim J, Massanet-Nicolau J, Kyazze G, Esteves S, Penumathsa B, Rodríguez J, Maddy J, Dinsdale R, Guwy A (2012) Integration of biohydrogen, biomethane and bioelectrochemical systems. Renewable Energy (in press)

Psenner R (1988) Alkalinity generation in a soft-water lake: watershed and in-lake processes. Limnol Oceanogr 33:1463–1475

Pullin MJ, Bertilsson S, Goldstone JV, Voelker BM (2004) Effects of sunlight and hydroxyl radical on dissolved organic matter: Bacterial growth efficiency and production of carboxylic acids and other substrates. Limnol Oceanogr 49:2011–2022

Qian J, Mopper K, Kieber DJ (2001) Photochemical production of the hydroxyl radical in Antarctic waters. Deep Sea Res Part I 48:741–759

Raghavan N, Steenken S (1980) Electrophilic reaction of the hydroxyl radical with phenol. Determination of the distribution of isomeric dihydroxycyclohexadienyl radicals. JACS 102:3495–3499

Randall C, Harvey V, Manney G, Orsolini Y, Codrescu M, Sioris C, Brohede S, Haley C, Gordley L, Zawodny J (2005) Stratospheric effects of energetic particle precipitation in 2003–2004. Geophys Res Lett 32:L05802

Ratte M, Bujok O, Spitzy A, Rudolph J (1998) Photochemical alkene formation in seawater from dissolved organic carbon: Results from laboratory experiments. J Geophys Res 103:5707–5717

Reche I, Pace ML, Cole JJ (1999) Relationship of trophic and chemical conditions to photobleaching of dissolved organic matter in lake ecosystems. Biogeochemistry 44:259–280

Reguera G, McCarthy KD, Mehta T, Nicoll JS, Tuominen MT, Lovley DR (2005) Extracellular electron transfer via microbial nanowires. Nature 435:1098–1101

Reitner B, Herndl GJ, Herzig A (1997) Role of ultraviolet-B radiation on photochemical and microbial oxygen consumption in a humic-rich shallow lake. Limnol Oceanogr 42:950–960

Rex M, Harris NRP, von der Gathen P, Lehmann R, Braathen GO, Reimer E, Beck A, Chipperfield MP, Alfier R, Allaart M (1997) Prolonged stratospheric ozone loss in the 1995–96 Arctic winter. Nature 389:835–838

Richard LE, Peake BM, Rusak SA, Cooper WJ, Burritt DJ (2007) Production and decomposition dynamics of hydrogen peroxide in freshwater. Environ Chem 4:49–54

Roberts EC, Priscu JC, Wolf C, Lyons WB, Laybourn-Parry J (2004) The distribution of microplankton in the McMurdo Dry Valley Lakes, Antarctica: response to ecosystem legacy or present-day climatic controls? Polar Biol 27:238–249

Rochelle-Newall E, Fisher T (2002) Production of chromophoric dissolved organic matter fluorescence in marine and estuarine environments: an investigation into the role of phytoplankton. Mar Chem 77:7–21

Roden EE, Wetzel RG (1996) Organic carbon oxidation and suppression of methane production by microbial Fe(III) oxide reduction in vegetated and unvegetated freshwater wetland sediments. Limnol Oceanogr 41:1733–1748

Rontani JF (2001) Visible light-dependent degradation of lipidic phytoplanktonic components during senescence: a review. Phytochemistry 58:187–202

Rosenfeld JK (1979) Amino acid diagenesis and adsorption in nearshore anoxic sediments. Limnol Oceanogr 24:1014–1021

Rosenfeldt EJ, Linden KG (2004) Degradation of endocrine disrupting chemicals bisphenol A, ethinyl estradiol, and estradiol during UV photolysis and advanced oxidation processes. Environ Sci Technol 38:5476–5483

Rosenstock B, Zwisler W, Simon M (2005) Bacterial consumption of humic and non-humic low and high molecular weight DOM and the effect of solar irradiation on the turnover of labile DOM in the Southern Ocean. Microb Ecol 50:90–101

Rothfuss F, Conrad R (1992) Vertical profiles of CH_4 concentrations, dissolved substrates and processes involved in CH_4 production in a flooded Italian rice field. Biogeochemistry 18:137–152

Rozendal RA, Hamelers HVM, Molenkamp RJ, Buisman CJN (2007) Performance of single chamber biocatalyzed electrolysis with different types of ion exchange membranes. Water Res 41:1984–1994

Sadtler (1968) The Sadtler standard spectra 1968 edition. Sadtler Research Lab, Inc, Philadelphia

Safarzadeh-Amiri A, Bolton JR, Cater SR (1996) Ferrioxalate-mediated solar degradation of organic contaminants in water. Sol Energy 56:439–443

Safarzadeh-Amiri A, Bolton JR, Cater SR (1997) Ferrioxalate-mediated photodegradation of organic pollutants in contaminated water. Water Res 31:787–798

Sakugawa H, Takami A, Kawai H, Takeda K, Fujiwara K, Hirata S (2000a) The occurrence of organic peroxide in seawater. In: Handa N, Tanoue E, Hama T (eds) Dynamics and characterization of marine organic matter. TERRAPUB, Kluwer, pp 231–240

Salonen K, Vähätalo A (1994) Photochemical mineralisation of dissolved organic matter in Lake Skjervatjern. Environ Int 20:307–312

Salonen K, Kairesalo T, Jones R (1992) Dissolved organic matter in lacustrine ecosystems: Energy-source and system regulator. Hydrobiology 229:1–291

Samuilov V, Bezryadnov D, Gusev M, Kitashov A, Fedorenko T (2001) Hydrogen peroxide inhibits photosynthetic electron transport in cells of cyanobacteria. Biochemistry (Moscow) 66:640–645

Sandbeck KA, Ward DM (1981) Fate of immediate methane precursors in low-sulfate, hot-spring algal-bacterial mats. Appl Environ Microbiol 41:775–782

Sarmiento JL, Slater R, Barber R, Bopp L, Doney SC, Hirst A, Kleypas J, Matear R, Mikolajewicz U, Monfray P (2004) Response of ocean ecosystems to climate warming. Global Biogeochem Cy 18:3001–3023

Schindler D, Turner M, Stainton M, Linsey G (1986) Natural sources of acid neutralizing capacity in low alkalinity lakes of the Precambrian Shield. Science 232:844–847

Schink B (1997) Energetics of syntrophic cooperation in methanogenic degradation. Microbiol Mol Biol Rev 61:262–280

Schmitt-Kopplin P, Hertkorn N, Schulten HR, Kettrup A (1998) Structural changes in a dissolved soil humic acid during photochemical degradation processes under O_2 and N_2 atmosphere. Environ Sci Technol 32:2531–2541

Schmittner A (2005) Decline of the marine ecosystem caused by a reduction in the Atlantic overturning circulation. Nature 434:628–633

Schulz S, Conrad R (1995) Effect of algal deposition on acetate and methane concentrations in the profundal sediment of a deep lake (Lake Constance). FEMS Microbiol Ecol 16:251–260

Schulz S, Conrad R (1996) Influence of temperature on pathways to methane production in the permanently cold profundal sediment of Lake Constance. FEMS Microbiol Ecol 20:1–14

Schwarzenbach RPGP, Imboden DM (1993) Environmental organic chemistry. Wiley, New York, pp 436–484

Scully N, Lean D (1994) The attenuation of ultraviolet radiation in temperate lakes (With 8 figures and 5 tables). Arch Hydrobiol Beih Ergebn Limnol 43:135–144

Scully N, McQueen D, Lean D, Cooper W (1996) Hydrogen peroxide formation: the interaction of ultraviolet radiation and dissolved organic carbon in lake waters along a 43–75? N Gradient. Limnol Oceanogr 41:540–548

Senesi N (1990) Molecular and quantitative aspects of the chemistry of fulvic acid and its interactions with metal ions and organic chemicals: Part II. The fluorescence spectroscopy approach. Analyt Chim Acta 232:77–106

Serban A, Nissenbaum A (1986) Humic acid association with peroxidase and catalase. Soil Biol Biochem 18:41–44

Shiller AM, Duan S, van Erp P, Bianchi TS (2006) Photo-oxidation of dissolved organic matter in river water and its effect on trace element speciation. Limnol Oceanogr 51(4):1716–1728

Shriner RLHW, Cox RFB (1943) p-Nitrophenyl Isocyanate. Org Synth Coll 2:453–455

Siegel DA, Michaels AF (1996) Quantification of non-algal light attenuation in the Sargasso sea: implications for biogeochemistry and remote sensing. Deep Sea Res Part II 43:321–345

Sikorski RJ, Zika R (1993a) Modeling mixed-layer photochemistry of H_2O_2: physical and chemical modeling of distribution. J Geophys Res 98:2329–2340

Sikorski RJ, Zika R (1993b) Modeling mixed-layer photochemistry of H_2O_2: optical and chemical modeling of production. J Geophys Res 98:2315–2328

Simankova MV, Kotsyurbenko OR, Stackebrandt E, Kostrikina NA, Lysenko AM, Osipov GA, Nozhevnikova AN (2000) *Acetobacterium tundrae* sp. nov., a new psychrophilic acetogenic bacterium from tundra soil. Arch Microbiol 174:440–447

Sizova MV, Panikov NS, Tourova TP, Flanagan PW (2003) Isolation and characterization of oligotrophic acido-tolerant methanogenic consortia from a Sphagnum peat bog. FEMS Microbiol Ecol 45:301–315

Skoog A, Wedborg M, Fogelqvist E (1996) Photobleaching of fluorescence and the organic carbon concentration in a coastal environment. Mar Chem 55:333–345

Smith RC, Baker KS (1981) Optical properties of the clearest natural waters (200–800 nm). Appl Opt 20:177–184

Song R, Westerhoff P, Minear RA, Amy GL (1996) Interaction between bromine and natural organic matter. (Minear RA, Amy GL (eds), Water disinfection and natural organic matter, Americal Chemical Society, Washington, pp 298–321

Southworth BA, Voelker BM (2003) Hydroxyl radical production via the photo-Fenton reaction in the presence of fulvic acid. Environ Sci Technol 37:1130–1136

Stedmon CA, Markager S (2005) Tracing the production and degradation of autochthonous fractions of dissolved organic matter by fluorescence analysis. Limnol Oceanogr 50:1415–1426

Stedmon CA, Markager S, Tranvik L, Kronberg L, Slätis T, Martinsen W (2007) Photochemical production of ammonium and transformation of dissolved organic matter in the Baltic Sea. Mar Chem 104:227–240

Steelink C (2002) Peer Reviewed: investigating humic acids in soils. Anal Chem 74:326–333

Steinberg SM, Venkatesan MI, Kaplan IR (1987) Org Geochem of sediments from the continental margin off southern New England, U.S.A.—part I. Amino acids, carbohydrates and lignin. Mar Chem 21:249–265

Stiller M, Nissenbaum A (1999) Geochemical investigation of phosphorus and nitrogen in the hypersaline Dead Sea. Geochim Cosmochim Acta 63:3467–3475

Ström L, Ekberg A, Mastepanov M, Røjle Christensen T (2003) The effect of vascular plants on carbon turnover and methane emissions from a tundra wetland. Glob Change Biol 9:1185–1192

Strome D, Miller MC (1978) Photolytic changes in dissolved humic substances. Int Ver Theor Angew Limnol 20:1248–1254

Stumm W, Lee GF (1961) Oxygenation of ferrous iron. Ind Eng Chem 53:143–146

Sun MY, Lee C, Aller RC (1993) Anoxic and Oxic Degradation of ^14C-labeled Chloropigments and a 14C-labeled Diatom in Long Island Sound sediments. Limnol Oceanogr 38:1438–1451

Suzumura M, Ingall ED (2004) Distribution and dynamics of various forms of phosphorus in seawater: insights from field observations in the Pacific Ocean and a laboratory experiment. Deep Sea Res Part I 51:1113–1130

Takeda K, Takedoi H, Yamaji S, Ohta K, Sakugawa H (2004) Determination of hydroxyl radical photoproduction rates in natural waters. Anal Sci 20:153–158

Tanaka K, Suda Y, Kondo N, Sugahara K (1985) O_3 tolerance and the ascorbate-dependent H_2O_2 decomposing system in chloroplasts. Plant Cell Physiol 26:1425–1431

Thauer RK (1998) Biochemistry of methanogenesis: a tribute to Marjory Stephenson. Microbiology 144:2377–2406

Thauer RK, Jungermann K, Decker K (1977) Energy conservation in chemotrophic anaerobic bacteria. Bacteriolog Rev 41:100

Thauer RK, Kaster AK, Seedorf H, Buckel W, Hedderich R (2008) Methanogenic archaea: ecologically relevant differences in energy conservation. Nature Rev Microbiol 6:579–591

Thebrath B, Rothfuss F, Whiticar M, Conrad R (1993) Methane production in littoral sediment of Lake Constance. FEMS Microbiol Lett 102:279–289

Thomas DN, Lara RJ (1995) Photodegradation of algal derived dissolved organic carbon. Mar Ecol Prog Ser Oldendorf 116:309–310

Tranvik LJ (1992) Allochthonous dissolved organic matter as an energy source for pelagic bacteria and the concept of the microbial loop. Hydrobiology 229:107–114

Tranvik L, Kokalj S (1998) Decreased biodegradability of algal DOC due to interactive effects of UV radiation and humic matter. Aquat Microb Ecol 14:301–307

Tranvik LJ, Downing JA, Cotner JB, Loiselle SA, Striegl RG, Ballatore TJ, Dillon P, Knoll L, Kutser T, Larsen S (2009) Lakes and reservoirs as regulators of carbon cycling and climate. Limnol Oceanogr 54:2298–2314

Twardowski MS, Donaghay PL (2002) Photobleaching of aquatic dissolved materials: Absorption removal, spectral alteration, and their interrelationship. J Geophys Res 107:3091

Uchida M, Nakatsubo T, Horikoshi T, Nakane K (1998) Contribution of micro-organisms to the carbon dynamics in black spruce (Picea Mariana) forest soil in Canada. Ecol Res 13:17–26

Uchida M, Nakatsubo T, Kasai Y, Nakane K, Horikoshi T (2000) Altitudinal differences in organic matter mass loss and fungal biomass in a subalpine coniferous forest, Mt. Fuji, Japan. Arct Antarct Alp Res 32:262–269

Upton M, Hill B, Edwards C, Saunders J, Ritchie D, Lloyd D (2000) Combined molecular ecological and confocal laser scanning microscopic analysis of peat bog methanogen populations. FEMS Microbiol Lett 193:275–281

Utsumi M, Belova SE, King GM, Uchiyama H (2003) Phylogenetic comparison of methanogen diversity in different wetland soils. J Gen Appl Microbiol 49:75–83

Vähätalo AV, Järvinen M (2007) Photochemically produced bioavailable nitrogen from biologically recalcitrant dissolved organic matter stimulates production of a nitrogen-limited microbial food web in the Baltic Sea. Limnol Oceanogr 52:132–143

Vähätalo AV, Wetzel RG (2004) Photochemical and microbial decomposition of chromophoric dissolved organic matter during long (months–years) exposures. Mar Chem 89:313–326

Vahatalo AV, Salkinoja-Salonen M, Taalas P, Salonen K (2000) Spectrum of the quantum yield for photochemical mineralization of dissolved organic carbon in a humic lake. Limnol Oceanogr 45:664–676

Valentine RL, Zepp RG (1993) Formation of carbon monoxide from the photodegradation of terrestrial dissolved organic carbon in natural waters. Environ Sci Technol 27:409–412

Vione D, Merlo F, Maurino V, Minero C (2004) Effect of humic acids on the Fenton degradation of phenol. Environ Chem Lett 2:129–133

Vione D, Falletti G, Maurino V, Minero C, Pelizzetti E, Malandrino M, Ajassa R, Olariu RI, Arsene C (2006) Sources and sinks of hydroxyl radicals upon irradiation of natural water samples. Environ Sci Technol 40:3775–3781

Vione D, Minero C, Maurino V, Olariu R-L, Arsene C, KMG M (2011) Photochemical transformation processes in surface waters. In: Maes KJ, Willems JM (Eds), Photochemistry: UV/VIS spectroscopy, photochemical reactions and photosynthesis, Nova Science Publishers, Chapter 9

Vione D, Lauri V, Minero C, Maurino V, Malandrino M, Carlotti ME, Olariu RI, Arsene C (2009) Photostability and photolability of dissolved organic matter upon irradiation of natural water samples under simulated sunlight. Aquat Sci 71:34–45

Voelker BM, Morel FMM, Sulzberger B (1997) Iron redox cycling in surface waters: effects of humic substances and light. Environ Sci Technol 31:1004–1011

von Gunten U, Oliveras Y (1997) Kinetics of the reaction between hydrogen peroxide and hypobromous acid: implication on water treatment and natural systems. Water Res 31:900–906

Waiser MJ, Robarts RD (2000) Changes in composition and reactivity of allochthonous DOM in a prairie saline lake. Limnol Oceanogr 45:763–774

Weiss R, Carmack ECC, Koropalov V (1991) Deep-water renewal and biological production in Lake Baikal. Nature 349:665–669

Westerhoff P, Yoon Y, Snyder S, Wert E (2005) Fate of endocrine-disruptor, pharmaceutical, and personal care product chemicals during simulated drinking water treatment processes. Environ Sci Technol 39:6649–6663

Westermann P (1994) The effect of incubation temperature on steady-state concentrations of hydrogen and volatile fatty acids during anaerobic degradation in slurries from wetland sediments. FEMS Microbiol Ecol 13:295–302

Wetzel RG (1984) Detrital dissolved and particulate organic carbon functions in aquatic ecosystems. Bull Mar Sci 35:503–509

Wetzel RG (1992) Gradient-dominated ecosystems: sources and regulatory functions of dissolved organic matter in freshwater ecosystems. Hydrobiology 229:181–198

Wetzel RG, Hatcher PG, Bianchi TS (1995) Natural photolysis by ultraviolet irradiance of recalcitrant dissolved organic matter to simple substrates for rapid bacterial metabolism. Limnol Oceanogr 40:1369–1380

White EM, Vaughan PP, Zepp RG (2003) Role of the photo-Fenton reaction in the production of hydroxyl radicals and photobleaching of colored dissolved organic matter in a coastal river of the southeastern United States. Aquat Sci 65:402–414

White EM, Kieber DJ, Sherrard J, Miller WL, Mopper K (2010) Carbon dioxide and carbon monoxide photoproduction quantum yields in the Delaware Estuary. Mar Chem 118:11–21

Whiticar MJ (1999) Carbon and hydrogen isotope systematics of bacterial formation and oxidation of methane. Chem Geol 161:291–314

Williams RT, Crawford RL (1985) Methanogenic bacteria, including an acid-tolerant strain, from peatlands. Appl Environ Microbiol 50:1542–1544

Winfrey M, Zeikus J (1979) Anaerobic metabolism of immediate methane precursors in Lake Mendota. Appl Environ Microbiol 37:244–253

Winter AR, Fish TAE, Playle RC, Smith DS, Curtis PJ (2007) Photodegradation of natural organic matter from diverse freshwater sources. Aquat Toxicol 84:215–222

Worakit S, Boone D, Mah R, Abdel-Samie M, El-Halwagi M (1986) *Methanobacterium alcaliphilum* sp. nov., an H_2-utilizing methanogen that grows at high pH values. Int J Syst Bacteriol 36:380–382

Wu F, Tanoue E (2001) Molecular mass distribution and fluorescence characteristics of dissolved organic ligands for copper (II) in Lake Biwa, Japan. Org Geochem 32:11–20

Wu FC, Mills RB, Cai YR, Evans RD, Dillon PJ (2005) Photodegradation-induced changes in dissolved organic matter in acidic waters. Can J Fish Aquat Sci 62:1019–1027

Xie H, Zafiriou OC, Cai WJ, Zepp RG, Wang Y (2004) Photooxidation and its effects on the carboxyl content of dissolved organic matter in two coastal rivers in the southeastern United States. Environ Sci Technol 38:4113–4119

Yamashita Y, Tanoue E (2004) In situ production of chromophoric dissolved organic matter in coastal environments. Geophys Res Lett 31 [doi: 101029/2004GL019734]

Yamashita Y, Tanoue E (2008) Production of bio-refractory fluorescent dissolved organic matter in the ocean interior. Nature Geosci 1:579–582

Yang ST, Guo M (1990) Kinetics of methanogenesis from whey permeate in packed bed immobilized cells bioreactor. Biotechnol Bioeng 36:427–436

Yocis BH, Kieber DJ, Mopper K (2000) Photochemical production of hydrogen peroxide in Antarctic waters. Deep Sea Res Part I 47:1077–1099

Yoshioka T, Mostofa KMG, Konohira E, Tanoue E, Hayakawa K, Takahashi M, Ueda S, Katsuyama M, Khodzher T, Bashenkhaeva N (2007) Distribution and characteristics of molecular size fractions of freshwater-dissolved organic matter in watershed environments: its implication to degradation. Limnology 8:29–44

Zafiriou OC, True MB (1979a) Nitrate photolysis in seawater by sunlight. Mar Chem 8:33–42

Zafiriou OC, True MB (1979b) Nitrite photolysis in seawater by sunlight. Mar Chem 8:9–32

Zafiriou OC, Joussot-Dubien J, Zepp RG, Zika RG (1984) Photochemistry of natural waters. Environ Sci Technol 18:356A–371A

Zafiriou OC, True MB, Hayon E (1987) Consequences of OH radical reaction in sea water: formation and decay of Br2− ion radical. In: Photochemistry of environmental aquatic systems Am Chem Soc, Washington, pp 89–105

Zeikus J, Weimer P, Nelson D, Daniels L (1975) Bacterial methanogenesis: acetate as a methane precursor in pure culture. Arch Microbiol 104:129–134

Zepp RG, Hoigne J, Bader H (1987a) Nitrate-induced photooxidation of trace organic chemicals in water. Environ Sci Technol 21:443–450

Zepp RG, Skurlatov Y, Pierce J (1987b) Algal-induced decay and formation of hydrogen peroxide in water: its possible role in oxidation of anilines by algae. In: Zika RG, Cooper WJ (eds) Photochemistry of environmental aquatic systems, ACS symp Ser 327. Am Chem Soc, Washington, pp 213–224

Zepp RG, Faust BC, Hoigne J (1992) Hydroxyl radical formation in aqueous reactions (pH 3–8) of iron (II) with hydrogen peroxide: the photo-Fenton reaction. Environ Sci Technol 26:313–319

Zepp RG, Callaghan T, Erickson D (1998) Effects of enhanced solar ultraviolet radiation on biogeochemical cycles. J Photochem Photobiol, B 46:69–82

Zepp R, Erickson D III, Paul N, Sulzberger B (2011) Effects of solar UV radiation and climate change on biogeochemical cycling: interactions and feedbacks. Photochem Photobiol Sci 10:261–279

Zhang Y, Zhu L, Zeng X, Lin Y (2004) The biogeochemical cycling of phosphorus in the upper ocean of the East China Sea. Estuar Coast Shelf Sci 60:369–379

Zhang Y, van Dijk MA, Liu M, Zhu G, Qin B (2009a) The contribution of phytoplankton degradation to chromophoric dissolved organic matter (CDOM) in eutrophic shallow lakes: field and experimental evidence. Water Res 43:4685–4697

Zhang Y, Liu M, Qin B, Feng S (2009b) Photochemical degradation of chromophoric-dissolved organic matter exposed to simulated UV-B and natural solar radiation. Hydrobiology 627:159–168

Zhang D, Pan X, Mostofa KMG, Chen X, Mu G, Wu F, Liu J, Song W, Yang J, Liu Y (2010) Complexation between Hg(II) and biofilm extracellular polymeric substances: an application of fluorescence spectroscopy. J Hazard Mat 175:359–365

Zhao Y, Yu Y, Feng W, Shen Y (2003) Growth and production of free-living heterotrophic nanoflagellates in a eutrophic lake–Lake Donghu, Wuhan, China. Hydrobiology 498:85–95

Zhou X, Mopper K (1990) Determination of photochemically produced hydroxyl radicals in seawater and freshwater. Mar Chem 30:71–88

Zika RG (1981) Marine organic photochemistry. In: Elsevier Oceanography Series, vol 31, pp 299–325

Zinder SH (1990) Conversion of acetic acid to methane by thermophiles. FEMS Microbiol Lett 75:125–137

Zinder SH (1993) Physiological ecology of methanogens. In: Ferry JG (Ed) Methanogenesis: Ecology, Physiology, Biochemistry and Genetics, Chapman and Hall, New York pp 128–206